Winter 1997

The chemistry and dry deposition of atmospheric nitrogen at a rural site in the northeastern United States

Barry Lee Lefer
University of New Hampshire, Durham

THE CHEMISTRY AND DRY DEPOSITION OF ATMOSPHERIC NITROGEN AT A RURAL SITE IN THE NORTHEASTERN UNITED STATES

BY

BARRY LEE LEFER

B. A., University of Virginia, 1989
M.S., University of New Hampshire, 1992

DISSERTATION

Submitted to the University of New Hampshire
in Partial Fulfillment of
the Requirements for the Degree of

Doctor of Philosophy
in
Earth Sciences

December, 1997

UMI Number: 9819679

UMI
300 North Zeeb Road
Ann Arbor, MI 48103

This dissertation has been examined and approved.

Robert W. Talbot

Dissertation Director, Dr. Robert W. Talbot
Research Associate Professor of Earth Sciences

John D. Aber

Dr. John D. Aber
Professor of Natural Resources

Jack E. Dibb

Dr. Jack E. Dibb
Research Associate Professor of Earth Sciences

William H. McDowell

Dr. William H. McDowell
Associate Professor of Natural Resources

J. William Munger

Dr. J. William Munger
Research Associate, Division of Applied Sciences
Harvard University

21 Nov 1997

Date

ACKNOWLEDGMENTS

First, I would like to thank my committee: Robert Talbot, Jack Dibb, Bill Munger, John Aber, and Bill McDowell. I greatly appreciate their help and guidance. I extend my profound thanks to my dissertation advisor, Robert Talbot, for his patience and assistance, for constantly challenging me to learn, and then letting me figure things out for myself. I thank Jack Dibb for many illuminating discussions and challenging questions. I thank Bill Munger for promptly and patiently answering my innumerable questions and providing chemical and meteorological support necessary to interpret this atmospheric N dataset. I am deeply indebted to John Aber for introducing me to the field of forest ecosystem research, both here and in Ireland. I also grateful to Bill McDowell for his encouragement and reminders to keep focused on the important things.

I would like to thank the numerous members of the Talbot research group who performed critical roles in the collection and analysis of these gas and aerosol samples. Eric Scheuer provided expert help and guidance in the lab and field, which made this work possible. The Talbot/Scheuer work study corps, lead by Kristen Olson, Mandy Fifield, Barry Moushegian, and Garry Seid , assisted on numerous field expeditions and cheerfully and untiringly extracted and analyzed thousands of samples.

I am grateful to the people of the Global Atmospheric Chemistry Group and the Complex Systems Research Center for making this a very exciting and enjoyable place to work. Extra praise goes to my officemates (Carolyn Jordan*, Paul Carroll, Dean Moosavi, Ruth Varner, and Matt Loomis) for their help with everything from collecting samples and reviewing manuscripts, to keeping me from becoming overwhelmed. I am also thankful for the excellent support of Linda Tibbetts and Karen Bushold which allowed me to focus on science and not worry about the other side of research.

The persons deserving the most recognition are my friends and family. During my tenure on the New Hampshire seacoast I particularly enjoyed the company of Patrick Crill and the Durham Firecats (Gregg Annis, Jeff Bass and Ben Auger). They offered me a much need outlet for my passion for football and taught me the importance of sharing a good pint with friends. Finally, I express my deepest feelings of appreciation to my wife Maggie, for her undying encouragement, understanding, and companionship.

This work was sponsored by the U.S. Department of Energy's National Institute for Global Environmental Change [NIGEC] (DE-FC03-90ER61010). My graduate education was sponsored a National Aeronautics and Space Administration GSRP fellowship, a grant from the Northeast Regional Center of NIGEC (901214-HAR#4), and a Dissertation Fellowship from the University of New Hampshire.

TABLE OF CONTENTS

LIST OF TABLES

LIST OF FIGURES

ABSTRACT

THE CHEMISTRY AND DRY DEPOSITION OF ATMOSPHERIC NITROGEN AT A RURAL SITE IN THE NORTHEASTERN UNITED STATES

by

Barry L. Lefer

University of New Hampshire, December, 1997

Measurements of N gas (HNO_3, NH_3) and aerosol (NO_3^-, NH_4^+) species were made between 1991-1995 to examine the nature of atmospheric N chemistry and to estimate the importance of N dry deposition to the Harvard Forest (Petersham, MA). This U.S. site was influenced by aged rural air masses advected from the northwest (NW) and fresh industrial emissions from the southwest (SW). Mean midday HNO_3 and aerosol N mixing ratios were four times higher in SW surface winds.

Diel cycles provided evidence of the entrainment of HNO_3 and aerosol NO_3^- from aloft as the nocturnal inversion broke down. HNO_3 made up about 20% of NO_Y at midday, while the sum of measured NO_Y species accounted for 60-80% of NO_Y suggesting that PAN and other organic nitrates were significant at this predominantly oak site. The deposition velocity (V_d) of HNO_3 was estimated using the modified-Bowen ratio (MBR) and an inferential method. Hourly averaged V_d for HNO_3 ranged from ≈ 1 cm s^{-1} at night to ≈ 6 cm s^{-1} at midday. HNO_3 deposition was typically 3-4 times higher than the measured NO_Y flux. Measurement bias, storage effects, and the flux of other NO_Y species probably contributed to this discrepancy.

NH_3 levels were suppressed by atmospheric SO_4^{2-} to mixing ratios of 200-300 pptv, below the NH_3 compensation point of the canopy. The SO_4^{2-} regulation of NH_X ($NH_3 + NH_4^+$) partitioning changed exponentially as a function of air temperature. The bulk aerosol was as a mixture of submicron ammonium (bi)sulfate aerosols with smaller amounts of soil particles. Aerosols from the SW were rarely neutralized, especially when SO_4^{2-} concentrations were greater than ≈ 100 nmol m^{-3}, suggesting an upper limit for NH_X emissions from this region. Aerosol NO_3^- was 4-8 times lower than NH_4^+, and associated with supermicron Ca^{2+}. The higher V_d of coarse mode NO_3^- resulted in similar dry deposition fluxes of 1 kg N ha^{-1} yr^{-1} for both N aerosol species. These aerosol deposition fluxes were considerably smaller than measured N ($NO_3^- + NH_4^+$) wet deposition (≈ 8 kg N ha^{-1} yr^{-1}) and estimates of HNO_3 inputs (1-7 kg N ha^{-1} yr^{-1}) to this forest ecosystem.

CHAPTER 1

INTRODUCTION

As an result of industrial and agricultural processes, humankind has inadvertently accelerated the biogeochemical cycling of nitrogen (N). Anthropogenic activities such as fossil fuel combustion, animal husbandry, and fertilizer application practices have increased the fluxes of nitrogen oxides (NO_x = NO and NO_2) and ammonia (NH_3) to the atmosphere. Since NH_3 acts as the principal neutralizing agent for atmospheric acids and NO_x is involved in both the production and destruction of tropospheric ozone (O_3), changes in the mixing ratios of these nitrogen gases directly impact the chemistry of the troposphere. The human induced enhancement of atmospheric NO_x and NH_3 has also increased the rate of atmospheric N deposition to the biosphere [Schell, 1987], potentially inducing N-limited ecosystems to remove CO_2 from the atmosphere at a faster rate [Peterson and Mellilo, 1985; Schindler and Bayley, 1993]. A better understanding of the consequences of increased N mobilization requires a closer look at the factors regulating the chemistry and deposition of atmospheric N.

Besides regulating the rate of ozone (O_3) production, NO_x also affects tropospheric mixing ratios of hydroxyl (OH) and hydroperoxy (HO_2) radicals. By controlling these critical atmospheric oxidants, NO_x directly regulates the oxidative removal rates of many trace gases and is indirectly involved in most atmospheric reaction cycles. NO_x is directly emitted from combustion processes as NO, but rapidly reacts with various oxidants (e.g., O_3, HO_2, organic peroxy radicals (RO_2)) to form NO_2. In the presence of sunlight, the photodissociation of NO_2 can regenerate NO in a matter of minutes, while slower reactions, occurring over a period of hours to days, may further oxidize NO_2 to nitric acid (HNO_3) or peroxyacetylnitrate (PAN). At night, NO_2 can be oxidized (via O_3) to NO_3 or subsequently react with NO_3 to form N_2O_5, which hydrolyses on aerosol surfaces to produce HNO_3 and aerosol nitrate (NO_3^-) [Richards, 1983; Dentener and Crutzen, 1993]. The family of reactive nitrogen trace species composed of NO, NO_2, NO_3, N_2O_5, HNO_3, aerosol NO_3^-, PAN and other organonitrates is collectively known as NO_y.

The less reactive NO_y reservoir species (PAN and HNO_3) have different atmospheric fates. PAN is only stable at cold temperatures and essentially insoluble, and as such has the potential to be transported long distances in the cold upper troposphere. Thus delivered to remote regions, PAN can thermally decompose to

NO_x in subsiding air. Although HNO_3 can react with various gases and particles (e.g., ammonia (NH_3) and soil/dust particles) to form nitrate containing aerosols it is also very water soluble and readily adsorbs onto surfaces. The dry deposition of HNO_3, is active over short distances, consequently, HNO_3 is efficiently removed from the atmosphere via both wet and dry deposition processes. Given the slow removal mechanisms of the other NO_Y components, the removal of HNO_3 is the primary atmospheric NO_Y sink and represents the termination of the radical reaction chain that produces O_3 [Logan, 1983].

In contrast, NH_3 is not actively involved in photochemical reactions, however it is the dominant atmospheric base, and as such determines the overall acidity of cloudwater, precipitation and atmospheric aerosols. Important sources of NH_3 include the decay of domestic livestock wastes, volatilization loses from fertilizers, biomass burning, and senescing vegetation [Schlesinger and Hartley, 1992]. Several studies indicate that growing vegetation can passively adsorb or emit NH_3 directly through leaf stomata [Denmead et al., 1976; Farquhar et al., 1980; Langford and Fehsenfeld, 1992]. Once NH_3 is released to the atmosphere, it has an average tropospheric lifetime on the order of hours to days before either: (1) reacting with H_2SO_4 or HNO_3 to form a fine mode aerosol; (2) being scavenged by wet deposition; or (3) directly dry depositing to the earth's surface. While aerosol NH_4^+ may be involved in long range transport if vertically advected into the free troposphere, NH_3 is typically deposited near its source.

As atmospheric N deposition has increased, some temperate forests have responded to this supplementary N with increased growth rates [Kauppi et al., 1992], while others have experienced serious damage [Vann et al., 1992]. Nitrogen has historically been a limiting nutrient for forest ecosystems, however, the extra addition of anthropogenically fixed N may eventually lead to a N saturated system [Aber et al., 1989], where nitrogen availability is in excess of biotic demand. Symptoms of N saturation include soil acidification [van Breemen et al., 1987], nitrate leaching [van Miegroet et al., 1992], and decreased stand growth rates [Schulze, 1989]. However, it is still uncertain what the critical atmospheric N loading rates are that lead to the problems associated with N saturation. Estimates of the critical N load to forests range from 2-30 kg N ha^{-1} yr^{-1} [Aren, 1983; Nilsson, 1978; Gunderson, 1991]. The critical N load is likely to be a function of other parameters such as: species composition, soil chemistry, hydrology, land-use history, plant/microbial interactions, and other biogeochemical factors.

The nitrogen loading of an ecosystem is accomplished by: [1] the wet deposition of dissolved NO_3^-, NH_4^+, and organic nitrogen (DON) in rain, fog, and snow; as well as [2] the dry deposition of N-containing aerosols and gases. Currently, much of the northeastern U.S. is receiving greater than 7 kg N $ha^{-1}yr^{-1}$ from wet deposition ($NO_3^- + NH_4^+$) alone [NADP/NTN, 1997]. Yet studies by Hanson and Lindberg [1991] show that dry deposition to plant surfaces can account for between 20 to 70% of total atmospheric N inputs. Given the

relatively high confidence in the quantification of the wet N deposition flux, the current large uncertainties in the estimates of total N deposition could be significantly reduced by a better understanding of the factors which regulate dry N deposition.

The goal of this thesis was to obtain hourly measurements of N gas and aerosol mixing ratios at the Harvard Forest (Petersham, MA) and to use this information to measure the importance of N dry deposition to this forest ecosystem. Measurements of HNO_3, NH_3, and soluble aerosol composition were made at two heights above, and one below, the mixed canopy primarily during the summer months between 1991 and 1995. Hence, this dataset was used to: (1) identify the chemical and physical factors which regulate the mixing ratios of water soluble N gases (HNO_3 and NH_3) and aerosols (NO_3^- and NH_4^+) at this rural northeastern U.S. site, and (2) estimate the dry deposition fluxes of these gases and particles to this mixed forest canopy and examine how they compare to other measurements of wet and dry N deposition to this ecosystem.

The following three chapters represent self contained papers, each with an abstract, introduction, conclusion, and references. In Chapter 2 [Lefer et al., 1997a], HNO_3 and NH_3 mixing ratios were reported for a variety of environmental conditions and related to diurnal and seasonal courses. Evidence of heterogeneous HNO_3 production and controls on NH_3 mixing ratios, such as the NH_3 compensation point, are examined. In Chapter 3 [Lefer et al., 1997b], the hourly deposition velocity of HNO_3 was estimated using modified-Bowen ratio and inferential approaches. The similarity of several hours of data for these two techniques enables the calculation of a canopy resistance for HNO_3. An inferential model of HNO_3 deposition was compared to eddy covariance measurements of the NO_y flux and multiple factors which contribute to the uncertainty associated with these methods are investigated. In Chapter 4, [Lefer and Talbot, 1997] the summertime composition and size distribution of water soluble aerosol species were reported and the dry deposition fluxes of particulate NH_4^+ and NO_3^- were calculated from empirical models. The primary NH_4^+ and NO_3^- aerosol production pathways were explored and the estimates of the contribution of N aerosols was compared to measured gaseous and precipitation N fluxes at this site. Chapter 5 ("Concluding Remarks"), summarizes the main conclusions, discusses the potential for further analysis of this dataset, and outlines directions for future experiments.

References

Aber, J.D., K.J. Nadelhoffer, P. Steudler, and J.M. Melillo, Nitrogen saturation in northern forest ecosystems, *BioScience*, *39* (6), 378-386, 1989.

Åren, G., Model analysis of some consequences of acid precipitation on forest growth, in *Ecological effects of acid deposition*, pp. 233-244, National Swedish Environment Protection Board, Solna, 1983.

Denmead, O.T., J.R. Freney, and J.R. Simpson, A closed ammonia cycle within a plant canopy, *Soil Biol. Biochem.*, *8*, 161-164, 1976.

Dentener, F.J., and P.J. Crutzen, Reaction of N_2O_5 on tropospheric aerosols: Impact on the global distributions of NO_x, O_3 and OH, *Journal of Geophysical Research*, *98*, 7149-7163, 1993.

Farquhar, G.D., P.M. Firth, R. Weselaar, and B. Weir, On the gaseous exchange of ammonia between leaves and the environment: determination of the ammonia compensation point, *Plant Physiology*, *66*, 710-714, 1980.

Gunderson, P., Nitrogen deposition and the forest nitrogen cycle, *Forest Ecology and Management*, *44*, 15-28, 1991.

Hanson, P.J., and S.E. Lindberg, Dry deposition of reactive nitrogen compounds: a review of leaf, canopy, and non-foliar measurements, *Atmospheric Environment*, *25A* (8), 1615-1634, 1991.

Kauppi, P.E., K. Mielikäinen, and K. Kuusela, Biomass and carbon budget of European forests, 1971-1990, *Science*, *256*, 70-74, 1992.

Langford, A.O., and F.C. Fehsenfeld, Natural Vegetation as a Source or Sink for Atmospheric Ammonia - A Case Study, *Science*, *255* (5044), 581-583, 1992.

Lefer, B.L., and R.W. Talbot, Aerosol nitrate and ammonium at a northeastern U.S. site, *Atmospheric Environment*, *submitted December*, 1997.

Lefer, B.L., R.W. Talbot, and J.W. Munger, Nitric acid and ammonia at a rural northeastern U.S. site, *Journal of Geophysical Research*, *submitted December* 1997a.

Lefer, B.L., R. W. Talbot, and J. W. Munger, Deposition of nitric acid vapor to a mid-latitude forest, *Atmospheric Environment*, *submitted December*, 1997b.

Logan, J.A., Nitrogen oxides in the troposphere: global and regional budgets, *Journal of Geophysical Research*, *88* (C15), 10,785-10,807, 1983.

NADP/NTN, National Atmospheric Deposition Program (NRSP-3)/National Trends Network, NADP/NTN Coordination Office, Natural Resource Ecology Laboratory, Colorado State University, Fort Collins, Colorado, 80523, February 17, 1997.

Nilsson, J., Critical loads for sulphur and nitrogen, in *Air Pollution and Ecosystems, Proc. Symp.*, edited by P. Mathy, pp. 85-91, D. Reidel Publishing Company, Dordrecht, 1978.

Peterson, B.J., and J.M. Melillo, The potential storage of carbon caused by eutrophication of the biosphere, *Tellus*, *37B*, 117-127, 1985.

Richards, L.W., Comments on the oxidation of NO_2 to nitrate—day and night, *Atmospheric Environment*, *17* (2), 397-402, 1983.

Schell, R.W., A historical perspective of atmospheric chemicals deposited on a mountain top peat bog in Pennsylvania, *International Journal of Goal Geology*, *8*, 147-173, 1987.

Schindler, D.W., and S.E. Bayley, The biosphere as an increasing sink for atmospheric carbon: estimates from increased nitrogen deposition, *Global Biogeochemical Cycles*, *7* (4), 717-734, 1993.

Schlesinger, W.H., and A.E. Hartley, A global budget for atmospheric NH_3, *Biogeochemistry*, *15*, 191-211, 1992.

Schulze, E.-D., Air pollution and forest decline in a spruce *Picea abies* forest, *Science*, *244*, 776-783, 1989.

Vann, D.R., G.R. Strimbeck, and A.H. Johnson, Effects of ambient levels of airborne chemicals on freezing resistance of red spruce foliage, *Forest Ecology and Management*, *51*, 69-79, 1992.

van Breemen, N., J. Mulder, and J.J.M. van Grinsven, Impacts of acid atmospheric deposition on woodland soils in The Netherlands: II N-transformations, *Soil Science Society of America Journal*, *51*, 1634-1640, 1987.

van Miegroet, H., D.W. Cole, and N.W. Foster, Nitrogen distribution and cycling, in *Atmospheric deposition and forest nutrient cycling*, edited by D.W. Johnson, and S.E. Lindberg, pp. 178-196, Springer-Verlag, New York, 1992.

CHAPTER 2

NITRIC ACID AND AMMONIA AT A RURAL NORTHEASTERN U.S. SITE

Abstract

Hourly mixing ratios of HNO_3, NH_3 and various other trace gas and aerosol species were determined at Harvard Forest in central Massachusetts between 1991-95 in order to: (1) measure diurnal and seasonal variability; and (2) define the important meteorological and chemical factors regulating the levels of HNO_3 and NH_3 in this rural atmosphere. Harvard Forest receives air masses from both urban and rural source regions resulting in mean midday HNO_3 mixing ratios four times higher when surface winds were from the SW ($\approx$ 2000 pptv) as opposed to the NW ($\approx$ 500 pptv) windsector. The HNO_3 diel cycle provides evidence of entrainment of HNO_3 from aloft as the nocturnal inversion breaks down. Gaseous NH_3 mixing ratios are typically 200-300 pptv and on average exhibit little diel variability. High levels of atmospheric sulfate consistently suppress NH_3 concentrations below the predicted NH_3 compensation point of the canopy, even during periods when total NH_X mixing ratios are quite high. The aerosol SO_4^{2-} regulation of NH_X partitioning changes as a function of temperature. At the same SO_4^{2-} mixing ratio, colder ambient temperatures result in lower NH_3/NH_X. On average HNO_3 makes up about 20% of NO_Y at midday. The sum of the measured NO_Y species (NO, NO_2, HNO_3, and particulate NO_3^-) typically account for 60-80% of NO_Y suggesting that PAN and other organic nitrates are a significant fraction of NO_Y at this predominantly oak forested site.

2.1 Introduction

The family of odd nitrogen trace species known as NO_Y ($NO_Y \equiv NO + NO_2 + NO_3 + N_2O_5$ + nitric acid (HNO_3) + aerosol nitrate ($NO_{3(p)}^-$) + peroxyacetylnitrate (PAN) + other organonitrates) is integral to the chemistry of the atmosphere. Besides regulating the rate of ozone (O_3) production and destruction reaction sequences, NO and NO_2 also affect tropospheric mixing ratios of hydroxyl (OH) and hydroperoxy (HO_2) radicals. By controlling these critical atmospheric oxidants, NO_X ($NO + NO_2$) is effectively involved in most atmospheric reaction cycles and the NO_X mixing ratio controls oxidative removal rates of many trace gases.

NO_X is directly emitted from combustion processes as NO, but rapidly reacts with various oxidants (e.g., O_3, HO_2, organic peroxy radicals (RO_2)) to form NO_2. In the presence of sunlight, the photodissociation of NO_2 can regenerate NO in a matter of minutes, while slower reactions, occurring over a period of hours to days, may further oxidize NO_2 to nitric acid (HNO_3) or peroxyacetylnitrate (PAN). At night, NO_2 can be oxidized (via O_3) to NO_3 or subsequently react with NO_3 to form N_2O_5, which hydrolyses on aerosol surfaces to produce HNO_3 [Richards, 1983; Dentener and Crutzen, 1993].

The less reactive NO_Y reservoir species (PAN and HNO_3) have different atmospheric fates. PAN is only stable at cold temperatures and essentially insoluble, and as such has the potential to be transported long distances in the cold upper troposphere. Thus delivered to remote regions, PAN can thermally decompose to NO_X in subsiding air. Although HNO_3 can react with various gases and particles (e.g., ammonia (NH_3) and soil/dust particles) to form nitrate containing aerosols, it is also very water soluble and readily adsorbs onto surfaces. The dry deposition of HNO_3 is active over short distances, consequently, HNO_3 is efficiently removed from the atmosphere via both wet and dry deposition processes. Given the slow removal mechanisms of the other NO_Y components, the removal of HNO_3 is the primary atmospheric NO_Y sink and represents the termination of the radical reaction chain that produces O_3 [Logan, 1983].

Further interest in the fate of HNO_3 has been linked to the "fertilization" of N-limited ecosystems by atmospheric deposition [Schindler and Bayley, 1993]. As anthropogenic emissions of NO have steadily increased over the past several decades [Gschwandtner et al., 1986], so has the deposition of atmospheric nitrogen [Schell, 1987], thereby potentially inducing some systems to incorporate even more atmospheric CO_2 [Peterson and Mellilo, 1985]. These investigations have highlighted the shortage of information regarding boundary layer HNO_3 mixing ratios and deposition fluxes, largely due to the difficulty in obtaining reliable ambient measurements. Even more scarce, and probably more difficult to acquire, are accurate measurements of gaseous NH_3 [Williams et al., 1992], another potentially important source of N to the biosphere.

In addition to being an important nutrient for plant growth, NH_3 is the only gaseous base found in significant quantities in the atmosphere, and it is therefore fundamental in determining the overall acidity of cloudwater, precipitation and atmospheric aerosols. Important sources of NH_3 include the decay of domestic livestock wastes, volatilization losses from fertilizers, biomass burning, and senescing vegetation [Schlesinger and Hartley, 1992]. Several studies indicate that growing vegetation can passively absorb or emit NH_3 directly through leaf stomata [Denmead et al., 1976; Farquhar et al, 1980; Langford and Fehsenfeld, 1992]. When ambient NH_3 mixing ratios are below a certain "compensation point", determined by the partial pressure of NH_3 within leaf stomata and perhaps the physiological state of the plant, NH_3 can escape to the atmosphere. The stomatal uptake of NH_3 is essentially the reverse process. Farquhar et al. [1980] noted that the compensation point of snap beans (*Phaseolus vulgaris*) was temperature dependent and could be described as the equilibrium NH_3 vapor pressure above an ammonium solution at a fixed pH of 6.8 (estimated to be the pH of the stomatal cell walls) and a NH_4^+ concentration of 46 μM. Langford and Fehsenfeld [1992] observed a nearly identical relationship for the regulation of background NH_3 mixing ratios for air passing over the Roosevelt National Forest in Colorado, and suggested that the NH_3 compensation point was a non-species specific mechanism perhaps related to photorespiration and assimilation.

Once NH_3 is released to the atmosphere, it has an average tropospheric lifetime on the order of hours to days before either: (1) reacting with H_2SO_4 or HNO_3 to form a fine aerosol; (2) being scavenged by wet deposition; or (3) directly dry depositing to the earth's surface. While NH_4^+ may be involved in long range transport if vertically advected into the free troposphere, NH_3 is typically deposited near its source.

Automated instruments to continuously measure atmospheric levels of NH_3 [Wyers et al., 1993] and HNO_3 [Buhr et al., 1995] have only recently been developed, consequently few long-term or high-resolution data sets exist for either species. The available longer term NH_3 measurements (weekly sample integration) indicate a seasonal cycle with summertime maxima and wintertime minima for the Harvard Forest in Petersham, MA [Tjepkema et al., 1981]. Higher resolution (2 hour integration) summertime data at other sites show similar diurnal trends with nighttime minima and daytime maxima for NH_3 [Langford et al., 1992]. It is thought the seasonal and diel cycles of NH_3 arise from warmer temperatures leading to greater NH_3 emission rates.

Several years of weekly HNO_3 measurements reveal different trends for various regions of the U.S. [Meyers et al., 1991]. Variable HNO_3 seasonal trends may be a consequence of episodic HNO_3 events occurring throughout the year [Edgerton et al., 1992]. The typical HNO_3 diel signal of higher values midday and lower levels at night[Parrish et al., 1986]is thought to be a result of photochemical HNO_3 production and surface deposition [Kleinman et al., 1994].

In the present study, hourly measurements of HNO_3 and NH_3 have been obtained during 1991-1995 at a nonurban continental site for a wide range of meteorological conditions. Over the same period, NO, NO_x, NO_y and other important trace gas species and meteorological parameters were continuously measured [Munger et al., 1996, 1997]. The purposes of this study were: (1) to ascertain the representativeness of this composite dataset, (2) to identify general seasonal and diurnal trends in the mixing ratios of HNO_3 and NH_3 at this site, (3) to establish how these mixing ratios depend on characteristic meteorological parameters such as wind direction and temperature, and (4) to examine HNO_3 relative to the other reactive nitrogen species measured.

2.2 Methods

2.2.1 Site description and ancillary measurements

The Harvard Forest in Petersham (42°32' N, 72°11' W; elevation 340m) is located in a wooded, rural area of central Massachusetts. The nearest large cities are Boston and Hartford, 100 km to the east and southwest, respectively. This 50-70 year old predominantly oak forest (mixed with maple, beech, birch, cherry, spruce, and pine) has an average canopy height of 23 m near the sampling site. Since the middle of 1990, the Harvard group has made continuous measurements of various atmospheric trace gases (NO, NO_2, NO_y, CO, CO_2, H_2O, O_3, and a suite of non-methane hydrocarbons) from the top of this 30 meter tower [Goldstein et al., 1995; Goulden et al., 1996; Munger et al., 1996]. In addition, numerous micrometeorological and radiative properties (including wind speed, wind direction, temperature, relative humidity, photosynthetically active radiation (PAR), solar albedo, and net radiative flux) are continuously monitored by a variety of instruments collaboratively operated by both Harvard and the State University of New York (SUNY) at Albany [Moore et al., 1996]. The fast response nature of most of these sensors enables the eddy covariance determination of fluxes of heat, momentum, NO_y, CO_2, and O_3 [Wofsy et al., 1993; Goulden et al., 1996; Moore et al., 1996; Munger et al., 1996, 1997].

2.2.2 UNH gas sampling methods and protocols

Water soluble gases were sampled with a mist chamber, also known as a nebulizing-reflux chamber [Cofer et al., 1985; Talbot et al., 1990]. A mist chamber concentrates the water-soluble gases from a large volume (≈1000 L) of air into a small volume (≈ 10 mL) of stripping solution, in this case, ultra-pure water was used. The dissolved ions in the stripping solution were quantified by ion chromatography. The mist chamber/ion chromatography (MC/IC) method has been continually developed and improved over the past 10

years and has proven in various intercomparison studies to be very effective at sampling gaseous HNO_3, HCOOH, CH_3COOH, and SO_2 [Keene et al., 1989; Talbot et al., 1990; Stecher et al., 1997].

A teflon membrane (Zefluor™, Gelman Products Inc.) was used as an aerosol prefilter to prevent water soluble aerosols from being dissolved in the mist chamber stripping solution. A custom-made teflon filter holder, designed to minimize internal surface area by omitting any backup filter support, attaches directly to the glass inlet of the mist chamber sampler. Operating at a flowrate of 30 slpm, this downward-facing prefilter collects a bulk sample of aerosol particles with a diameter between ≈ 10 nm [Dibb and Anderson, 1996 personal communication] and at least 50 μm for windspeeds up to 5 m s^{-1} [Davies, 1968; Davies and Subari, 1982]. Aerosol filter samples were stored in a freezer and within a week of their collection were treated with 200 μL of MeOH (to allow more complete wetting of teflon) and then extracted with two 10 ml aliquots of deionized water. Immediately after their generation, mist chamber samples and aerosol extracts were stored in 30-ml HDPE amber bottles, preserved with 100 μl of $CHCl_3$ and kept on ice until their transfer to a refrigerator. All samples were analyzed within 2 months of collection by ion chromatography for major ion species (including NO_3^- and $NH_4^+{}_{(aq)}$). Details of the ion chromatographic chemical analysis of water soluble gas and aerosol samples are described in Talbot et al.[1992, 1997] and Lefer et al. [1994].

The hourly sampling protocol involved collecting 45-50 minute integrated mist chamber and aerosol prefilter samples simultaneously from three levels (29, 24 and 10 m above ground) with the remaining 10-15 minutes available to rinse the mist chambers, to change the prefilters, and to periodically collect mist chamber blanks. Unless otherwise noted, this paper will discuss the gas and aerosol samples collected from the uppermost sampling height at 29 m, some 6-7 m above the canopy. Hourly mist chamber samples were continuously collected for 12-30 hour long periods on 70 dates between 1991-1995 (Table 2.1). The majority of the sampling occurred during the growing season (May - August). The entire Harvard Forest dataset, including the University of New Hampshire (UNH) gas and aerosol data, is available on-line via anonymous ftp at io.harvard.edu in the directory pub/nigec/UNH and the Web site www-as.harvard.edu.

Table 2.1. Mist Chamber HNO_3 and NH_3 sampling dates. HNO_3 data collected on all days, NH_3 data only collected on dates with *.

Year	Julian Day
1991	165*, 166*, 168*, 169*, 223*, 225*, 226*, 227*, 280, 281, 282, 283
1992	143, 144, 146, 147, 148, 192, 193, 194, 245, 246, 248, 249
1993	62, 79, 80, 81, 118, 119, 121, 200*, 201*, 202*, 203*, 204*
1994	144*, 153*, 154*, 155*, 156*, 161*, 162*, 167*, 168*, 215*, 216*, 217*, 202*, 235*, 236*, 237*, 238*
1995	116*, 117*, 120*, 122*, 159*, 160*, 161*, 164*, 165*, 166*, 167*, 168*, 169*, 213*, 214*, 215*, 219*, 220*, 221*

2.2.3 Potential sampling artifacts

Any HNO_3 or NH_3 measurement technique that employs a prefilter is susceptible to certain positive and negative artifacts [Appel and Tokiwa, 1981; Cadle et al., 1982]. The easiest way to minimize prefilter reactions is to sample for a shorter period of time (smaller volume of air), thereby reducing the aerosol loading on the teflon prefilter. Our 45 minute integrated samples (1.3 m^3) were relatively short considering that most studies which observed prefilter problems (see below) typically sampled for 6-24 hours integrating much larger volumes of air (5-20 m^3).

On a Teflon filter, particulate NH_4NO_3 can dissociate into HNO_3 and NH_3 [Appel et al., 1981] resulting in significant positive HNO_3 [Spicer et al., 1982; Appel et al., 1988] and NH_3 [Appel et al, 1988] errors. While NH_4NO_3 is unstable at typical tropospheric temperatures and relative humidities [Stelson and Seinfeld, 1982], the reactions producing ammonium (bi)sulfate are generally thought to be irreversible [Tang, 1980]. Consequently, Tang et al. [1980], suggested that substantial NH_4NO_3 formation will not occur until almost all atmospheric sulfate is completely neutralized. The studies that observed positive HNO_3 and NH_3 artifacts occurred in the western United States where NH_4NO_3 is more prevalent due to lower regional SO_2 emissions [Hidy, 1978; Wolff, 1984]. The substantial SO_4^{2-} wet deposition flux to the northeastern U.S. [National Acid Deposition Program, 1997] indicates that NH_4NO_3 volatilization should be less of problem when sampling this generally sulfate rich acidic atmosphere.

A potential negative HNO_3 artifact can occur when HNO_3 reacts with basic soil [Forrest et al., 1982] or seasalt particles [Savoie and Prospero, 1982] on the prefilter. As suggested above, the northeastern U.S. aerosol is generally acidic although this acidity can be mitigated by high soil dust emissions occurring as a result of drought or agricultural practices. Since aerosol SO_4^{2-}, Ca^{2+} (an indicator of soil dust), and Na^+ levels on the prefilter were measured for each sample, we can safely say that these sampling artifacts are insignificant for the vast majority of our samples [Lefer and Talbot, 1997].

2.2.4 Mist chamber technical specifications

This MC/IC gas sampling system had average detection limits of 5 parts per trillion by volume (pptv) for HNO_3 and 12-40 pptv NH_3, assuming an average solution volume of 15 mL, an average sampled air volume of 1350 L, analytical detection limits (in μmol/L) of 0.02 (NO_3^-) and 0.05 (NH_4^+), and/or a minimum NH_4^+ concentration of 2x the average blank of 0.09 μmol/L. While the mist chambers did not have a detectable NO_3^- blank, in some cases there was a slight NH_4^+ blank that tended to decrease over the course of the sampling period. Since blanks were collected several times a day, this was easily accounted for in the blank subtraction protocol.

The mist chamber samplers have been shown on multiple occasions to have 100% collection efficiency for HNO_3 (Talbot et al., 1990; Talbot et al., 1997). A single stage NH_3 dilution system was constructed to determine the mist chamber's collection efficiency for NH_3. This simple dilution system consisted of a NH_3/N_2 cylinder ($\approx$ 1 ppmv), a high pressure liquid N_2 dewar, two Teledyne-Hastings mass flowmeters, and a 1.1 meter long 2.0 cm I.D. Pyrex tube with 3.1 mm add port and a 6.35 mm sample port (near opposite ends). The flowrate of the NH_3 cylinder was not measured during an actual calibration run, however, this flowrate was measured before and after each calibration run with a bubble flowmeter and was always found to be invariant. The concentrated NH_3 was transported via a 1-m length of 1/8" O.D. Silcosteel™ tubing (Restek Inc.) and added into the core of the N_2 flow. The flowrate and volume of the dilution N_2 was measured by an integrating mass flowmeter upstream from the glass manifold. Approximately 1-m downstream from the NH_3 add port, the NH_3/N_2 mixture was sampled directly from the core of the manifold with a mist chamber.

The NH_3 mixing ratio delivered from the cylinder (821±40 ppbv) was determined by sampling (n=12) directly from the Silcosteel™ tubing. The cylinder gas was bubbled through 2 H_2O bubblers in series followed by a mass flowmeter. No NH_4^+ was ever detected in the 2nd bubbler. For a typical ambient NH_3 mixing ratio (370 pptv), the mist chamber had a mean (±std. dev.) collection efficiency of 99% (±9.2%) (n=9). Similar NH_3 collection efficiencies were observed for both higher and lower NH_3 levels. A mist chamber

collection efficiency of 100% was used for determining the mixing ratios of both HNO_3 and NH_3 in our ambient air measurements.

The uncertainties assigned to the atmospheric mixing ratios reported for MC/IC samples were calculated using the error propagation formula [Knoll, 1979] and applying it to the uncertainties associated with the following measurements: air volume, water volume, ion concentration, blank subtraction, and collection efficiency. The reported mixing ratios of HNO_3 and NH_3 have overall uncertainties of ±11% and ±18%, respectively. The accuracy of the ion chromatographic determinations of NO_3^- and NH_4^+ in mist chamber samples were referenced to NIST certified aqueous standards, however at this point there are no certified low level (sub-ppbv) gaseous standards to directly determine the overall accuracy of any measurement of these and many other trace gases [Crosley, 1994].

2.3 Results

2.3.1 Diel cycles of HNO_3 and NH_3

Hourly observations collected between Julian Days 165-169 (14-18 June) of 1991 (Figure 2.1) depict diurnal and synoptic variations typical of summertime observations at Harvard Forest. On day 165, north-northwest winds advected an air mass to the site with low HNO_3 and moderately high NH_3 mixing ratios (≈ 150 and 500 pptv, respectively). The next day, an air mass arriving from the west-southwest contained less NH_3 but much higher HNO_3 levels that peaked near mid-day (at approximately 4000 pptv). On the following day, southerly winds (Day 168, Figure 2.1) brought little gaseous NH_3 to this site with moderate levels of HNO_3. Thus changes in synoptic flow patterns strongly influenced the day-to-day mixing ratios of HNO_3 and NH_3.

While changes in mixing ratios of both species were often related to changes in wind direction or the height of the mixed layer, day 215 of 1995 (Figure 2.2a) is a good example of "typical" diurnal behavior at this site because of consistent winds from the south-southeast throughout the day. Under these conditions, NH_3 levels usually do not vary much while mixing ratios of HNO_3 frequently increase from a morning low to peak at mid-day, and then decrease throughout the afternoon. Less common at this site is to have north-northeast winds, (Figure 2.2b) which resulted in a distinct NH_3 diel cycle starting with representative NH_3 mixing ratios in the morning, rapidly rising to a mid-day maximum, which decline throughout the afternoon and evening.

Previous studies have shown that the mixing of polluted and clean air masses commonly results in lognormal distributions of atmospheric species for one specific site, particularly for primary pollutants (e.g., Georgopoulos and Seinfeld, 1982; Parrish et al., 1991). Both the HNO_3 and NH_3 datasets contained a wide

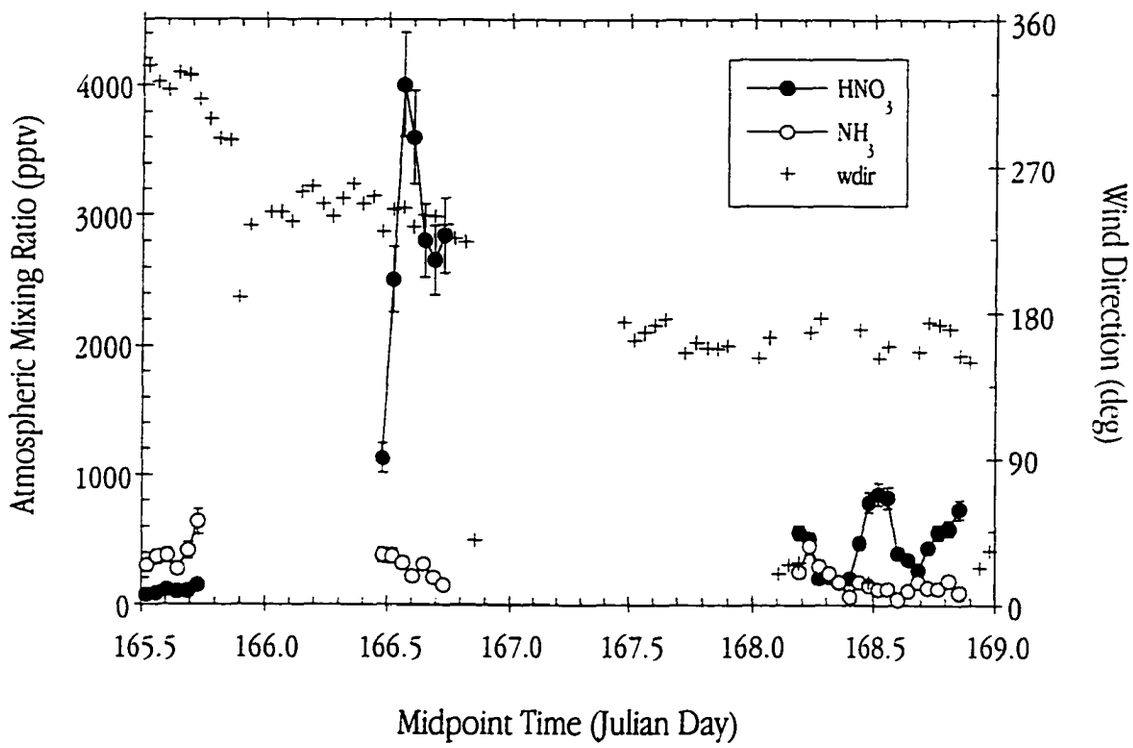

Figure 2.1. Hourly integrated mixing ratios of HNO_3 and NH_3 and average wind direction for the period June 14-17, 1991 (Julian Day (JD) 165-168). Error bars represent measurement uncertainty.

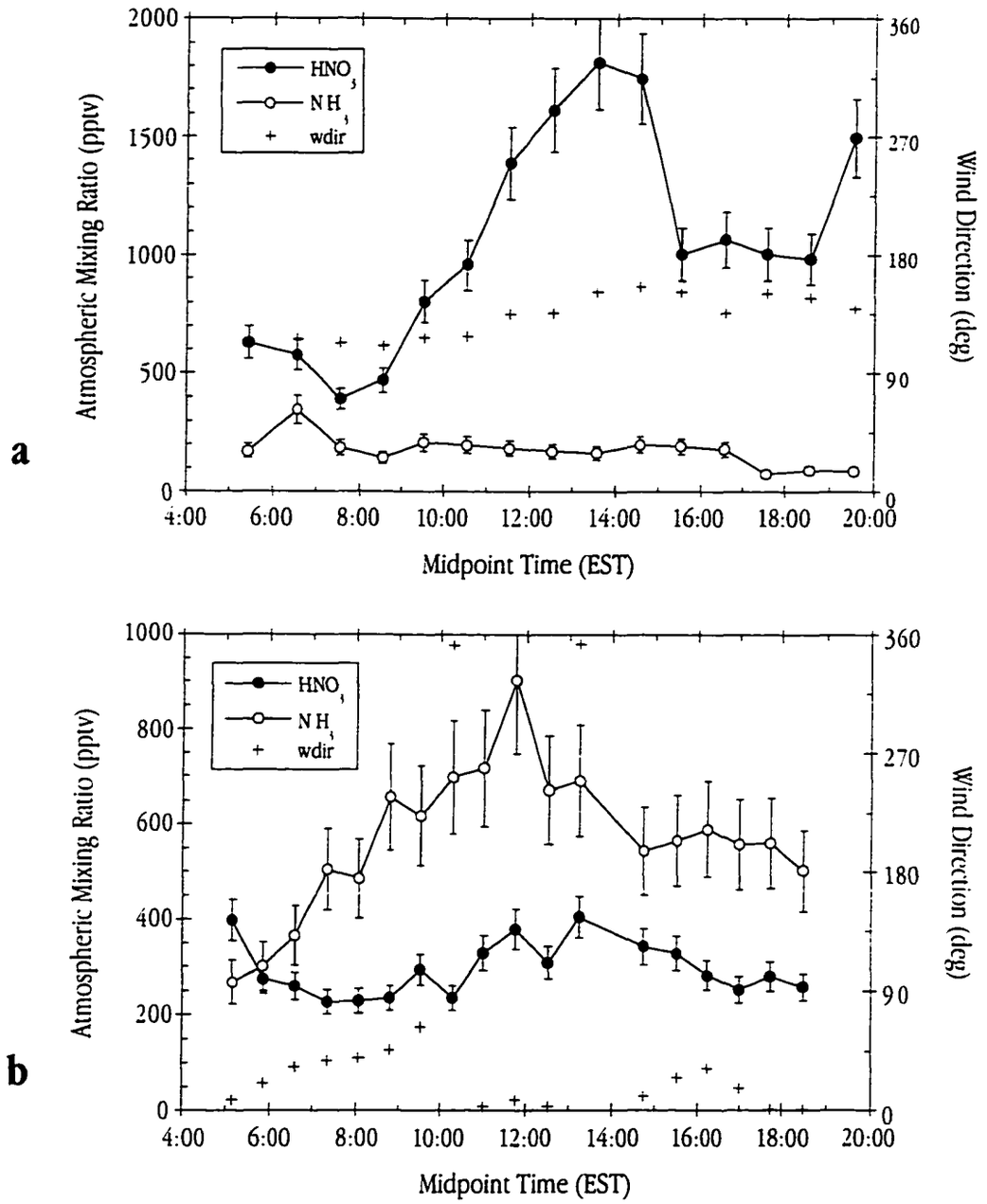

Figure 2.2. [a] Hourly integrated mixing ratios of HNO_3 and NH_3 and average wind direction for August 3, 1995 (JD 215). Error bars represent measurement uncertainty; [b] Same as Figure 2a, but for June 14, 1995 (JD 165).

range of lognormally distributed values. Consequently, the mean values may be strongly influenced by a few very high values, in such cases, both mean and median values are plotted. Consolidation and hourly binning of this 1991-1995 summertime dataset produced a composite mean diel cycle of HNO_3 at this site that is bimodal with nighttime and daytime mixing ratios of 400 and 900 pptv, respectively (Figure 2.3a). The composite median HNO_3 diel cycle displays less variability (Figure 2.3a) on account of the low HNO_3 mixing ratios in NW surface winds (Figure 2.3b), which occurred twice as often as SW winds during our sampling (see Figure 2.3b and section 2.4.1). The same data processing procedure yielded composite average and median NH_3 diel cycles that show mixing ratios consistently in the 200-400 pptv range (Figure 2.3a).

2.3.2 Windsector and season

Diel changes in the HNO_3 mixing ratio for the southwest (SW) and northwest (NW) wind sectors are on the order of 2000 pptv and 500 pptv, respectively (Figure 2.3b). In addition to having a lower amplitude, the NW diel cycle also starts from lower baseline HNO_3 mixing ratios. This pattern matches that previously noted by Munger et al. [1996] for NO_y and NO_x who defined the primary surface-wind direction sectors at this site as the north-northwesterly (270-45°), the southwesterly (180-270°) and the easterly (45-180°). The NH_3 diel cycle did not change as a function of windsector (not shown). However, mean and median mixing ratios of NH_3 and HNO_3 are different for the NW and SW wind sectors (Table 2.2). On average, an air mass with surface winds from the SW wind sector contains 3-4 times more HNO_3 and significantly less NH_3 ($p = 0.038$) than one with winds from the NW wind sector (Table 2.2).

Over a 5 year period, the majority (66%) of HNO_3 samples were collected in the summer (June, July, August) while 23% and 10% of the samples were collected in spring (March, April, May) and fall (September, October, November), respectively. No samples were collected in the winter (December, January, February). The measured HNO_3 mixing ratios were lowest in early spring (Figure 2.4), and highest in late summer to early fall (days 210-240 of 1994). The NH_3 levels peak in July and August (Figure 2.4b) with lower mixing ratios observed in the spring. An exponential relationship ($r^2 = 0.82$) between NH_3 levels and air temperature is evident for the summer of 1995 (Figure 2.5). At times the temperature dependence of the NH_3 breaks down, as shown for August 1995 (Figure 2.5). Data from other earlier years contain similar dual temperature relationships, but for purposes of clarity, only one year of summertime NH_3 data is included in Figure 2.5.

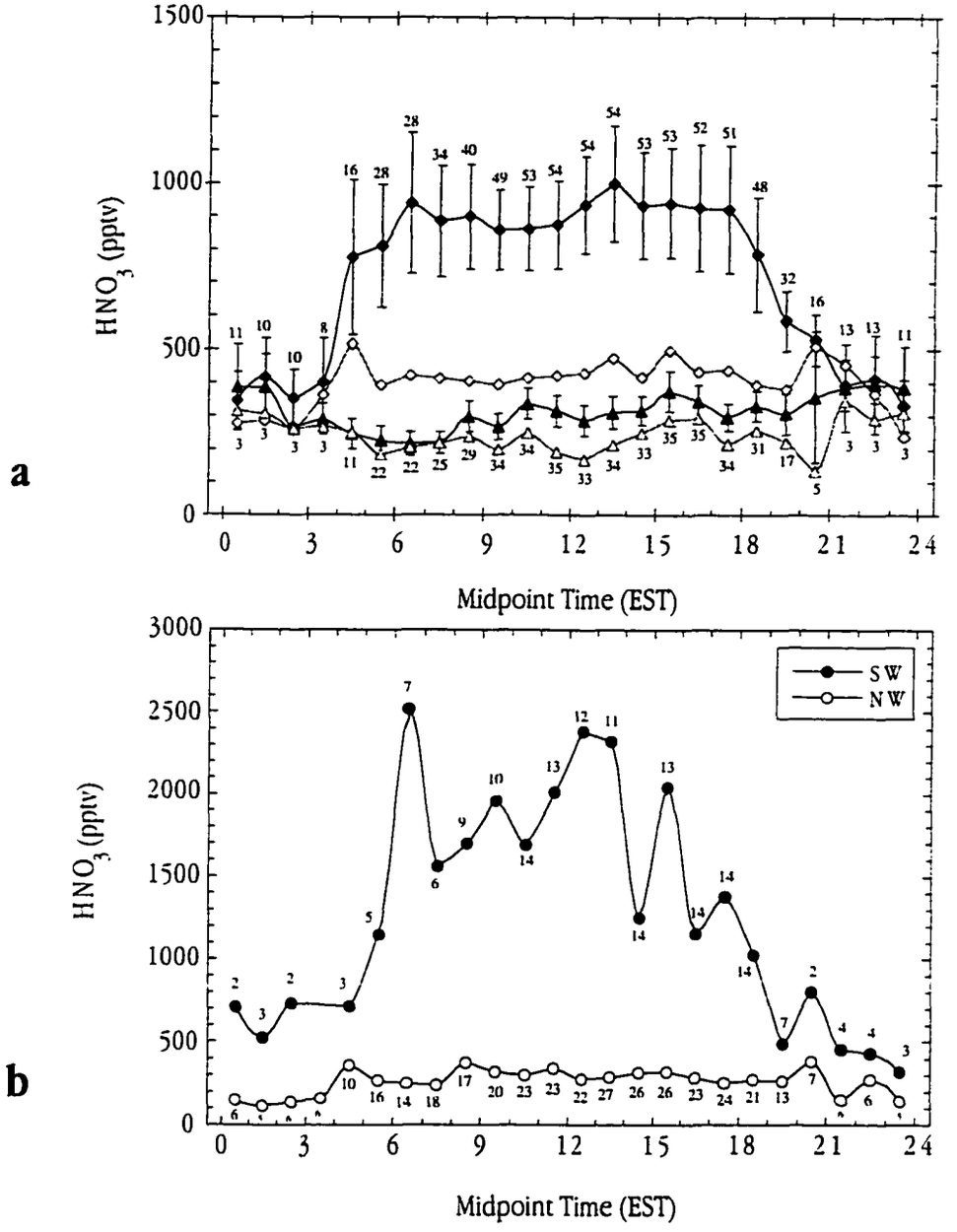

Figure 2.3 [a] Mean (filled symbols) and median (open symbols) diel cycles of HNO_3 (diamonds) and NH_3 (triangles) for all wind sectors. Error bars represent standard error of mean. Numbers above or below bars are number of hourly samples averaged.; [b] Median HNO_3 diel cycles for the dominant wind sectors: 180°-270° is southwest (SW); 270°-45° is northwest (NW). Values above or below points are number of samples.

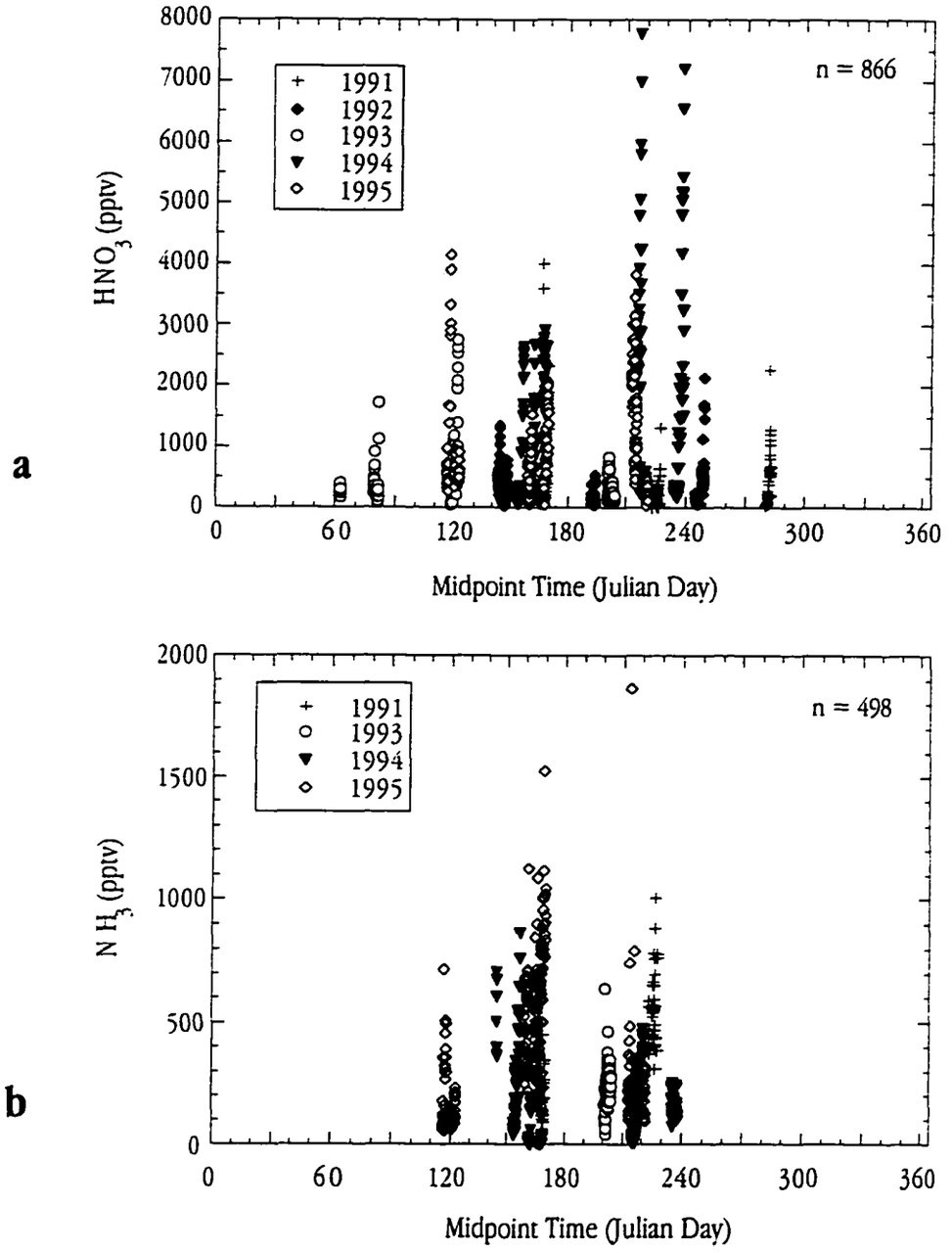

Figure 2.4. [a] Hourly integrated HNO_3 mixing ratios plotted versus Julian day. All samples collected between 1991-1995 on days listed in Table 2.1. Measurement uncertainty of ±11% not shown to keep figure legible; [b] Same as Figure 4a, except for NH_3. Measurement uncertainty of 17% not shown

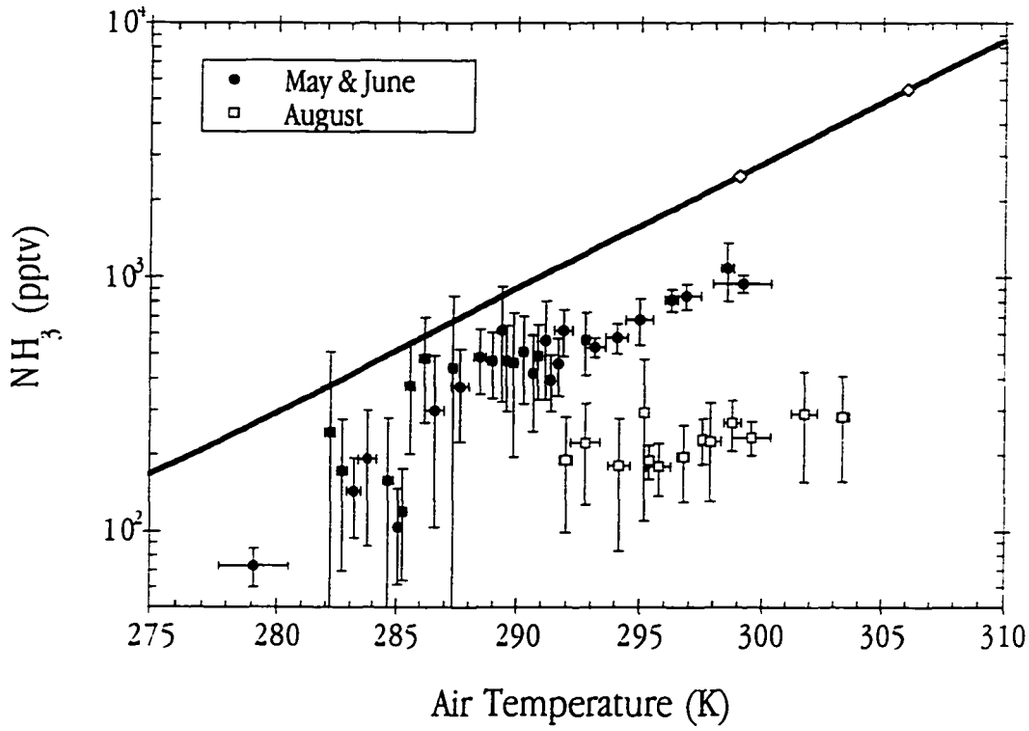

Figure 2.5. Temperature dependence of gaseous NH_3 mixing ratios collected for two different periods in the summer of 1995: 01 May - 18 June, 1995 (May, June) and 01-09 August, 1995 (August). Each symbol represents the average of five individual 1-hour measurements spanning the temperature range indicated by the horizontal bars. The vertical bars represent the standard deviation of the five samples. The solid line corresponds to the calculated NH_3 vapor pressure above a solution with 46 μM [NH_4^+] and pH 6.8 [Farquhar et al., 1980].

Table 2.2. Summary statistics of mixing ratios at UNH sampling times and selected surface-wind direction sectors. Statistics include: number of samples (n), 25th percentile (25%), standard deviation (s.d.), and 75th percentile (75%).

Species	Statistic	All Sectors	NW	E	SW
HNO_3, pptv	n*	788	370	154	187
	25%**	217	154	297	454
	median	423	271	512	1239
	mean	828	482	653	1712
	s.d.	1045	585	520	1566
	75%**	984	538	896	2533
NH_3, pptv	n	463	234	90	113
	25%	142	179	133	124
	median	245	281	194	224
	mean	231	353	309	292
	s.d.	254	260	229	266
	75%	452	471	467	436
NO_X, pptv	n	443	231	110	81
	25%	782	641	1406	1979
	median	1458	910	3396	4078
	mean	3647	1340	5214	8080
	s.d.	7011	1221	6737	12844
	75%	3794	1522	6091	7497
NO_Y, pptv	n	662	359	135	156
	25%	1861	1485	3228	3616
	median	3481	2290	4484	5592
	mean	5191	3038	6871	8655
	s.d.	5947	2428	5875	9022
	75%	6099	3772	8557	10972
$\{NO_Y\text{-}NO_X\}$, pptv	n	395	227	92	69
	25%	992	976	933	1015
	median	1793	1629	2095	2457
	mean	2466	1985	2952	3429
	s.d.	2266	1468	2963	2942
	75%	3017	2548	3412	5483

*Northwest (NW) is 270°-45°, East (E) is 45° - 180°, and Southwest (SW) is 180°-270°.

2.4 Discussion

2.4.1 Representativeness of the composite dataset

To extract meaning from a non-continuous dataset it is necessary to determine what time period the composite dataset most closely represents. Certainly, the mean and median values reported in Table 2.2 are not necessarily comparable to overall annual values due to the lack of wintertime (Dec.-Feb.) data (Table 2.1). Due to the availability of a continuous dataset of many chemical species and meteorological parameters made by Harvard University (HU) from the same tower, (e.g., Munger et al., 1996,1997) we can investigate how a parameter measured more or less continuously between 1991-1995 compares to the same parameter analyzed only for the UNH composite sampling times.

Table 2.3. Frequency of average hourly surface winds by sector (1991-95).

	n	NW	E	SW
UNH[b]	720	52%	20%	27%
1991-95[c]	33330	49%	19%	32%
Summer (1991-95)[d]	8466	44%	16%	39%

[a]Northwest (NW) is 270°-45°, East (E) is 45°-180°, and Southwest (SW) is 180°-270°.
[b]University of New Hampshire (UNH) HNO_3 and NH_3 sampling times.
[c]Harvard University (HU) continuous measurements.
[d]Summer is defined as June, July, and August.

Measurements of wind direction reveal that NW winds occur 49% and 52% of the time for continuous (HU) and composite (UNH) sampling, respectively. Similar good agreement is observed for the E and SW windsectors (Table 2.3). However, it appears that the SW sector is under represented (Δ -12%) and NW similarly over represented (Δ 8%) in the composite dataset when compared to summer-only HU observations (Table 2.3). On a diel basis, the median NO_y measured during UNH sampling times compares well with the median summertime NO_y diel (Figure 2.6), with the greatest differences occurring in the nighttime hours when UNH sample coverage was the lightest (Figure 2.3a). Summer and winter NO_y diel cycles vary considerably [Munger et al., 1996], consequently the UNH composite NO_y diel cycle between 0900-1300 is significantly different ($p < 0.05$) from the 1991-95 mean annual NO_y diel. Overall the composite dataset is most representative of summer conditions between the hours of 0500-2000 with a bias towards air masses with surface winds from the cleaner NW sector.

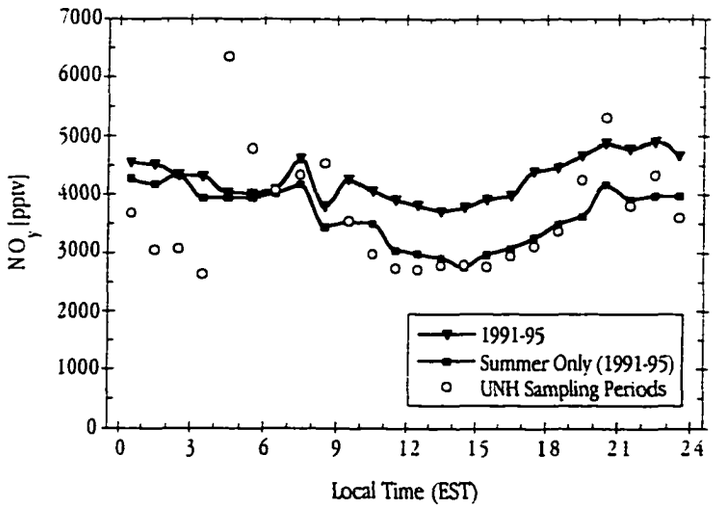

Figure 2.6 Median diel cycles of NO_y between 1991-95 for 3 different sets of data: all data; summertime only (June, July, and August); and UNH HNO_3 sampling periods listed in Table 2.1. Number of samples in each hourly group is ≈1200 for 1991-95 and ≈350 for summer only. UNH Sample number shown in Figure 3a for HNO_3 sampling times.

2.4.2 HNO_3

2.4.2.1 Comparison to other measurements. Table 2.4 is a compilation of HNO_3 measurements in rural North America, sorted in order of increasing sample integration time. This list, while not exhaustive, represents some of the more recent measurements. All the results, with the exception of this study, were obtained using Teflon/Nylasorb filterpacks which have previously been shown to compare reasonably well to the MC/IC technique [Talbot et al., 1990]. When comparing these values, note that all the sub-daily measurement campaigns mainly occurred during the summer months. Many of these high resolution projects do not include nighttime measurements (as noted in Table 2.4) which are generally lower [Edgerton et al., 1992] and may be biased by nonrepresentative meteorological conditions. While the daily and weekly HNO_3 sampling programs provide excellent seasonal and annual coverage, the long integration times may mask hourly and day/night variability that is useful in understanding the processes influencing the atmospheric chemistry of HNO_3.

The overall hourly mean and median HNO_3 mixing ratio for Harvard Forest agrees quite well with other measurements in rural North America (Table 2.4). The large range of HNO_3 mixing ratios (26-7771 pptv) at Harvard Forest is indicative of the wide variety of air masses that influence this site. The smaller HNO_3 variability

Table 2.4. Nitric acid mixing ratios for various sites in rural North America (all mixing ratios reported as pptv).

Site (Latitude)	Mean ±SD (Median ± MAD)	Range	Integration (restrictions) Study Period	Method	Source
Harvard Forest, MA (42.5°N)	828±1045 (423±257)	26-7771	1-hr (episodic) Summers 1991-95	Mist Chamber	This Study
Candor, NC	670±330	30-1760	1 hr (daytime only) June-July 1992	Teflon/Nylon filter pack	Aneja et al., 1994b
Metter, Georgia	800		1 hr 26 June -16 August 1991	NO_y-NO_y with Nylon Filter [includes particulate NO_3^-]	Kleinman et al., 1994
Mt. Mitchell, NC	406±340 [1988] 498±210 [1989]	20-2000	2 hr (daytime only) Summers 1988-89	Teflon/Nylon filter pack	Aneja et al., 1994a
Niwot Ridge, CO	—	10-3000	1-4 hr (daytime only) All Seasons 1979-84	Teflon/Nylon filter pack	Parrish et al, 1986
Oak Ridge, TN	1649	697-2819	4-hr (daytime only) 15-18 September 1982	Teflon/Nylon filter pack	Meyers et al., 1989
Calgary, Alberta	420	20-4000	4-hr (daytime only) June-August 1982	Teflon/Nylon filter pack	Peake et al., 1985
Pittsburg, CA	—	300-1500	8-hr 05-08 February 1979	Teflon/Nylon & Teflon/NaCl filter pack	Appel et al., 1980
Whiteface Mtn., NY	200 [clean] 1000 [polluted]	100-3100	6/12-hr July 1982	Teflon/NaCl filter pack & diffusion denuder	Kelly et al., 1984
State College, PA	900 [Jan] 400 [Feb] 500 [Mar]	50-1400 [Jan] 100-810 [Feb] 100-2295 [Mar]	24 hr (15 days/month) Jan.-March 1984	Teflon/Nylon filter pack downstream of NH_3 denuder	Lewin et al., 1986
Niwot Ridge, CO	64 [Winter] 238 [Summer]	20-700	24-hr (episodic) All Season 1980-84	Teflon/Nylon filter pack	Parrish et al, 1986

Table 2.4. (continued)

Site (Latitude)	Mean ±SD (Median ± MAD)	Range	Integration (restrictions) Study Period	Method	Source
Howland, ME (45.2°N)	270±174∞ 425±154*	79-829∞ 154-329*	7 day 1987/1994-present Selected New England sites of National Dry Deposition Network (NDDN)	Teflon/Nylon filter pack	Selected New England sites of National Dry Deposition Network (NDDN) (see also : Edgerton et al., 1992)
Woodstock., NH (43.5°N)	241±123∞ 256±80*	58-605∞ 162-398*			
Lye Brook, VT (43.0°N)	677±331∞ 733±218*	201-1409∞ 352-1124*			
Connecticut Hill, NY (42.4°N)	921±324∞ 1038±359*	297-1911∞ 612-1911*			
Catskills, NY (42.4°N)	975±412∞ 1165±232*	291-1665∞ 736-1615*			
Abington, CT (41.9°N)	842±430∞ 1232±440*	197-1822∞ 430-1822*			

∞ Annual for 1994.
* Summer for 1994.

reported in most other studies is to some degree a consequence of longer sample integration times, especially the weekly sampling of the National Dry Deposition Network (NDDN) [Edgerton et al., 1992]. Ollinger et al. [1993] noted that mean HNO_3 levels for the NDDN sites in the northeastern U.S. decreased linearly with increasing latitude. Interestingly, Harvard Forest at 42.5°N with a mean hourly mixing ratio of 828 pptv fits this trend (Table 2.4). The gradient of decreasing HNO_3 values to the north of this site concurs with the calculations of Munger et al. [1997], who concluded that much of the NO_x emitted in the northeastern U.S. is deposited as HNO_3 within a few days.

2.4.2.2 HNO_3 Diel Trends. HNO_3 mixing ratios are lower at night and higher during the day at Harvard Forest (Figure 2.3a) and at other sites as well [Edgerton et al., 1992; Parrish et al., 1986]. Previous attempts to define the diel cycle of HNO_3 have shown similar patterns, with the highest mixing levels occurring in the afternoon [Parrish et al, 1986; Aneja et al, 1994a, Kleinman et al., 1994]. The distinctly different HNO_3 diel patterns for the SW and NW windsectors emphasize the respective urban and rural source regions for these air mass categories (Figure 2.3b). Earlier studies at Harvard Forest [e.g. Munger et al., 1996] labeled the SW and NW surface wind direction sectors as "polluted" and "clean" based on significantly higher midday NO_x and NO_y mixing ratios for the SW sector. Using a trajectory model, Moody et al. [1997] quantitatively determined the same air masses source regions and described their divergent chemical climatologies. Instead of using a meteorological parameter, Kleinman et al. [1994] subdivided HNO_3 data from rural Georgia into groups based on O_3 mixing ratios and in the process produced two HNO_3 diel patterns of similar shape and magnitude to those in Figure 2.3b.

The notable rise in early morning HNO_3 mixing ratios (≈ 0500 EST) (Figures 2.3a and 2.3b) is coincident with average time of summer sunrise as well as large increases in the heat flux, friction velocity, NO_x and NO_y mixing ratios, and NO_y deposition rate [Munger et al., 1996]. Due to low photochemical activity at this time of day, it is likely that this increase in HNO_3 could result from the entrainment of HNO_3 in "fossil" mixed layer air from the previous day as the new mixed layer develops [Kleinman et al., 1994]. Large increases in early morning NO_y deposition velocities [Munger et al., 1996] endorse this theory by demonstrating high concentrations of a readily-depositing NO_y species (e.g. HNO_3) in these air masses. Trainer et al. [1991] predict that some of the HNO_3 mixed down as the nocturnal boundary layer erodes is produced at night via heterogeneous reactions involving N_2O_5.

Another way to examine the early morning HNO_3 increase is to compare the 29 m HNO_3 measurements to the simultaneous below canopy (11 m) measurements. The largest cross canopy HNO_3

gradients (Figure 2.7a) occur in the early morning (0500-0700). While it is not possible from this dataset to discern whether this is residual or nocturnally produced HNO_3, it is interesting to note that these air parcels containing higher HNO_3 mixing ratios are also enriched in aerosol NO_3^- (Figure 2.7b). While not direct evidence of heterogeneous HNO_3 production, this may be evidence of heterogeneous nighttime particulate NO_3^- production [Li et al., 1993].

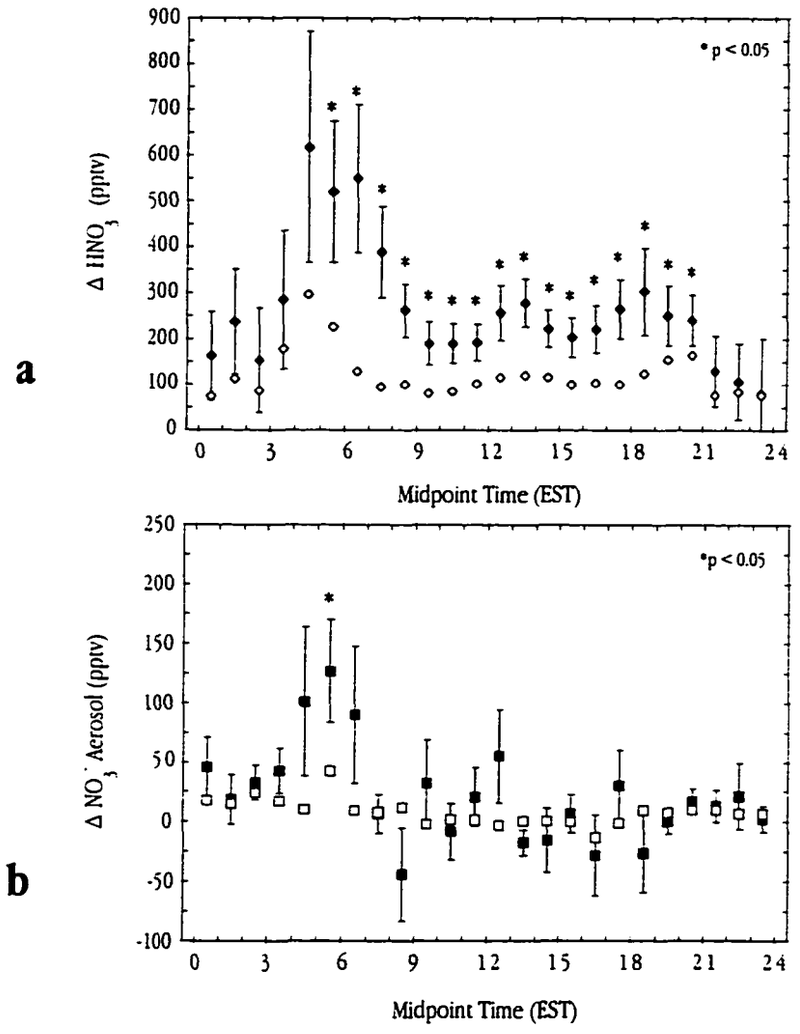

Figure 2.7. [a] Mean (filled symbol) and median (open symbol) diel cycle of difference between above canopy (29 m) and below canopy (11 m) HNO_3 mixing ratios. Canopy height is ≈ 22.5 m. Vertical bars correspond to standard error of mean. Number of samples averaged each hour same as in Figure 3a. [b] Same as Figure 7a, except for aerosol NO_3^- mixing ratios.

2.4.2.3 Seasonal differences in HNO_3. Munger et al. [1997] analyzed 7 years (1990-1996) of continuous hourly NO_Y flux measurements at this site and report the highest NO_Y deposition occurs during the months of May, July, and August and the lowest during December, January, and February. As the primary depositing species of NO_Y, the composite HNO_3 seasonal cycle (Figure 2.4), while lacking wintertime data, is consistent with these findings. Parrish et al. [1986] also report their maximum and minimum HNO_3 levels in late summer and winter, respectively. However, studies from other regions have observed significantly different HNO_3 seasonal cycles. In Cedar Creek, WY, the highest levels occur in the spring [Edgerton et al., 1992], while Bondville and Argonne, IL experience their peak HNO_3 concentrations in the winter [Meyers et al., 1991]. Seasonal differences in HNO_3 are believed to be a function of many interrelated physical and climatological factors which may also differ seasonally and geographically, including: homogeneous and heterogeneous production, dry deposition and wet removal, local biogenic isoprene emissions, boundary layer dynamics, and regional NO_x emission densities.

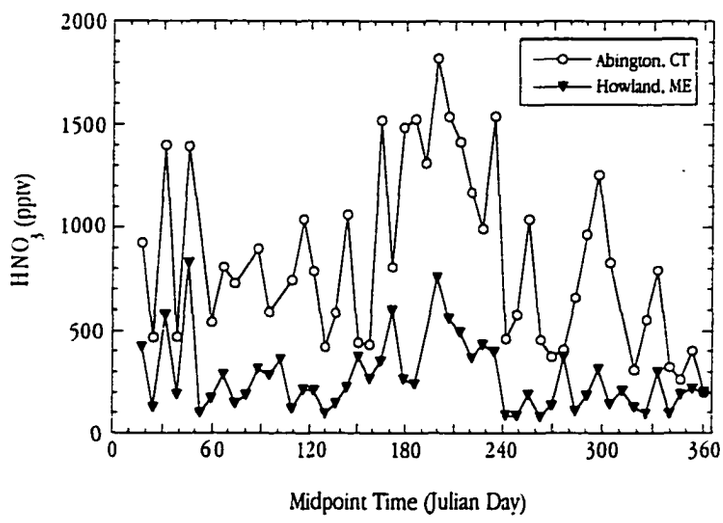

Figure 2.8. Weekly integrated HNO_3 mixing ratios for 1994 for two northeastern sites. Data is from National Dry Deposition Network (NDDN) sites in Abington, CT (ABT147) and Howland, ME (HOW132) [National Dry Deposition Network, 1996].

While the weekly NDDN samples will probably not be useful to determine the importance of some of these factors such as nighttime heterogeneous HNO_3 production, it is a good dataset to examine seasonal HNO_3 levels across the eastern U.S.. The 1994 data from two northeastern U.S. NDDN sites (Howland, ME and Abington, NY) were selected to highlight the two extremes in the regional HNO_3 latitudinal gradient. In 1994,

both of these sites report the highest sustained HNO_3 levels in July and August (≈ Days 180-240) (Figure 2.8) and lower mixing ratios in the winter, which is consistent with the HNO_3 and NO_Y deposition results at Harvard Forest [this study; Munger et al., 1997]. Peak July and August HNO_3 mixing ratios at Harvard Forest and other northeastern U.S. sites may be explained by additional HNO_3 production via organic nitrate pathways [Munger et al., 1997]. The coherence of the HNO_3 signals from these two sites, for both the long and short-term (episodic) events, suggests that similar factors control the HNO_3 levels throughout the northeastern U.S.. The regional HNO_3 concentration gradient reported by Ollinger et al. [1993] is also evident in these two records and most likely represents the deposition of HNO_3 as a large portion of the emitted NO_X is oxidized to HNO_3 and deposited within the region [Munger et al., 1997].

2.4.3 NH_3

2.4.3.1 Comparison to previous NH_3 measurements. The mean NH_3 mixing ratio of 321 pptv is equivalent to the 300 pptv and 420 pptv summertime mean observed for other forested sites in Oak Ridge, TN and Niwot Ridge, CO [Langford et al., 1992]. At Harvard Forest, ten years previous to this study, Tjepkema et al. [1981] observed summertime NH_3 mixing ratios in the range of 200-330 pptv using 7-day oxalic acid denuder measurements. The greater variability displayed in our hourly measurements is due to the damping of high frequency structure by the weekly integrated samples.

Our composite NH_3 diel cycle does not display the trend of higher daytime mixing ratios peaking in the afternoon and then gradually declining throughout the night observed at several other sites [Langford et al., 1992]. Some of the individual days that went into this composite do, however, demonstrate such a pattern, including day 165 of 1995 as shown in Figure 2.2b. Interestingly, some days with a flat NH_3 diel cycle display a more "typical" NH_X (NH_3 + NH_4^+) diel signal (Figure 2.9a).

Our composite of summer NH_3 levels generally fits in with the complete year of NH_3 concentrations measured by Tjepkema et al. [1981] at Harvard Forest in 1980. They found the highest NH_3 levels to occur in the summer, peaking in early August and decreasing rapidly to fall and winter lows of less than 50 pptv. As suggested by the "typical" seasonal and diel cycles of NH_3, boundary layer NH_3 levels are a general function of air temperature, with higher NH_3 mixing ratios associated with warmer temperatures [Langford et al., 1992]. Our observations of small, or no, diel variation of NH_3 mixing ratios on many days suggests that other factors also play a significant role in regulating NH_3 levels at the Harvard Forest.

2.4.3.2 Controls on boundary layer NH_3 levels. It is clear that air temperature is a primary controller of NH_3 in the boundary layer, as several other sites show a strong temperature dependence of NH_3

mixing ratios [Langford et al., 1992]. Higher air temperatures lead to greater emissions of NH_3 from its primary sources, cattle feedlots and fertilizer applications. Higher air temperatures also increase the vapor pressure of NH_3 over ammonium sulfate aerosols, thereby slowing the rate at which they are formed. As ambient NH_3 mixing ratios above vegetated systems approach the NH_3 compensation point, higher air temperatures increase the vapor pressure of NH_3 above the NH_4^+ dissolved in the water film lining stomatal cavities, increasing the NH_3 emitted by the canopy as predicted by Henry's Law [Langford and Fehsenfeld, 1992]. At Harvard Forest, due to the lack of nearby sources and high levels of SO_4^{2-} in the atmosphere, the ambient mixing ratios of NH_3 are more or less always below the NH_3 compensation point reported by Farquhar et al. [1980], suggesting that the canopy (or ecosystem) at Harvard Forest is continually losing NH_3 to the atmosphere. Similarly, based on the low nature of the few NH_3 mixing ratios reported for eastern forests, Langford et al. [1992] predicted these ecosystems would emit significant levels of NH_3.

For the months of May and June of 1995, the exponential relationship between averaged NH_3 mixing ratios and temperature (r^2=0.85) may perhaps define the NH_3 compensation point for this ecosystem. If so, this particular NH_3 compensation point is lower than that previously observed by Farquhar et al. [1980] for snap beans and confirmed by Langford and Fehsenfeld [1992] for a lodgepole-ponderosa pine/ spruce-fir forest. The Farquhar et al. [1980] NH_3 compensation point is plotted as a function of air temperature for comparison (Figure 2.5). Another fundamental determinant of NH_3 levels at most sites is their proximity to NH_3 sources. With mean and median mixing ratios between 200-350 for all wind sectors, this suggests that there are few significant sources of NH_3 near Harvard Forest. While mean NH_3 levels from the "clean" NW sector are significantly greater than those from the "polluted" SW sector, total NH_x levels, and therefore total NH_3 emissions, are greater in the SW wind sector. Thus significant levels of NH_3 are emitted from the SW sector, however a large fraction of the NH_3 is soon converted to $NH_4^+{}_{(p)}$, resulting in low ambient NH_3 mixing ratios.

As described earlier in section 2.3, NH_3 can rapidly react with H_2SO_4 to produce ammonium (bi)sulfate aerosols. In an acidic atmospheric environment dominated by SO_4^{2-}, Tang [1980] predicted that a primary control on the gaseous/particulate partitioning of ammonia is the level of atmospheric SO_4^{2-}. This control is clearly demonstrated by comparing two consecutive days (JD 159-160) in 1995. On day 159 (1995), north winds brought high levels of NH_x (3-5 ppbv) and high SO_4^{2-} levels (≈ 1-2 ppbv) to Harvard Forest (Figure 2.9a) and NH_3 accounts for 9-25% of NH_x. On day 160, easterly winds advected moderate levels of NH_x (≈ 500-800 pptv) and very little aerosol SO_4^{2-} (<500 pptv) resulting in the opposite situation with the majority of the NH_x (67-91%) present as NH_3 instead of aerosol NH_4^+ (Figure 2.9a).

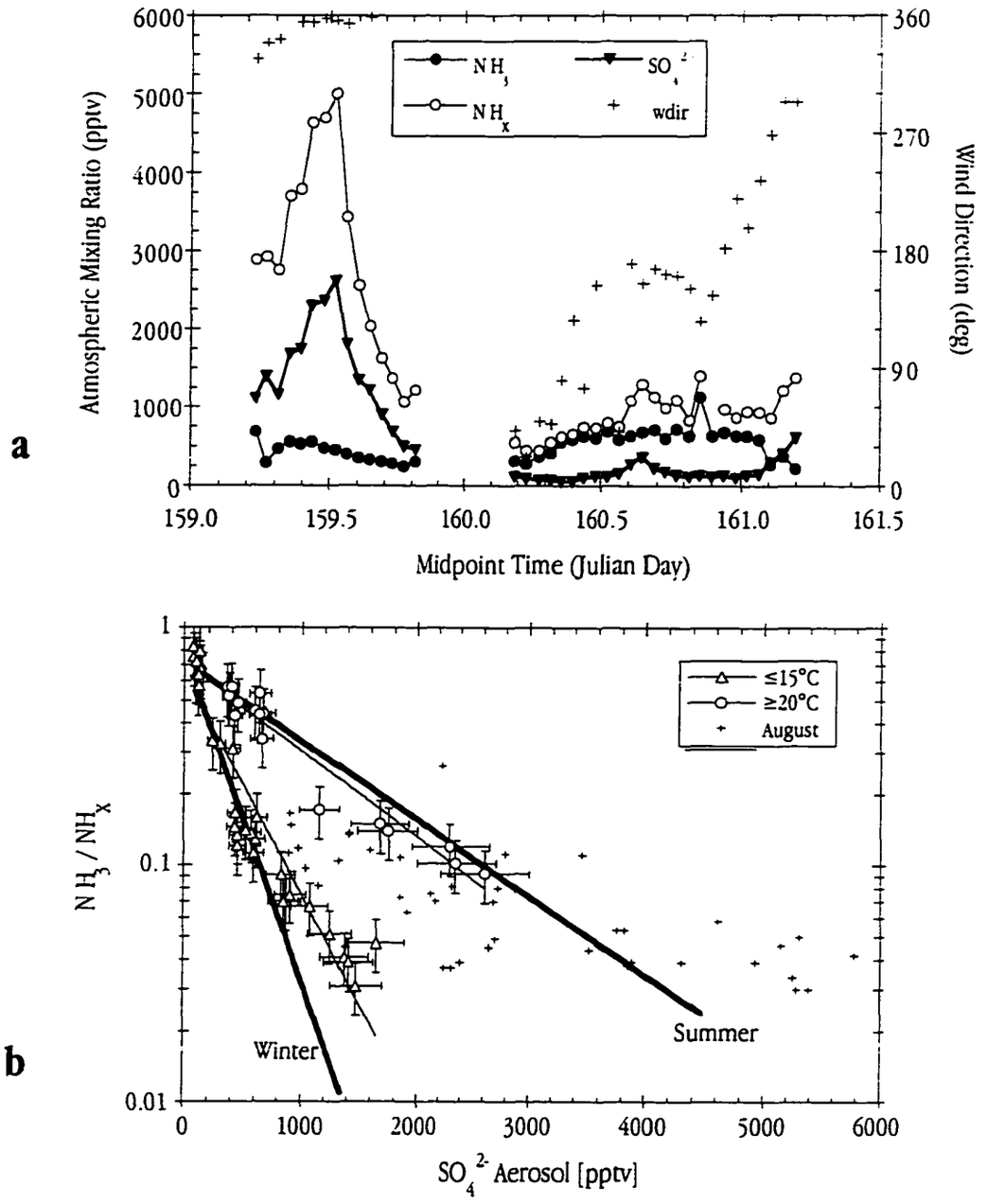

Figure 2.9. [a] Dependence of gaseous/particulate partitioning of ammonia on atmospheric sulfate. Wind direction and hourly NH_3 and NH_x and aerosol SO_4^{2-} mixing ratios for June 8 and 9, 1995 (JD 159 and 160). Measurement uncertainty not shown. [b] Dependence of NH_3/NH_x partitioning on atmospheric sulfate and air temperature. Open symbols represent samples collected in May and June, 1995 at two different temperature ranges (≤15°C (triangles) and ≥20°C (circles)). Vertical bars show the uncertainty of the partition ratio as determined by propagation of errors. Horizontal bars represent SO_4^{2-} measurement uncertainty. Plus symbol corresponds to August 1995 samples. Error bars for these samples are not shown to keep figure legible. Thick lines represent relationships reported by Langford et al. [1992] from compilation of winter and summer results.

Average aerosol SO_4^{2-} mixing ratios for the "polluted" SW sector are 2.3 times higher than the NW sector, resulting in significantly different ($p < 0.001$) mean (± std. deviation) NH_3/NH_x ratios of 0.39 (±0.22) and 0.23 (±0.22) for the NW and SW wind sectors, respectively. Langford et al. [1992] collected available data from various studies which simultaneously determined NH_3, NH_4^+, and SO_4^{2-} mixing ratios. Breaking up the data into wintertime and summertime measurements, they observed negative exponential relationships between the fraction of NH_x as NH_3 and total atmospheric sulfate. The steeper slope of the wintertime data was attributed to decreased wintertime NH_3 emissions and the lower equilibrium vapor pressure of NH_3 over ammonium sulfate aerosols at colder temperatures.

Separating our May and June 1995 NH_3 data into two groups based on the air temperature, ≤15°C and ≥20 °C, we observed exponential relationships describing the partitioning of NH_3 and NH_4^+ as a function of $SO_4^{2-}{}_{[p]}$ (Figure 2.9b). The squared correlation coefficients are 0.91 and 0.93 for the ≤15°C and ≥20°C groups, respectively. These relationships are quite similar to those reported by Langford et al. [1992], which, for comparison, have been included in Figure 2.9b (thicker lines). Not included in this analysis, but also shown in Figure 2.9b, are NH_3 data from August 1995. All the data collected during August represent sampling periods in which the air temperature was 19°C or greater. With the exception of the samples with quite high SO_4^{2-} mixing ratios (> 3500 pptv), most of the remaining August samples fall somewhere between the ≤15°C and ≥20 °C ammonia-to-sulfate relationships described above. August 1995 is same period for which the relationship between NH_3 and temperature shown in Figure 2.5 does not apply.

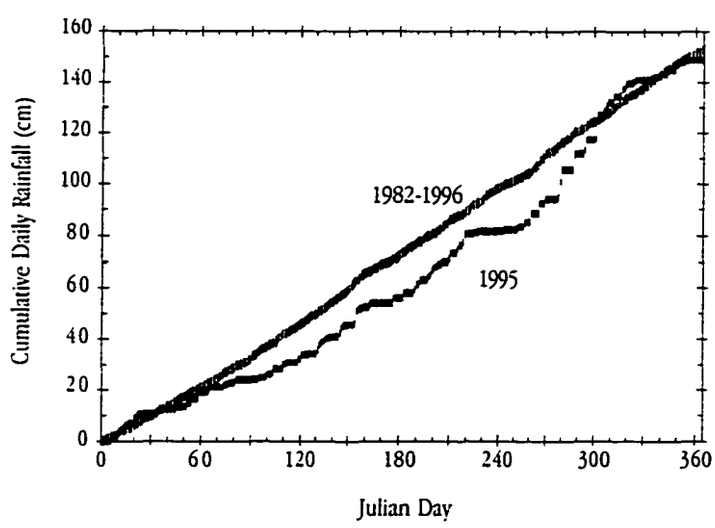

Figure 2.10. Cumulative daily rainfall at the Quabbin Reservoir NADP site for 1995 and 14 year average for years 1982-1996 [NADP/NTN, 1997].

In addition to being a warmer time period (Figure 2.5), the August samples also contained on average significantly more SO_4^{2-} and less NH_3 relative to NH_4^+ (Figure 2.9b). However, the majority of the August samples were collected within temperature and SO_4^{2-} ranges observed during summer and still contained less NH_3 (Figures 2.5 and 2.9b). Langford and Fehsenfeld [1980] also observed a deviation from the predicted compensation point at higher temperatures and speculated that lower NH_3 emissions were related to water stress. At Harvard Forest, 1995 was drier than average with a period of drought occurring from early August through mid-September as shown by cumulative daily rainfall (Figure 2.10). These data further suggest that for vegetation experiencing water (or other physiological) stress, which encourages reduced stomate apertures, the exchange of NH_3 is also restricted, effectively suppressing a plant's NH_3 compensation point.

2.4.4 NO_Y and HNO_3

The NO_Y diel cycle at Harvard Forest, with lower mixing ratios at midday and higher levels at night, has been attributed to changes in the height of the boundary layer and the vertical distribution of NO_Y [Munger et al., 1996]. At night, NO_X emissions accumulate below the stable nocturnal boundary layer. As the mixed layer grows the next morning, boundary layer NO_Y concentrations are diluted by the entrainment of air lower in NO_Y from aloft. For the UNH sampling periods this process resulted in median midday and midnight NO_Y mixing ratios of ≈ 3000 and 4000 pptv, respectively (Figure 2.6). The range of NO_Y values and diel trend are similar to those observed at other flatland rural sites in North America [Parrish et al., 1993].

Four of the individual components of NO_Y (NO, NO_2, HNO_3, $NO_{3(p)}^-$) were simultaneously measured at Harvard Forest. NO and NO_2 rapidly interconvert between each other as function of sun intensity, oxidant concentrations (O_3 and peroxy radicals), and temperature (Parrish et al., 1990). Thus, when considering a composite dataset collected under a variety of conditions, it is more meaningful to look at NO_X, the sum of NO and NO_2. NO_X is, at all times, the largest fraction of NO_Y at Harvard Forest (Figure 2.11)

At night NO_X accounts for more than 60% of NO_Y while no other measured species contributes more than a 10% share of NO_Y (Figure 2.11). Nitric acid is the next most abundant measured NO_Y species with a midday maxima of 20% of NO_Y occurring at the same time as the NO_X minima, indicative of the photochemical oxidation of NO_2 to HNO_3. At night, all the NO in the surface layer is titrated to NO_2 by reaction with O_3 and other oxidants. As the sun rises, NO_2 photolysis begins and the NO contribution increases from essentially zero to a high of about 10% of NO_Y around 0800 EST (Figure 2.11). Aerosol NO_3^- is a minor fraction of NO_Y at this site accounting for 3-7% of NO_Y at any time of the day.

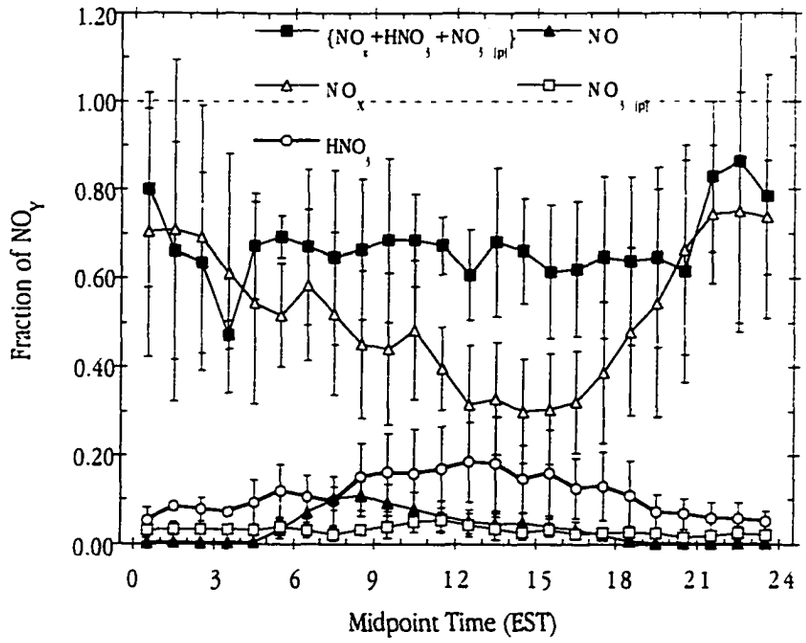

Figure 2.11 Median partitioning ratio of individual and sum of measured NO_Y species as a function of time of day. Vertical bars represent median absolute deviation (MAD). Sample numbers for this composite diel are the same as HNO_3 diel in Figure 2.3a.

The sum of these four NO_Y species accounted for 60-80% of NO_Y, with the median of the unmeasured residual remaining fairly constant (≈ 1500-2500 pptv) throughout the day (Figure 2.11). In air masses with winds from the urban SW windsector, the mean (± std. deviation) "unmeasured" NO_Y fraction was 23% (±14%) of NO_Y. The NW and E windsectors brought even higher levels of these "unmeasured" NO_Y compounds, with both sectors having, on average (± std. deviation), 60% ± 20% of NO_Y contributed by the sum of $NO_X + HNO_3 + NO_{3\,[p]}^-$.

Typically, NO_X, HNO_3, and PAN are the major reactive nitrogen species at most sites [Parrish et al., 1993]. Recent studies suggest that various other organic nitrates may also be an important component of NO_Y at forested sites [Trainer et al., 1991]. The majority of the "unmeasured" NO_Y at Harvard Forest is most likely PAN and other organic nitrates. In contrast to HNO_3, PAN is only a temporary NO_Y reservoir since it thermally decomposes back to NO_X. For a site in Scotia, PA, situated in an oak forest, mid-day summertime PAN mixing ratios can get as high as 2000 pptv and can account for as much as 30-40% of NO_Y [Trainer et al., 1991]. Oak forests like Harvard Forest emit large amounts of isoprene in the summer months [Goldstein et al., 1997]. Since the oxidation products of isoprene are thought to be important precursors of PAN [Trainer et al., 1991], one would expect significant PAN levels at Harvard Forest. Since it quickly degrades at summertime surface

temperatures. PAN tends to have a diel cycle similar to HNO_3. The diel cycle of the NO_Y residual does appear to decrease in the evening (2200-0100) as expected (Figure 2.11). However, the larger variability in the nighttime values due to the lower sampling coverage make this a non-significant difference.

The quantity $\{NO_Y\text{-}NO_X\}$ describes the sum of HNO_3, PAN, and other oxidized reactive N species. The linear relationship between HNO_3 and $\{NO_Y\text{-}NO_X\}$ (slope = 0.55, $r^2 = 0.86$) indicates that HNO_3 is typically about half of the oxidized NO_Y in air masses arriving from the SW windsector (Figure 2.12). While more variable, on average about 25% of $\{NO_Y\text{-}NO_X\}$ is HNO_3 in the NW and E surface wind sectors. Trainer et al. [1991] modeled the photochemical production of organic nitrates, such as butyl and isoprene nitrates, and predicted that these reactive N compounds may contribute as much as 1000 pptv to NO_Y at night and 3000 pptv or more to NO_Y mid-day. These high levels appear possible in light of the unusual results observed for several early evening hours between April 27 and 30, 1993. During these hours an air mass with easterly surface winds contained less than 1 ppbv of HNO_3, 4-5 ppbv of NO_X, and more than 8 ppbv of "unidentified" oxidized NO_Y, presumably PAN and other organic nitrates (Figure 2.12).

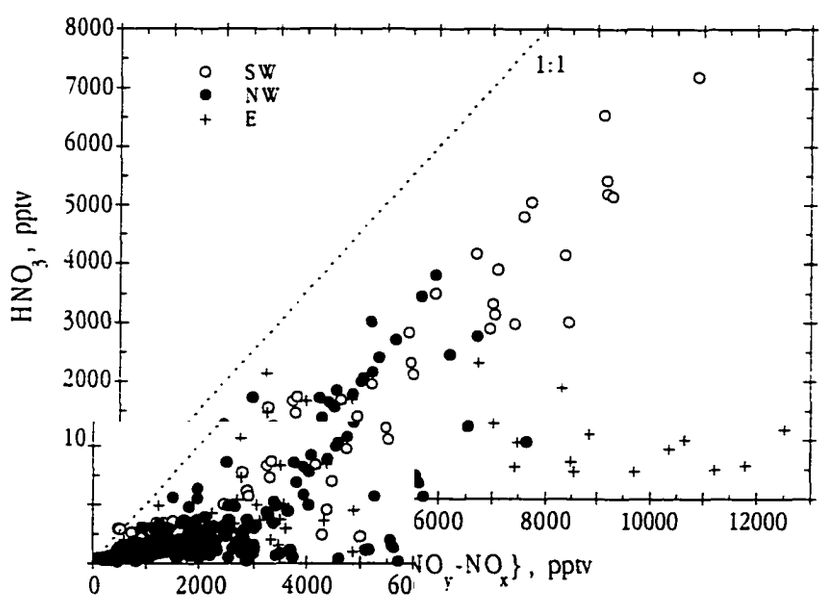

Figure 2.12. Relationship between HNO_3 and oxidized fraction of NO_Y, defined as $\{NO_Y\text{-}NO_X\}$, for the three surface wind sectors: 180°-270° is southwest (SW); 270°-45° is northwest (NW); 45°-180° is east (E). Error bars not shown.

2.5 Conclusions

Mean summertime HNO_3 mixing ratios at Harvard Forest agree well with results from other rural sites and fit in with the latitudinal HNO_3 gradient for the northeastern U.S.. This site receives air masses from both urban and rural source regions resulting in mean and median HNO_3 levels four times higher when surface winds were from the SW as opposed to the NW windsector. High early morning HNO_3 and aerosol NO_3^- mixing ratios and cross canopy gradients provide evidence of the entrainment of these species from aloft into the newly developing mixed layer. This behavior is consistent with theories of nocturnal heterogeneous HNO_3 and aerosol NO_3^- production in the "fossil" mixed layer.

The importance of acidic SO_4^{2-} aerosols in regulating the gaseous NH_3 levels at Harvard Forest is demonstrated by the low NH_3 mixing ratios and the exponential relationships between the NH_3/NH_x partitioning ratio and aerosol SO_4^{2-} concentrations. In the sulfate rich atmosphere above Harvard Forest, NH_3 mixing ratios appear to be suppressed below the NH_3 compensation point, suggesting that this N limited ecosystem is routinely losing N to the atmosphere though canopy NH_3 emissions. Air temperature is another factor controlling the NH_3 levels at this site. However it is difficult to apportion the controls on NH_3 between the temperature response of the NH_3 compensation point and the temperature sensitivity of NH_3/H_2SO_4 production. The temperature response of these two controls have similar results with warmer temperatures resulting in both greater NH_3 canopy emissions and a larger NH_3/NH_x ratios for a given SO_4^{2-} concentration. It appears that other factors, such as water stress, may also limit NH_3 mixing ratios at this site, as occurred in August 1995 when the air temperature relationship for NH_3 breaks down.

On average HNO_3 makes up about 20% of NO_Y at midday. PAN and perhaps other organic nitrates are believed to make up a significant fraction of NO_Y at Harvard Forest since the sum of the measured NO_Y species (NO, NO_2, HNO_3, and NO_3^-) typically account for between 60-80% of the summertime NO_Y over the course of a day. HNO_3 makes up about half of the oxidized NO_Y in polluted SW winds. However, unmeasured oxidized NO_Y species comprise ≈ 75% of the $\{NO_Y\text{-}NO_X\}$ in surface winds from the NW and E sectors, suggesting significant production of organic nitrates in these air masses.

2.6 Acknowledgments

This research was funded by the US Department of Energy's (DOE) National Institute for Global Environmental Change (NIGEC) through the NIGEC Northeast Regional Center at Harvard University (DOE Cooperative Agreement DE-FC03-90ER61010). Financial support does not constitute an endorsement by the DOE of the views expressed in this article/report. The work at the University of New Hampshire (UNH) is sported by subcontract 901214-HAR#4 from Harvard University, under the Northeast Regional Center of NIGEC, to the Research Foundation of UNH. The excellent technical assistance of Eric Scheuer and comments by Jack Dibb are gratefully acknowledged. The UNH gas and aerosol dataset for Harvard Forest is available via anonymous ftp at io.harvard.edu in the directory pub/nigec/UNH and the Web site www-as.harvard.edu.

2.7 References

Aneja, V.P., C.S. Clairborn, Z. Li, and A. Murthy, Trends, seasonal variations, and analysis of high-elevation surface nitric acid, ozone, and hydrogen peroxide, *Atmospheric Environment*, *28* (10), 1781-1790, 1994a.

Aneja, V.P., M. Das, D.-S. Kim, and B.E. Hartsell, Measurements and analysis of photochemical oxidants and trace gases in the rural troposphere of the southeast United States, *Israel Journal of Chemistry*, *34*, 387-401, 1994b.

Appel, B.R., and Y. Tokiwa, Atmospheric particulate nitrate sampling errors due to reactions with particulate and gaseous strong acids, *Atmospheric Environment*, *15*, 1087-1089, 1981.

Appel, B.R., Y. Tokiwa, and M. Haik, Sampling of nitrates in ambient air, *Atmospheric Environment*, *15*, 283-289, 1981.

Appel, B.R., S.M. Wall, Y. Tokiwa, and M. Haik, Simultaneous nitric acid, particulate nitrate and acidity measurements in ambient air, *Atmospheric Environment*, *14*, 549-554, 1980.

Appel, B.R., Y. Tokiwa, E.L. Kothny, R. Wu, and V. Povard, Evaluation of procedures for measuring atmospheric nitric acid and ammonia, *Atmospheric Environment*, *22* (8), 1565-1573, 1988.

Buhr, S.M., M.P. Buhr, F.C. Fehsenfeld, J.S. Holloway, U. Karst, R.B. Norton, D.D. Parrish, and R.E. Sievers, Development of a semi-continuous method for the measurement of nitric acid vapor and particulate nitrate and sulfate, *Atmospheric Environment*, *29* (19), 2609-2624, 1995.

Cadle, S.H., R.J. Countess, and N.A. Kelly, Nitric acid and ammonia in urban and rural locations, *Atmospheric Environment*, *16* (10), 2501-2506, 1982.

Cofer III, W.R., V.G. Collins, and R.W. Talbot, Improved aqueous scrubber for collection of soluble atmospheric trace gases, *Environmental Science & Technology*, *19* (6), 557-560, 1985.

Crosley, D.R., Issues in the measurement of reactive nitrogen compounds in the atmosphere, Report # MP-94-035, SRI International, Menlo Park, March 1994.

Davies, C.N., The entry of aerosols into sampling tubes and heads, *British Journal of Applied Physics*, ser.2,*1*, 921-392, 1968.

Davies, C.N., and M. Subari, Aspiration above wind velocity of aerosols with thin-walled nozzles facing at right angles to the wind direction, *Journal of Aerosol Science*, *13* (1), 59-71, 1982.

Denmead, O.T., J.R. Freney, and J.R. Simpson, A closed ammonia cycle within a plant canopy, *Soil Biol. Biochem.*, *8*, 161-164, 1976.

Dentener, F.J., and P.J. Crutzen, Reaction of N_2O_5 on tropospheric aerosols: Impact on the global distributions of NO_x, O_3 and OH, *Journal of Geophysical Research*, *98*, 7149-7163, 1993.

Edgerton, E.S., T.F. Lavery, and R.P. Boksleitner, Preliminary data from the USEPA dry deposition network: 1989, *Environmental Pollution*, *75*, 145-156, 1992.

Farquhar, G.D., P.M. Firth, R. Weselaar, and B. Weir, On the gaseous exchange of ammonia between leaves and the environment: determination of the ammonia compensation point, *Plant Physiology*, *66*, 710-714, 1980.

Forrest, J., D.J. Spandau, R.L. Tanner, and L. Newman, Determination of atmospheric nitrate and nitric acid employing a diffusion denuder with a filter pack, *Atmospheric Environment*, *16* (6), 1473-1485, 1982.

Georgopoulos, G.P., and J.H. Seinfeld, Statistical distribution of air pollutant concentrations, *Environmental Science & Technology*, *15* (7), 401A-416A, 1982.

Goldstein, A.H., C.M. Spivakovsky, and S.C. Wofsy, Seasonal variations of nonmethane hydrocarbons in rural New England: Constraints on OH concentrations in northern latitudes, *Journal of Geophysical Research*, *100*, 21,023-21,033, 1995.

Goldstein, A.H., M.L. Goulden, J.W. Munger, S.C. Wofsy, and C.D. Geron, Season course of isoprene emissions from a midlatitude deciduous forest, *Journal of Geophysical Research*, *in press*, 1997.

Goulden, M.L., J.W. Munger, S.-M. Fan, B.C. Daube, and S.C. Wofsy, Exchange of carbon dioxide by a deciduous forest: response to interannual climate variability, *Science*, *271*, 1576-1578, 1996.

Gschwandtner, G., K. Gschwandtner, K. Eldridge, C. Mann, and D. Mobley, Historic emissions of sulfur and nitrogen oxides in the United States from 1900 to 1980, *Journal of the Air Pollution Control Association*, *36*, 139-149, 1986.

Hidy, G.M., Spatial and temporal distribution of airborne sulfate in parts of the U.S., *Atmospheric Environment*, *12*, 735-752, 1978.

Keene, W.C., R.W. Talbot, M.O. Andreae, K. Beecher, H. Berresheim, M. Castro, J.C. Farmer, J.N. Galloway, M.R. Hoffmann, S.-M. Li, J.R. Maben, J.W. Munger, R.B. Norton, A.A.P. Pszenny, H. Puxbaum, H. Westberg, and W. Winiwarter, An intercomparison of measurement systems for vapor and particulate phase concentrations of formic and acetic acids, *Journal of Geophysical Research*, *94* (D5), 6457-6472, 1989.

Kelly, T.J., R.L. Tanner, L. Newman, P.J. Galvin, and J.A. Kadlecek, Trace gas and aerosol measurements at a remote site in the northeast U.S., *Atmospheric Environment*, *18* (12), 2565-2576, 1984.

Kleinman, L., Y.-N. Lee, S.R. Springston, L. Nunnermacker, X. Zhou, R. Brown, K. Hallock, P. Klotz, D. Leahy, J.H. Lee, and L. Newman, Ozone formation at a rural site in the southeastern United States, *Journal of Geophysical Research*, *99* (D2), 3469-3482, 1994.

Knoll, G.F., *Radiation detection and measurement*, 816 pp., John Wiley & Sons, New York, 1979.

Langford, A.O., and F.C. Fehsenfeld, Natural Vegetation as a Source or Sink for Atmospheric Ammonia - A Case Study, *Science*, *255* (5044), 581-583, 1992.

Langford, A.O., F.C. Fehsenfeld, J. Zachariassen, and D.S. Schimel, Gaseous ammonia fluxes and background concentrations in terrestrial ecosystems of the United States, *Global Biogeochemical Cycles*, *6* (4), 459-483, 1992.

Lefer, B.L., R.W. Talbot, R.C. Harriss, J.D. Bradshaw, S.T. Sandholm, J.O. Olson, G.W. Sachse, J. Collins, M.A. Shipham, D.R. Blake, K.I. Klemm, K. Gorzelska, and J. Barrick, Enhancement of acidic gases in biomass-burning impacted air masses over Canada, *Journal of Geophysical Research*, *99* (D1), 1721-1738, 1994.

Lefer, B.L., and R.W. Talbot, Aerosol nitrate and ammonium at a northeastern U.S. site, *Atmospheric Environment*, *submitted December*, 1997.

Lefer. B.L., R. W. Talbot, and J. W. Munger, Deposition of nitric acid vapor to a mid-latitude forest. *Atmospheric Environment, submitted December*, 1997.

Lewin, E.E., R.G. DePena, and J.P. Shimshock, Atmospheric gas and particle measurements at a rural northeastern U. S. site, *Atmospheric Environment, 20* (1), 59-70, 1986.

Li, S.-M., K.G. Anlauf, and H.A. Wiebe, Heterogeneous nighttime production and deposition of particle nitrate at a rural site in North America during summer 1988, *Journal of Geophysical Research, 98* (D3), 5139-5157, 1993.

Logan, J.A., Nitrogen oxides in the troposphere: global and regional budgets, *Journal of Geophysical Research, 88* (C15), 10,785-10,807, 1983.

Meyers, T.P., B.J. Huebert, and B.B. Hicks, HNO_3 deposition to a deciduous forest, *Boundary-Layer Meteorology, 49*, 395-410, 1989.

Meyers, T.P., B.B. Hicks, R.P.J. Hosker, J.D. Womack, and L.C. Satterfield, Dry deposition inferential measurement techniques--II. Seasonal and annual deposition rates of sulfur and nitrate, *Atmospheric Environment, 25A* (10), 2361-2370, 1991.

Moody, J.L., J.W. Munger, A.H. Goldstein, D.J. Jacob, and S.C. Wofsy, Harvard Forest regional-scale air mass composition by PATH (Patterns in atmospheric transport history), *Journal of Geophysical Research, submitted*, 1997.

Moore, K.W., D.R. Fitzjarrald, R.K. Sakai, M.L. Goulden, J.W. Munger, and S.C. Wofsy, Seasonal variation in radiative and turbulent exchange at a deciduous forest in central Massachusetts, *Journal of Applied Meteorology, 35*, 122-134, 1996.

Munger, J.W., S.C. Wofsy, P.S. Bakwin, S.-M. Fan, M.L. Goulden, B.C. Daube, and A.H. Goldstein, Atmospheric deposition of reactive nitrogen oxides and ozone in a temperate deciduous forest and a subarctic woodland: 1. Measurements and mechanisms, *Journal of Geophysical Research, 101* (D7), 12,639-12,657, 1996.

Munger, J.W., S.-M. Fan, P.S. Bakwin, M.L. Goulden, A.H. Goldstein, A.S. Colman, and S.C. Wofsy, Regional budgets for nitrogen oxides from continental sources: variations of rates for oxidation and deposition with season and distance from source regions, *Journal of Geophysical Research, in press*, 1997.

NADP/NTN, National Atmospheric Deposition Program (NRSP-3)/National Trends Network, NADP/NTN Coordination Office, Natural Resource Ecology Laboratory, Colorado State University, Fort Collins, Colorado, 80523, February 17, 1997.

Ollinger, S.V., J.D. Aber, G.M. Lovett, S.E. Millham, R.G. Lathrop, and J.M. Ellis, A spatial model of atmospheric deposition for the northeastern U.S., *Ecological Applications, 3* (3), 459-472, 1993.

Parrish, D.D., M.P. Buhr, M. Trainer, R.B. Norton, J.P. Shimshock, C. Fehsenfeld, K.G. Anlauf, J.W. Bottenheim, Y.Z. Tang, H.A. Wiebe, J.M. Roberts, R.L. Tanner, L. Newman, V.C. Bowersox, K.J. Olszyna, E.M. Bailey, M.O. Rodgers, T. Wang, H. Berresheim, U.K. Roychowdhury, and K.L. Demerjian, The total reactive oxidized nitrogen levels and the partitioning between the individual species at six rural sites in eastern North America, *Journal of Geophysical Research, 98* (D2), 2927-2939, 1993.

Parrish, D.D., M. Trainer, M.P. Buhr, B.A. Watkins, and F.C. Fehsenfeld, Carbon monoxide concentrations and their relation to concentrations of total reactive oxidized nitrogen at two rural U.S. sites, *Journal of Geophysical Research*, *96* (D5), 9309-9320, 1991.

Parrish, D.D., R.B. Norton, M.J. Bollinger, S.C. Liu, P.C. Murphy, D.L. Albritton, F.C. Fehsenfeld, and B.J. Huebert, Measurements of HNO_3 and NO_3^- particulates at a rural site in the Colorado mountains, *Journal of Geophysical Research*, *91* (D5), 5379-5393, 1986.

Peake, E., M.A. MacLean, and H.S. Sandhu, Total inorganic nitrate (particulate nitrate and nitric acid) observations in Calgary, Alberta, *Journal of the Air Pollution Control Association*, *35* (3), 250-253, 1985.

Peterson, B.J., and J.M. Melillo, The potential storage of carbon caused by eutrophication of the biosphere, *Tellus*, *37B*, 117-127, 1985.

Savoie, D.L., and J.M. Prospero, Particle size distribution of nitrate and sulfate in the marine atmosphere, *Geophysical Research Letters*, *9* (10), 1207-1210, 1982.

Schell, R.W., A historical perspective of atmospheric chemicals deposited on a mountain top peat bog in Pennsylvania, *International Journal of Goal Geology*, *8*, 147-173, 1987.

Schlesinger, W.H., and A.E. Hartley, A global budget for atmospheric NH_3, *Biogeochemistry*, *15*, 191-211, 1992.

Schindler, D.W., and S.E. Bayley, The biosphere as an increasing sink for atmospheric carbon: estimates from increased nitrogen deposition, *Global Biogeochemical Cycles*, *7* (4), 717-734, 1993.

Spicer, C.W., J.E. Howes, T.A. Bishop, L.H. Arnold, and R.K. Stevens, Nitric acid measurement methods: an intercomparison, *Atmospheric Environment*, *16*, 1487-1500, 1982.

Stecher III, H.A., G.W. Luther III, D.L. MacTaggart, S.O. Farwell, D.R. Crosley, W.D. Dorko, P.D. Goldan, N. Beltz, U. Krischke, W.T. Luke, D.C. Thornton, R.W. Talbot, B.L. Lefer, E.M. Scheuer, R.L. Benner, J. Wu, E.S. Saltzman, M.S. Gallagher, and R.J. Ferek, Results of the Gas-Phase Sulfur Intercomparison Experiment (GASIE): Overview of experimental setup, results and general conclusions, *Journal of Geophysical Research*, *102* (D13), 16,219-16,236, 1997.

Stelson, A.W., and J.H. Seinfeld, Relative humidity and pH dependence of the vapor pressure of ammonium nitrate-nitric acid solutions, *Atmospheric Environment*, *16*, 993-1000, 1982.

Talbot, R.W., A.S. Vijgen, and R.C. Harriss, Measuring tropospheric HNO_3: problems and prospects for nylon filter and mist chamber, *Journal of Geophysical Research*, *95* (D6), 7553-7542, 1990.

Talbot, R.W., A.S. Vijgen, and R.C. Harriss, Soluble species in the Arctic summer troposphere: acidic gases, aerosols, and precipitation, *Journal of Geophysical Research* (D15), 16,531-16,545, 1992.

Talbot, R.W., J.E. Dibb, B.L. Lefer, E.M. Scheuer, J.D. Bradshaw, S.T. Sandholm, S. Smyth, D.R. Blake, N.J. Blake, G.W. Sachse, J.E. Collins, and G.L. Gregory, Large-scale distributions of tropospheric nitric, formic, and acetic acids over the western Pacific basin during wintertime, *Journal of Geophysical Research*, *In press*, 1997.

Tang, I.N., On the equilibrium partial pressures of nitric acid and ammonia in the atmosphere, *Atmospheric Environment*, *14*, 819-828, 1980.

Tjepkema, J.D., R.C. Cartica, and H.F. Hemond, Atmospheric concentration of ammonia in Massachusetts and deposition on vegetation, *Nature*, *249*, 445-446, 1981.

Trainer, M., M.P. Buhr, C.M. Curran, F.C. Fehsenfeld, E.Y. Hsie, S.C. Liu, R.B. Norton, D.D. Parrish, E.J. Williams. B.W. Gandrud, B.A. Ridley, J.D. Shetter, E.J. Allwine, and H.H. Westberg, Observations and modeling of the reactive nitrogen photochemistry at a rural site, *Journal of Geophysical Research*, *96* (D2). 3045-3063, 1991.

Williams, E.J., S.T. Sandholm, J.D. Bradshaw, J.S. Schendel, A.O. Langford, P.K. Quinn, P.J. LeBel, S.A. Vay, P.D. Roberts, R.B. Norton, B.A. Watkins, M.P. Buhr, D.D. Parrish, J.G. Calvert, and F.C. Fehsenfeld. An intercomparison of five ammonia measurement techniques, *Journal of Geophysical Research*. *97* (D11), 11591-11611, 1992.

Wofsy, S.C., M.L. Goulden, J.W. Munger, S.-M. Fan, P.S. Bakwin, B.C. Daube, S.L. Bassow, and F.A. Bazzaz, Net exchange of CO_2 in a mid-latitude forest, *Science*, *260*, 1314-1317, 1993.

Wolff, G.T., On the nature of nitrate in coarse continental aerosols, *Atmospheric Environment*, *18* (5), 997-981. 1984.

Wyers, G.P., R.P. Otjes, and J. Slanina, A continuous-flow denuder for the measurement of ambient concentrations and surface-exchange fluxes of ammonia, *Atmospheric Environment*, *27A* (13), 2085-2090, 1993.

CHAPTER 3

DEPOSITION OF NITRIC ACID VAPOR TO A MID-LATITUDE FOREST

Abstract

The deposition velocity (V_d) of nitric acid vapor over a fully leafed mixed forest was estimated using the modified-Bowen ratio (MBR) and a dry deposition inferential model (DDIM). The MBR approach presumed a similarity between the diffusivities of HNO_3 and heat, while the DDIM method assumed the canopy resistance (R_c) to be zero. Hourly averaged DDIM HNO_3 deposition velocities varied diurnally, ranging from nighttime lows of ≈ 1 cm s^{-1} to midday highs of ≈ 6 cm s^{-1}. The similarity of results obtained from the MBR and the sum of the DDIM aerodynamic and boundary layer resistances suggests that R_c to HNO_3 deposition is quite small. Average and median inferential HNO_3 fluxes were -8.30 and -3.03 μmol m^{-2} hr^{-1}, respectively. At night, the estimates of HNO_3 deposition were similar to the eddy covariance NO_Y flux, however, daytime HNO_3 fluxes were typically 3-4 times higher than measured NO_Y deposition. It is likely that measurement bias, NO_X emissions, and storage effects may all contribute to the observed differences between the NO_Y and HNO_3 fluxes.

3.1 Introduction

Anthropogenic emissions of nitrogen oxides (NO and NO_2) have steadily increased over the past several decades [Gschwandtner et al., 1986], as has the deposition of atmospheric nitrogen [Schell, 1987]. Some temperate forests have responded to this supplementary nitrogen deposition with increased growth rates [Kauppi et al., 1992], while others have experienced serious damage [Vann et al., 1992]. Nitrogen has historically been a limiting nutrient for forest ecosystems, thus enhanced atmospheric N inputs may stimulate the rate at which these ecosystems sequester atmospheric CO_2 via photosynthesis [e.g., Peterson and Melillo, 1985; Schindler and Bayley, 1993]. Alternatively, it has been suggested that the extra addition of anthropogenically fixed nitrogen eventually leads to a nitrogen saturated ecosystem, where nitrogen availability is in excess of biotic demand [Aber et al., 1989; Schulze, 1989]. There are, in fact, forest ecosystems in Europe and North America that are displaying symptoms of nitrogen saturation [Aber, 1992; Lamersdorf and Meyer, 1993]. However, it is still uncertain what the critical atmospheric nitrogen loading rates are that lead to problems

associated with nitrogen saturation. Estimates of the critical nitrogen load to forests range from 2-30 kg N ha^{-1} y^{-1} [Åren, 1983; Nilsson, 1978; Gunderson, 1991]. The critical N load is likely to be a function of other parameters such as: species composition, soil chemistry, hydrology, land-use history, plant/microbial interactions, and other biogeochemical factors.

The nitrogen loading of an ecosystem is accomplished by: [1] the wet deposition of dissolved nitrate (NO_3^-), ammonium (NH_4^+), and organic nitrogen (DON) in rain, fog, and snow; as well as [2] the dry deposition of N-containing aerosols and gases (e.g., gaseous nitric acid (HNO_3) and ammonia (NH_3)). Currently, much of the northeastern U.S. is receiving greater than 7 kg N $ha^{-1}yr^{-1}$ from wet deposition ($NO_3^- + NH_4^+$) alone [National Acid Deposition Program, 1997]. Yet studies by Hanson and Lindberg (1991) show that dry deposition to plant surfaces can account for between 20 to 70% of total atmospheric N inputs. While it is relatively easy to quantify the amount of rainfall and the concentrations of dissolved N therein to obtain a wet deposition flux (wet deposition of fog and cloud water excluded), it has proven considerably more difficult to determine dry deposition rates of nitrogen containing gases and aerosols.

Gaseous nitrogen compounds can be characterized into different classes based on the mechanism controlling their deposition to vegetated surfaces: [1] compounds able to adsorb to many surfaces (HNO_3 and NH_3); [2] species that interact with leaves primarily by diffusion into stomata (NO_2 and possibly NH_3); and [3] gases that are not readily taken up by plants or plant surfaces (NO, N_2O) [Hosker and Lindberg, 1982]. While HNO_3 has the highest deposition velocity of the aforementioned N gases [Hanson and Lindberg, 1991], it is also typically the largest fraction of total reactive nitrogen ($NO_Y \equiv NO + NO_2 + NO_3 + HNO_3 + NO_3^-$ aerosol + N_2O_5 + peroxyacetyl nitrate (PAN) + other organic nitrates) in air a few days removed from combustion sources [Logan, 1983; Bytnerowicz et al., 1987]. The dry deposition or wet scavenging of HNO_3 from the atmosphere is the primary removal pathway for atmospheric NO_Y [Logan, 1983]. Given the relatively high confidence in the quantification of the wet N deposition flux, the current large uncertainties in the estimates of total atmospheric N deposition could be significantly reduced by a better understanding of the factors which regulate HNO_3 dry deposition.

In the present study hourly vertical gradients of HNO_3 summertime mixing ratios [Lefer et al., 1997] and air temperatures (1995 only) were obtained above a mid-latitude forest between 1991-95. Simultaneous measurements of the eddy covariance fluxes of sensible heat (Q_H), momentum (τ), and NO_Y [Moore et al., 1996; Munger et al., 1996] enabled us to: [1] estimate the dry deposition flux of HNO_3 using two different methods; [2] examine how these estimates of HNO_3 deposition compare to measurements of NO_Y dry

deposition; and [3] identify some of the factors which may reconcile the differences between these various estimates of HNO_3 deposition.

3.2 Methods

3.2.1 Site description

This study was conducted at the Environmental Measurement Site at Harvard Forest located in Petersham, Massachusetts (42.54°N, 72.18°W), approximately 100 km away from the urban centers of Boston and Hartford, to the east and southwest of Harvard Forest, respectively. Measurements were conducted from a 30-m micrometeorological tower that extended 6-7 meters above the forest canopy. This 50-70 year old predominantly red oak forest is mixed with red maple and scattered stands of hemlock and white pine. An approximate deciduous leaf area index (LAI) of 3.4 was determined for this site by leaf litter collection [Goulden, unpublished data]. The tower is situated in a moderately hilly area more than 1 km from the nearest paved road. At midday in the growing season 84% of the net radiation is on average balanced by the sum of the sensible (Q_H), latent (Q_E), and soil (Q_G) heat fluxes [Moore et al., 1996]. Individual days are typically much closer to being balanced (i.e., residual < 10% net radiation). However, days with winds from the southwest (SW) windsector (SW = 180°-270°) generally appear to have a poorer energy balance, which may be related to variations in surface-type or perhaps differences in biomass heat storage for the SW tower footprint [Moore et al., 1996]. As determined from wind profiles under neutral conditions, the zero plane displacement height (d) is approximately 19.8 m for the fully leafed canopy [Moore et al., 1996].

3.2.2 Sampling methods and instrumentation

Gaseous HNO_3 was sampled using a mist chamber [Talbot et al., 1990; Lefer et al., 1997] equipped with a teflon prefilter. The mist chamber device generates a fine mist which concentrates the HNO_3 from a large volume of air (≈ 1000 L) into a small volume of deionized water (≈ 10 mL). The nitrate (NO_3^-) concentrations in solution were quantified using a modified Dionex™ ion chromatograph (IC) [Talbot et al., 1994]. Ambient air was sampled for a period of 45-50 minutes at a flow rate of 30 standard L $min.^{-1}$ (slpm), as determined with an integrating linear mass flow meter (Teledyne-Brown Engineering, Hampton, VA). The mist chamber samplers used in this study had 100% collection efficiency for HNO_3 with a limit of detection of 5 parts per trillion by volume (pptv) for HNO_3 and an overall uncertainty of ±11% [Lefer et al., 1997].

Gaseous HNO_3 was simultaneously sampled from three mist chambers suspended 29, 24, and 11-m above the ground. The mist chamber sample extraction, rinsing, and refilling took approximately 10 minutes.

thus consecutive samples were collected with effectively one hour time resolution. Mist chamber extracts were placed in 30 mL high density polyethylene amber bottles, treated with 100 μL of $CHCl_3$ as a biocide, and refrigerated (for less than 2 months) until analyzed for dissolved NO_3^-. HNO_3 was continuously sampled for 12-30 hour periods on 70 mostly summertime days between 1991-1995 [Lefer et al., 1997].

Two platinum thermistors (model 43347, R.M. Young Company) in aspirated radiation shields were used to measure the air temperature at the 29 and 24-m levels. Both probes underwent a three point calibration (Campbell Scientific, Inc.) to achieve an absolute accuracy of ± 0.05 °C, thus a temperature gradient between the two probes could be determined with an accuracy of 0.1°C. One minute average signals (sampled at 1 Hz) from these sensors were stored in a model CR10 data logger (Campbell Scientific, Inc.).

An Applied Technologies, Inc. (model SWS-211/3K) three-axis sonic anemometer was mounted on a boom at 29-m oriented towards the prevailing west winds. This sonic anemometer was used to acquire the vertical and horizontal wind velocities, wind direction, and virtual air temperature at a rate of 4 Hz. The coordinate system of the anemometer was mathematically rotated to account for tilting of the sonic anemometer or deviations from horizontal streamlines. The NO_Y converter inlet was mounted on a separate boom at a slightly lower level (28.3-m) to minimize its potential influence on the micrometeorological measurements. The uncertainty and precision of the 8 Hz NO_Y measurement was estimated to be ± 6% and 4%, respectively [Munger et al., 1996]. A separate inlet at 29-m was attached to a LiCor 6262 CO_2/H_2O instrument which reported concentrations at 4-Hz. In this study, these high frequency measurements were used to calculate 30-min eddy-covariance fluxes of heat, momentum, water vapor and NO_Y at 29 m perpendicular to the mean streamline [Moore et al., 1996; Munger et al., 1996]. Further details of the data acquisition and analysis procedures are reported in Moore et al. [1996] and Munger et al. [1996]. The entire Harvard Forest dataset, including the University of New Hampshire (UNH) gas and aerosol dataset is available via anonymous ftp at io.harvard.edu in the directory pub/nigec/UNH and the Web site www-as.harvard.edu.

3.2.3 HNO_3 flux calculations

3.2.3.1 Modified Bowen-ratio technique. The flux of a species i (F_i) can be defined as:

$$F_i = -V_{d(i)} C_i \qquad [1]$$

or

$$F_i = \mathrm{K}_i \frac{dC_i}{dz} \qquad [2]$$

where $V_{d(i)}$ is the deposition velocity of i, C_i is the concentration of i, K_i is the diffusion coefficient (or diffusivity) of species i, and dC_i/dz is the concentration gradient of i. By convention, negative fluxes are

defined as a loss from the atmosphere. The modified-Bowen ratio technique (MBR) assumes that turbulence similarly mixes and equally transfers scalar quantities such as sensible heat (T) and C_i [Meyers et al., 1996].

The eddy covariance sensible heat flux:

$$Q_H = C_a \overline{w'T'} \qquad [3]$$

(where C_a is the heat capacity of air and $\overline{w'T'}$ is the product of the instantaneous deviations of horizontal windspeed (w') and temperature (T')) can also be expressed in terms of a diffusion coefficient and a temperature gradient:

$$Q_H = \mathrm{K}_H \frac{dT}{dz} \qquad [4].$$

Assuming that the scalar diffusivities of HNO_3 (K_{HNO_3}) and heat (K_H) are similar, then equations [1], [2], and (4) can be combined to give a solution for the deposition velocity of HNO_3 [Lee et al., 1993; Klemm et al., 1994]:

$$V_{d(HNO_3)} = -\frac{Q_H}{C_{HNO_3}} \frac{dC_{HNO_3}}{dz} \frac{dz}{dT} \frac{1}{\rho C_a} \qquad [5]$$

with density of air (ρ) and C_a included to convert Q_H to units of °C cm s^{-1}. The assumption of diffusion coefficient equality was originally based on some empirical results which demonstrated a similarity between the turbulent transfer of sensible heat and water vapor [Dyer and Hicks, 1970]. Studies comparing ozone (O_3) deposition measured via both eddy covariance and flux-gradient methods have shown that $\mathrm{K}_H \approx \mathrm{K}_{O_3}$ over grass surfaces [Droppo, 1985]. However, Raupach [1979] found that the inhomogenous temperature structure of a forest canopy can enhance turbulent processes even in near neutral conditions.

A second central assumption to this approach is the constancy of fluxes with height. This assumption implies that there are no sources or sinks of HNO_3 between the two sampling levels, or between the lower height and the canopy itself. Thus we are assuming no heterogeneous chemical reactions between HNO_3 and NH_3, no significant horizontal advection of HNO_3, and no uptake of HNO_3 onto the surface of basic aerosols or into fog droplets between two sampling heights and above the canopy. For example, Meixner et al. [1988] found that this assumption was not valid in conditions of high relative humidities (i.e., RH > 62%, the deliquescence point of NH_4NO_3 aerosols) or in the presence of fog where HNO_3 was scavenged by the wet surfaces. Given that NH_4NO_3 is a very minor species at this site [Lefer and Talbot, 1997] and that our gradient sampling was dominated by clear air conditions, we assume that such phenomena had a negligible influence on the observed HNO_3 gradients.

The MBR approach requires significant measurable gradients in the scalars being measured, in this case, HNO_3 and air temperature. The three sources of error in the ΔHNO_3 measurements include the precision of: the IC determination of NO_3^- (± 1%), the water sample volume (± 0.1%), and the integrated air volume (± 4 %). A propagation of errors uncertainty of twice these values estimate suggests that the ΔHNO_3 between the two levels needs to be at least 10% of the concentration at 29-m to be 95% confident that these two measurements are truly different. This estimate is supported by the more than 50 hours of side by side (or null gradient) HNO_3 sampling from 24 m in which the volume corrected HNO_3 concentration difference between two mist chambers was on average (± std. deviation) 6.2 (± 5.0)%. Given the variability of the null gradient testing, a detectable HNO_3 gradient was defined as Δ HNO_3 greater than 10% of the HNO_3 concentration at 29m. Due to the precision of the temperature sensors, ± 0.1°C was the minimum detectable temperature gradient. An example of gradient measurements of HNO_3 and air temperature (T) is shows that it is not always possible to measure detectable gradients (Figure 3.1). Null gradient testing (multiple sensors at the same height above the forest) confirms that the sensor bias is within the limits described above (Figure 3.2). All above canopy HNO_3 concentration gradient measurements made between 1991-1995 are summarized in Table 3.1.

3.2.3.2 Dry deposition inferential model (DDIM). In the dry deposition inferential model (DDIM), also known as a resistance analogy model, the deposition velocity is the inverse of three serial resistances [Hicks et al., 1987]:

$$V_{d(HNO_3)} = \frac{1}{R_a + R_b + R_c} \qquad [6]$$

that regulate the deposition of gases and small particles to a surface. The aerodynamic resistance (R_a) is a function of the atmospheric stability and can be described as a larger scale measure of the degree of turbulent mixing between the measurement height z and the quasi-laminar boundary layer just above the deposition surface. This resistance can be expressed as:

$$R_a = \frac{\bar{u}}{u_*^2} - \frac{\psi_H}{ku_*} \qquad [7]$$

where $\bar{u}$ is mean horizontal windspeed, u_* is friction velocity, ψ_H is a diabactic stability correction coefficient for the transfer of heat, and k is von Karman's constant ($k = 0.4$). u_* was defined as:

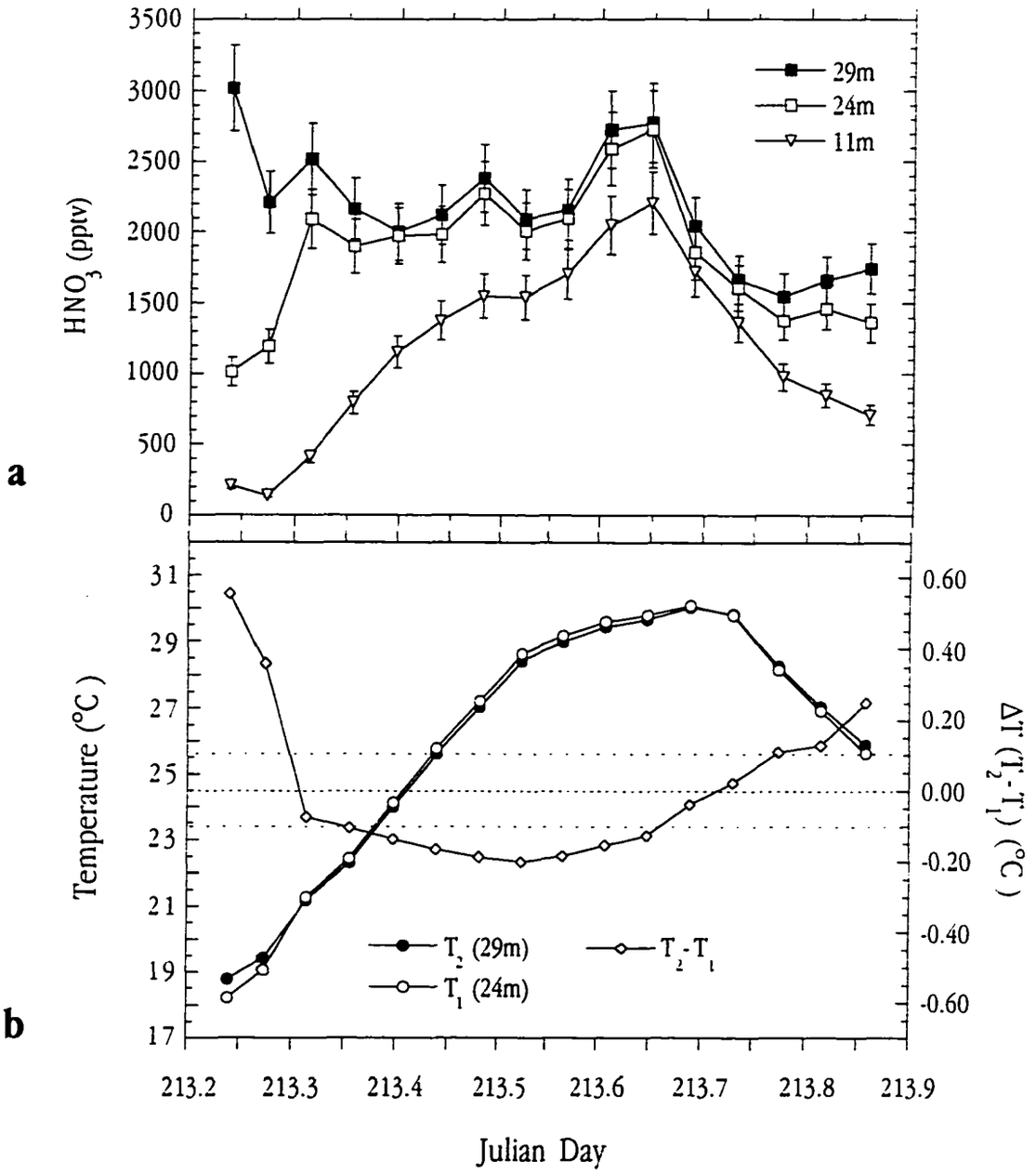

Figure 3.1. (a) Concentration of HNO_3 at three different levels for August 01, 1995. Error bars represent the measurement uncertainty.; (b) Average hourly air temperatures at 29 and 24m and Δ temperature for the same day. Uncertainty of each sensor is ± 0.05 °C. Dotted lines represent ± 0.1 °C accuracy for the Δ temperature measurement.

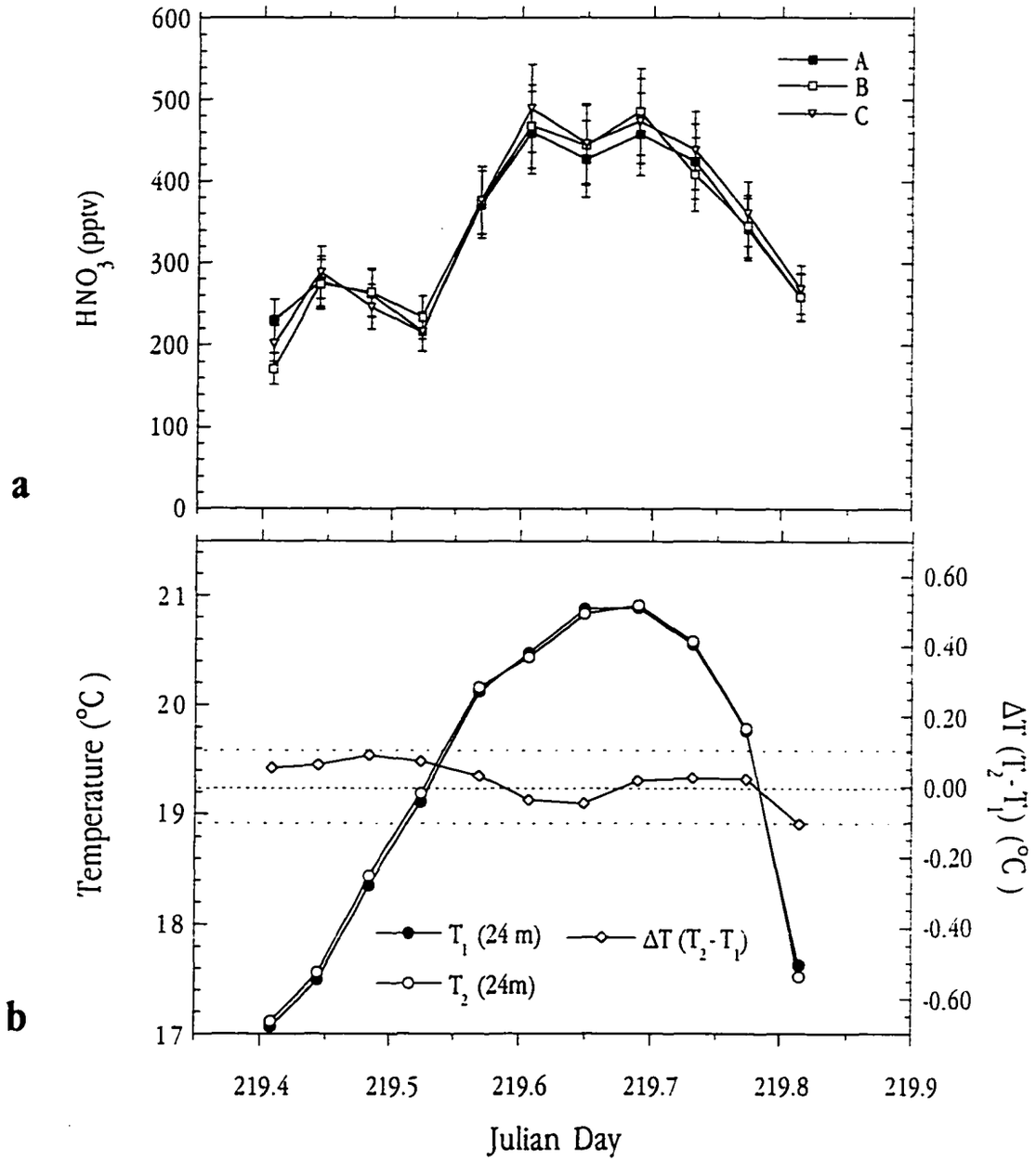

Figure 3.2. (a) Concentration of HNO_3 for three different mist chamber samplers at 24 m on August 07, 1995. Error bars represent the measurement uncertainty.; (b) Average hourly air temperatures for two sensors at 24m and Δ temperature for the same day. Uncertainty of each sensor is ± 0.05 °C. Dotted lines represent ± 0.1 °C accuracy of the Δ temperature measurement.

$$u_* = \sqrt{-\overline{u'w'}} = \sqrt{-\tau} \qquad [8]$$

where $\overline{u'w'}$ (or τ) is the eddy covariance momentum flux. ψ_H was adapted from Wesely and Hicks [19__] for stable conditions:

$$\psi_H = -5(z-d)/L \qquad [9a]$$

and for unstable conditions:

$$\psi_H = \exp\left[0.598 + 0.39\ln(-(z-d)/L) - 0.09(\ln(-(z-d)/L))^2\right] \qquad [9b]$$

where the measurement height (z) is 29-m, the zero plane displacement height (d) is 19.8-m, and L is the Monin-Obukhov length scale. Stable conditions are defined as $L < 0$ and unstable as $L > 0$ for:

$$L = -\rho C_p u_*^3 T / kgQ_H \qquad [10]$$

where T is absolute temperature, and g is the acceleration due to gravity.

The surface boundary layer resistance (R_b) describes the rate of molecular diffusion through the viscous sublayers on the leaf surface, and can be written as [Garratt and Hicks, 1973; Meyers et al., 1989]:

$$R_b \equiv (2/ku_*)(Sc/\mathrm{Pr})^{2/3} \cong 7.1/u_* \qquad [11]$$

using a Schmidt number (Sc) for HNO_3 of 1.22 and a Prandtl number (Pr) for air of 0.72.

The final stage of deposition in this model concerns the surface (or canopy) resistance (R_c) of leaf deposition pathways. The components of R_c include: uptake through the stomates and onto the mesophyll, adsorption onto the cuticular membrane, or deposition to other surfaces (e.g., branches, soil). Hanson and Lindberg [1991] have compiled HNO_3 conductance values for several tree species, however due to the strong affinity of HNO_3 for most surfaces, it is commonly assumed that R_c for HNO_3 is essentially 0 [Huebert and Robert, 1985; Meyers et al., 1989; Erisman, 1993; Lee et al., 1993; Geigert et al., 1994].

3.3 Results

3.3.1 Gradient measurements

Between 1991-1995 measurements of ambient HNO_3 concentrations were simultaneously determined from 29 and 24m (6 and 1 m above the forest canopy) for 642 individual hours. The HNO_3 concentration gradient measurement ($\Delta[HNO_3]$) was defined as the difference between the HNO_3 concentrations at 29m ($[HNO_3]_{29m}$) and 24m ($[HNO_3]_{24m}$). The strength or significance of $\Delta[HNO_3]$ was evaluated relative to $[HNO_3]_{29m}$ and termed the ratio G such that:

$$G = \Delta[HNO_3]/[HNO_3]_{29m} \qquad [12].$$

In this study, a detectable HNO_3 gradient, defined as G > 0.1, was observed for 380 of the 642 HNO_3 gradient measurements (Table 3.1). Given that the highest HNO_3 mixing ratios are found in air masses from the polluted SW, the largest HNO_3 gradients are also observed in this windsector (Table 3.1). Similarly, higher mixing ratios mean that only larger gradients would be significant for the SW sector. Undetectable HNO_3 gradients occurred 33% of the time when the difference between the two levels was less than 10% (i.e., -0.1 < G < 0.1). The frequency of non-significant gradients was similar for all surface wind sectors (Table 3.1).

Table 3.1. Summary of gradient status and ΔHNO_3 measurements for selected surface wind direction sectors[¶]. Statistics include: number of samples (n), 25th percentile (25%), standard deviation (s.d.), and 75th percentile (75%).

	Statistic	All Sectors	NW	E	SW
Gradient Status	Gradient Ratio (G)				
Deposition [# hours]	> 0.1	380	174	85	95
Undetectable [# hours]	-0.1 < G < 0.1	210	98	42	47
Emission [# hours]	< -0.1	52	32	13	2
$\Delta[HNO_3]$[‡] for Deposition	n	380	174	85	95
(nmol m^{-3})	25%	2.08	1.55	3.09	6.44
	median	5.24	2.72	5.55	14.1
	mean	9.06	5.99	7.57	16.6
	s.d.	10.6	9.42	7.51	12.6
	75%	12.5	6.59	8.76	25.3

[¶]Northwest (NW) wind sector is 270°-45°, east (E) is 45°-180°, and southwest (SW) is 180°-270°.
[‡] $\Delta[HNO_3] = [HNO_3]_{29m} - [HNO_3]_{24m}$.
[*] $G = \Delta[HNO_3]^{\Delta}/[HNO_3]_{29m}$.

Interesting, significant negative gradients (G < -0.1), which in this framework would signify HNO_3 emission, were observed 8% of the time. Sampling at the hourly time scale, Munger et al. [1996] also observed NO_Y "emission" at this site and attributed this to the storage of NO_Y in the subcanopy. Diel changes in concentration due to formation and breakdown of the nocturnal boundary layer or wind direction changes from polluted to clean wind sector can trap air with relatively high NO_Y mixing ratios in the subcanopy atmosphere. While this air still contains high levels of NO_Y it can be subsequently ventilated out of the canopy into relatively cleaner air and observed as NO_Y emission. Integrating flux measurements of daily or longer time periods

eliminates this problem. Our hourly results suggest much the same phenomenon is occasionally occurring for HNO_3.

3.3.2 Modified Bowen ratio (MBR)

Of the many hours for which gradient measurements were made, suitable high resolution temperature gradient measurements (i.e., $\Delta T \pm 0.1°C$) necessary for the MBR heat similarity calculation were only available for 89 hours of 1995. Of these, 16 and 22 hours were used for null gradient and below canopy measurements, respectively. The remaining 52 hours were tested to see if they met the following criteria: [1] the absolute value of ΔT was greater than 0.1°C; [2] ΔHNO_3 was more than 10% of the HNO_3 concentration at 29-m (i.e., $G > 0.1$), and [3] all other necessary measurements (e.g., Q_H) were available. Of these remaining hours, 11 hours did not meet both criteria 1 and 2, 11 additional hours had undetectable ΔT gradients, 12 more hours had undetectable $\Delta[HNO_3]$ gradients, and 9 hours lacked Q_H and other supporting micrometeorological measurements.

The meteorological and chemical conditions for the remaining 9 hours on 01-02 August, 1995 for which MBR measurements of the HNO_3 flux were made are summarized in Table 3.2 and Figure 3.1 (01 August, 1995 only). During these hours the wind was fairly steady (1-2 m/s) from the west and north. The results of the MBR HNO_3 flux calculations are shown in Table 3.3. For two of these hours, the temperature gradient did not agree with the direction of Q_H, resulting in a negative V_d. On both of these occasions (0600 EST each day), Q_H was quite small just after the transition from a positive to negative Q_H, and appears to be a time when the MBR technique breaks down [Meyers et al., 1996]. Aside from these two hours, the MBR calculated V_d of HNO_3 is approximately 2 cm s^{-1} for stable conditions and ranges from 3-12 cm s^{-1} during unstable periods (Figure 3.3). The MBR HNO_3 fluxes for these same times range from -5 to -44 μmol m^{-2} hr^{-1} and are consistently about 3 times the measured NO_y flux for the same hours (Figure 3.4, Table 3.3).

3.3.3 Dry deposition inferential model (DDIM)

The determination of the aerodynamic (R_a (eq. 7)) and boundary layer (R_b (eq. 11)) resistances used to calculate the V_d of HNO_3 are essentially a function of turbulence, as represented by u and u_*. During HNO_3 sampling periods, the average and median summertime (June, July, and August) values of u and u_* both exhibit a composite diel behavior coincident with the heat flux, with higher values midday and lower values at night (Figures 5a and 5b). Consequently, the diel cycle of V_d has the same pattern (Figure 3.6a) with nighttime values of u and u_* ($\approx$ 1.5 and 0.2 cm s^{-1}, respectively) resulting in a V_d of $\approx$ 1.5 cm s^{-1}. Typical midday values of 2.5 m s^{-1} and 0.6 m s^{-1} for u and u_* respectively, yield a V_d of $\approx$ 6 cm s^{-1}.

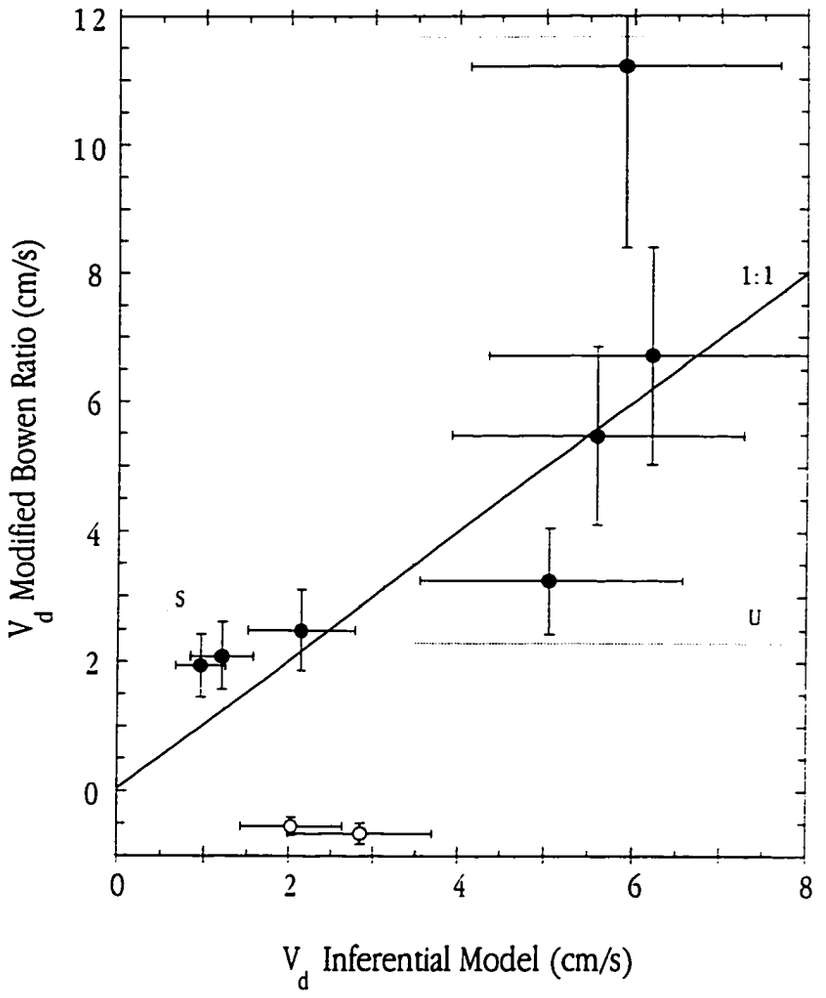

Figure 3.3. Comparison of deposition velocities calculated by modified-Bowen ratio (MBR) method and dry deposition inferential model (DDIM) for 01-02 August, 1995. Boxes with S and U indicate stable and unstable atmospheric conditions, respectively. Open symbols represent two time periods for which MBR approach did not work. Solid line is 1:1 line. Error bars represent the propagation of errors in uncertainty of each method.

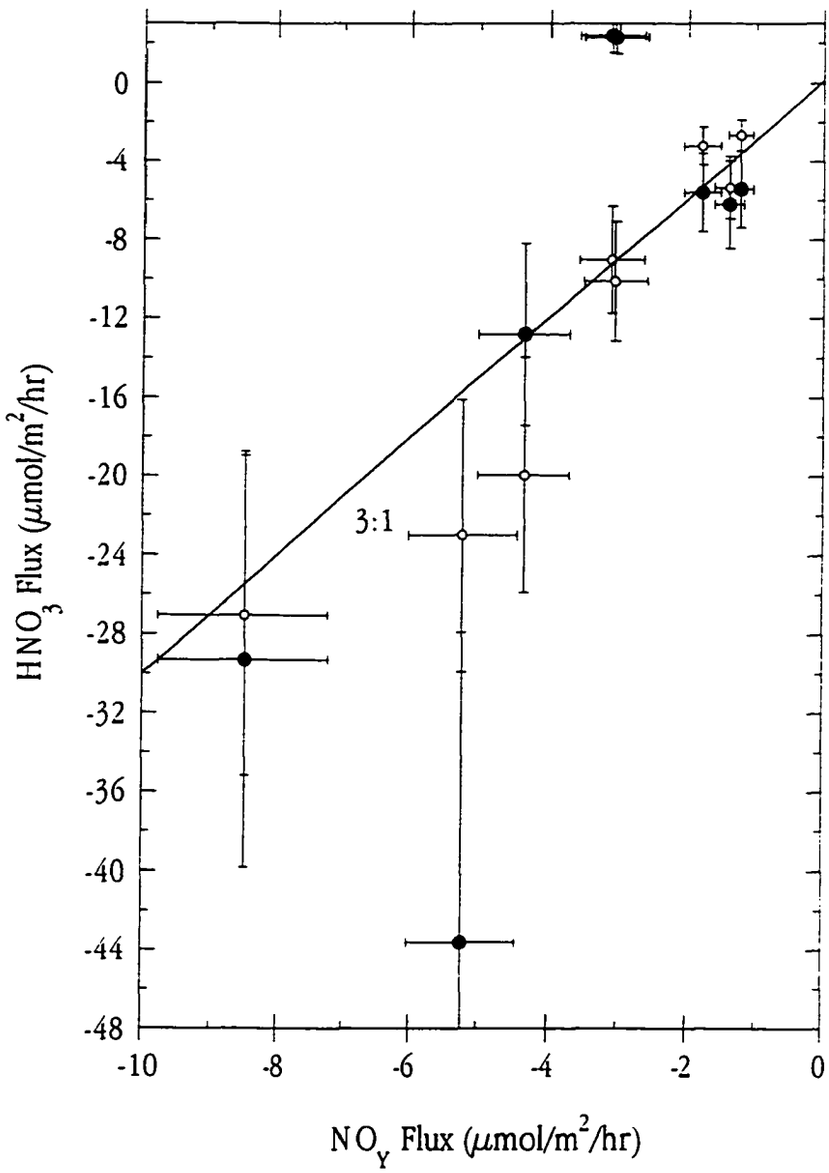

Figure 3.4. HNO_3 deposition flux via MBR (solid symbols) and DDIM (open symbols) versus the eddy covariance NO_Y flux. Solid line is 3:1 line and error bars represent propagation of errors uncertainty.

Over all the summer HNO_3 sampling periods (n=449), the average (± std. error) DDIM V_d at 29 m was 4.7 ± 0.12 cm s^{-1}. The average V_d for the for the southwestern (SW = 180°-270°) and northwest (NW = 70°-45°) windsectors are not statistically different (Figure 3.7a, Table 3.4). The significantly lower V_d for the E wind sector is puzzling. Other studies at this site [Goulden et al., 1996; Moore et al., 1996] have identified a slight tower shadowing effect when airflow is from behind the tower (45-135°). While the "shadowing" does increase the variability of u_* in this sector [Moore et al., 1996], we have no reason to believe that this would decrease u_* significantly. Easterly winds were often associated with cloudy conditions [Goulden et al., 1996], which may also be responsible for the change. Due to the relatively infrequent occurrence of easterly winds in this study (≈ 16%) and because we can not attribute the lower V_d in easterly winds to instrument bias, we did not remove these periods from the dataset.

Summertime HNO_3 concentrations exhibit an average composite diel cycle similar to V_d (Figures 3.6 and 3.7) but the two variables are generally uncorrelated. Higher HNO_3 concentrations are generally found at midday, due to the greater photochemical production rates at this time, and in winds from the polluted SW sector. Similarly, u_* and hence V_d, also tends to be greater midday when vertical mixing is enhanced due to greater solar heating. However, unlike [HNO_3], V_d is not significantly greater in the SW sector (Figure 3.7a). which likely explains the general lack of correlation between these two variables.

However, the larger midday values of both V_d and HNO_3 lead to the calculation of large midday HNO_3 deposition fluxes (≈ 11 μmol m^{-2} hr^{-1}). This effect is especially amplified in air masses from the SW sector (Figure 3.7c). In general, average nighttime HNO_3 deposition compares well with the observed eddy covariance NO_Y flux (Figure 3.8a). During the day, however, calculated HNO_3 fluxes are significantly greater (3-4 times larger) than measured NO_Y fluxes between 0800 and 1900 EST (Figures 3.8b and 3.8c).

3.3.4 Flux error analysis

The uncertainty of the various inputs to the MBR and DDIM approaches include : $\Delta T \pm 0.1$ °C (or a maximum of 10%), Δ[HNO_3] ± 10%, T ± 0.05°C, [HNO_3] ± 11%, Q_H ± 15%, u ± 15%, and u_* ± 15% [Munger et al., 1996; Lefer et al., 1997; Figures 1a and b]. Using these values we conducted a separate propagation of errors analysis [Erisman, 1993], which suggest that both the MBR and DDIM V_d values have an uncertainty of ±25%. The HNO_3 deposition flux measurements have uncertainties of ±22% and ±30% for the MBR and DDIM methods, respectively. These uncertainty values do not include the effect of any systematic bias resulting from correlation in the variables (see section 3.4.4).

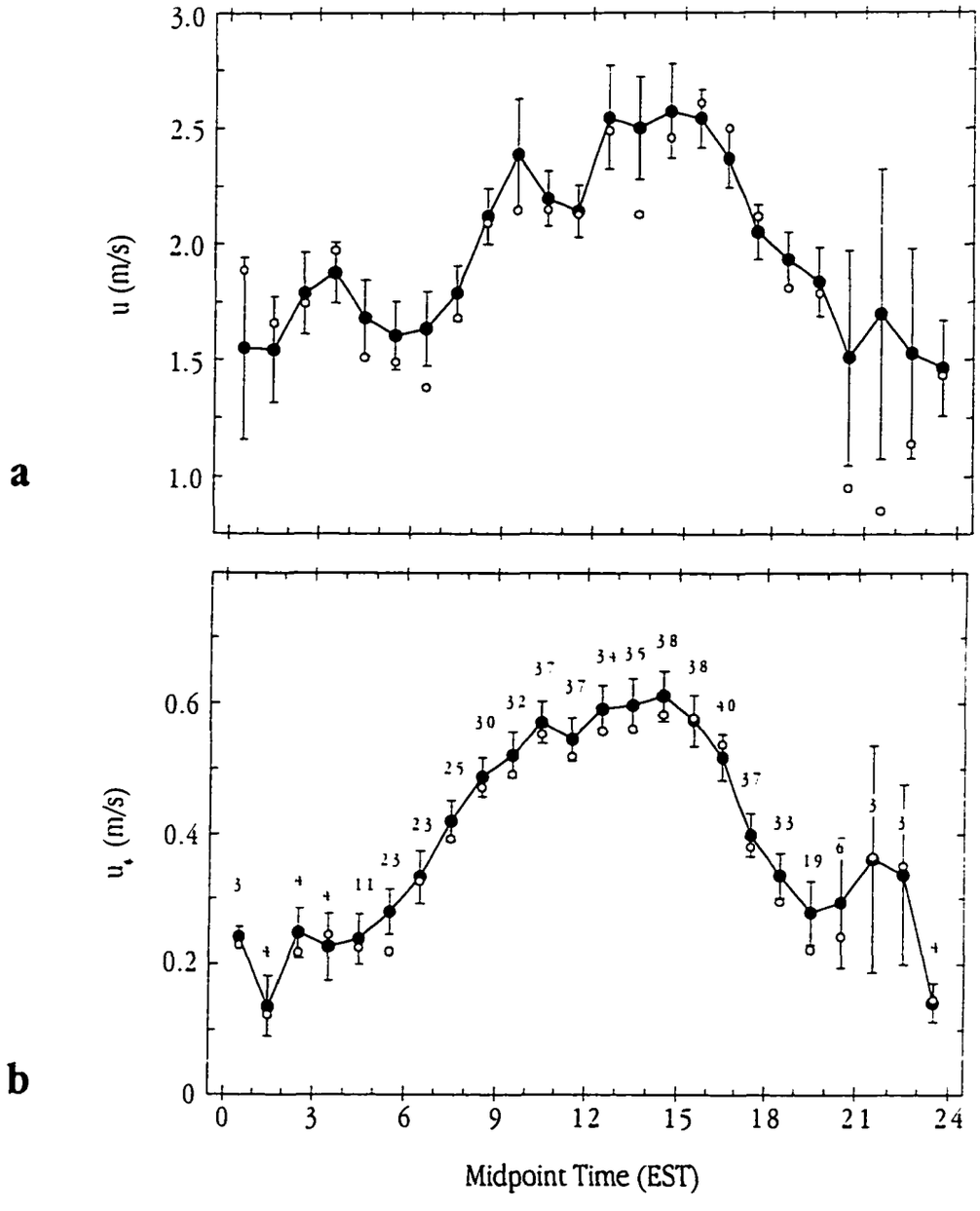

Figure 3.5. (a) Mean (filled symbol) and median (open symbol) diel cycle of hourly averaged horizontal windspeed at 29-m for HNO_3 summertime sampling periods. Vertical bars correspond to standard error of mean. Number of samples averaged are same as in Figure 3.5b.; (b) Same as Figure 3.5a, except for friction velocity. Values above symbols are number of samples.

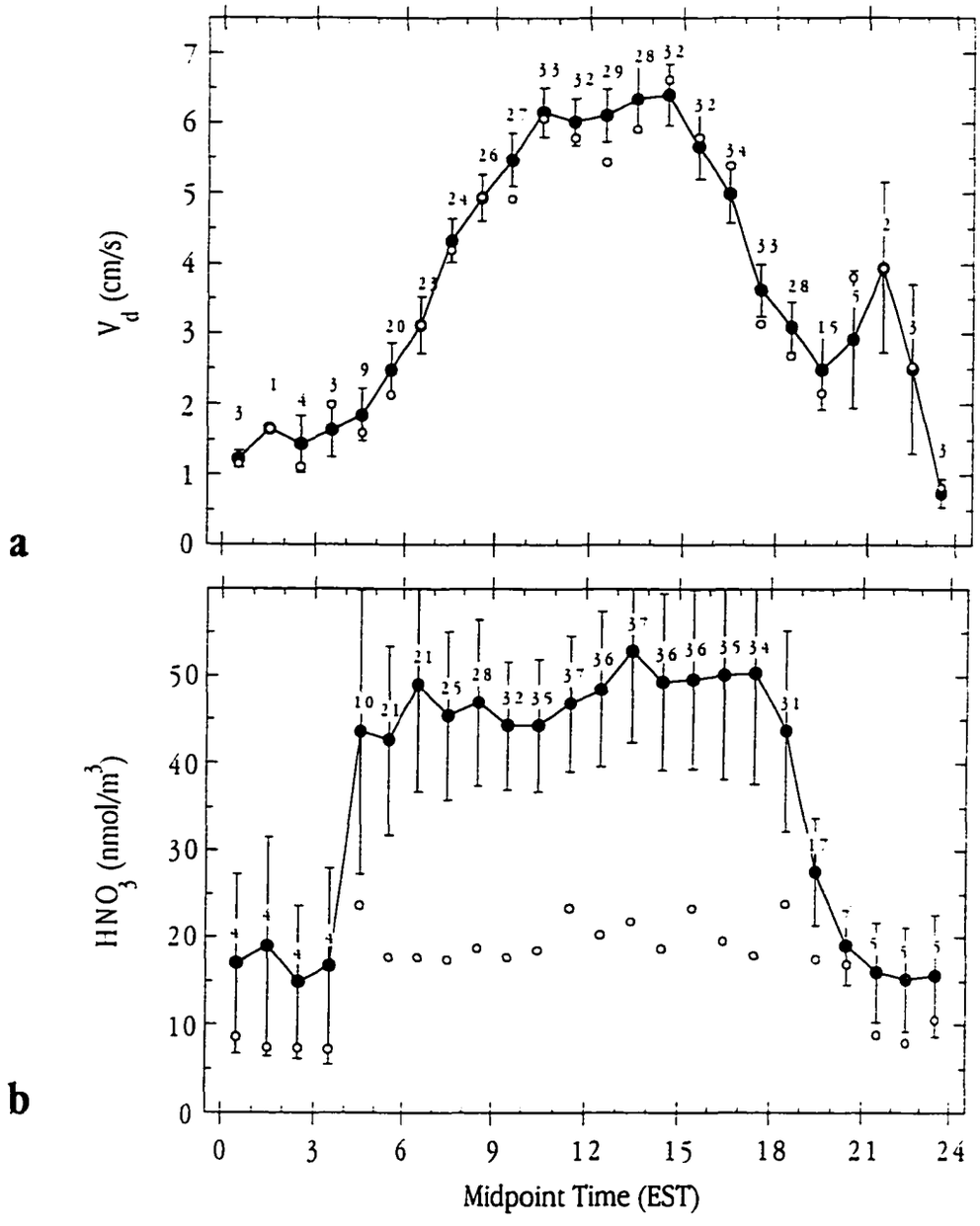

Figure 3.6. (a) Mean (filled symbol) and median (open symbol) diel cycle of DDIM deposition velocity at 29-m for HNO_3 summertime sampling periods. Vertical bars correspond to standard error of mean. Values above symbols are number of samples.; (b) Same as Figure 3.6a, except for HNO_3 concentration.

3.4 Discussion

3.4.1 Modified-Bowen ratio (MBR) HNO_3 deposition velocities

A paradox of any flux-gradient approach is that under turbulent conditions when the flux is expected to be greatest, the gradient can be small, and in our case, was often unmeasurable. This is shown in Figure 3.2, where the mid-day HNO_3 mixing ratios for Day 213 are not significantly different for the upper two sampling heights. Assuming a similarity with the heat flux has the additional drawback of having the heat flux cross zero twice each day in transition to and from unstable conditions (Figure 3.1), making the measurement of ΔT more difficult. Overall, these difficulties were equally apparent for gradient measurements of both HNO_3 and T, and tend to bias MBR[Q_H] similarity measurements to relatively stable periods [e.g., Lee et al., 1993].

The average ($\pm$ std. error) deposition velocity using the MBR approach over the forest was 4.7 ± 1.3 cm s^{-1} with a range of 1.9-11.2 (Table 3.3). These values are in general agreement with the DDIM V_d estimates for the same period (Table 3.3) and flux-gradient HNO_3 measurements of V_d (0.5-5.1 cm s^{-1}) over a deciduous forest [Meyers et al., 1989]. Studies employing the MBR technique to determine the V_d of HNO_3 include: Huebert and Robert [1985] over a Colorado grassland (V_d of 2.0-3.1 cm s^{-1}); Dollard et al. [1987] over a wheat field (V_d of 5 - 26 cm s^{-1}); Müller et al. [1993] over a mature wheat canopy (V_d of 0.6 - 5.0 cm s^{-1}); Meixner et al. [1988] over a coniferous forest (V_d of 0.3 - 39 cm s^{-1}); and Lee et al. [1993] over a lava surface (V_d of 0.3 -3.5 cm s^{-1}). In general, the HNO_3 deposition velocities are similar for these different surfaces, but also show considerable variability for studies over the same surface. However, it is difficult to compare the range of these measurements since most of these studies, this one included, were carried out for relatively short periods (a few hours) in a small range of environmental conditions. Overall, one might expect the taller canopies (e.g. forest vs. grass) to have a rougher surface, thus creating more turbulence and higher deposition velocities.

Problems with the MBR approach result from the violation of either the similarity or constant flux assumptions. While it is difficult to address the similarity assumption from our dataset, Raupach et al., [1979] suggest that the similarity assumption is more applicable in a region significantly above the canopy roughness elements. In some cases this region has been assumed to be at a level at least twice the height of the canopy [e.g., Meixner et al., 1988]. In this study we were limited by the tower height to a maximum level $\approx$ 1.3 times the canopy height.

A modeling exercise by Kramm and Dlugi [1994] has shown that the heterogeneous formation of NH_4NO_3 aerosol can overstate the [HNO_3] gradient, leading to an over estimate of the HNO_3 flux. The Kramm

Table 3.2. Hourly data for selected micrometeorological and chemical quantities for 01-02 August 1995 (JD 213-214).

Day (Julian)	Midpoint (EST)	Q_H (W/m^2)	LE (W/m^2)	R_n (W/m^2)	τ (cm^2/s^2)	L (m)	u_* (m/s)	u (m/s)	wdir (deg)	RH (%)	HNO_3@29m ($\mu mol/m^3$)	ΔHNO_3 ($\mu mol/m^3$)	T@29m (°C)	ΔT (°C)
213	6:35	8.2	63.8	115	-1069	-413	0.33	1.91	270	82.4	98.6E-3	45.3E-3	19.43	0.36
	8:32	76.6	242.4	384	-2911	-201	0.54	2.52	304	69.0	96.6E-3	11.9E-3	22.33	-0.11
	18:34	-39.8	21.9	-3	-1120	94	0.33	1.77	269	56.9	69.1E-3	7.7E-3	28.27	0.11
	19:33	-36.5	9.7	-42	-615	42	0.25	1.34	270	62.9	74.1E-3	8.8E-3	27.05	0.13
	20:35	-36.1	2.4	-42	-512	32	0.23	1.33	256	65.5	77.7E-3	17.0E-3	25.89	0.25
214	6:35	7.3	24.5	102	-320	-76	0.18	0.93	247	89.0	123.8E-3	86.8E-3	20.42	0.58
	8:32	35.9	210.2	256	-2055	-256	0.45	1.70	332	78.5	109.7E-3	22.2E-3	24.20	-0.14
	10:33	163.5	441.6	540	-1475	-34	0.38	1.31	327	69.2	108.1E-3	17.9E-3	25.94	-0.15
	11:37	163.1	462.9	600	-1629	-40	0.40	1.41	328	62.6	121.0E-3	12.8E-3	27.34	-0.16

Table 3.3. Data related to modified Bowen ratio calculation of the HNO_3 dry deposition flux for 01-02 August 1995 (JD 213-214).

Day (Julian)	Midpoint (EST)	R_a (s/m)	R_b (s/m)	R_r** (s/m)	V_d MBR (cm/s)	V_d DDIM (cm/s)	F NO_Y/[HNO_3] (cm/s)	F MBR (μmol/m^2/hr)	F DDIM (μmol/m^2/hr)	F NO_Y (μmol/m^2/hr)	Conservation Ratio[‡] @ 29-m	Conservation Ratio[‡] @ 24-m
213	6:35	15.3	19.9	-	-0.65	2.85	0.86	2.30	-9.48	-3.05	0.91	0.88
	8:32	5.8	12.0	0.3	5.49	5.59		-19.1	-18.0		0.89	0.92
	18:34	27.3	19.4	-6.6	2.49	2.14	0.56	-6.20	-5.08	-1.40	0.93	0.92
	19:33	56.9	26.2	-35	2.09	1.20	0.67	-5.58	-3.09	-1.80	0.93	0.91
	20:35	76.3	28.7	-53	1.94	0.95	0.44	-5.43	-2.58	-1.24	-	-
214	6:35	13.0	36.3	-	-0.54	2.03	0.69	2.39	-8.32	-3.10	0.86	0.82
	8:32	5.5	14.3	11	3.25	5.05	1.11	-12.8	-18.4	-4.36	0.86	0.80
	10:33	-2.17*	16.9	-8.0	11.21	5.91	1.35	-43.6	-23.3	-5.24	0.87	0.85
	11:37	-1.17*	16.1	-1.2	6.72	6.21	1.95	-29.3	-25.9	-8.50	0.91	0.88
			Average ± std. error		4.7 ± 1.3¶			-17.4 ± 5.5¶				

*Negative R_a values replaced by 0 in all calculations (e.g., V_d and R_r).
**Assuming $R_r = [V_d\ MBR]^{-1}$, $R_r = R_r - (R_a + R_b)$.
¶Average without two hours with negative MBR V_d.
‡Conservation ratio = $[HNO_3] / ([HNO_3]+[NO_3^-])$.

and Dlugi [1994] model was parameterized for a European atmosphere where $[NH_3] \geq [HNO_3]$ are both on the order of 1 ppbv. Due to the low ambient mixing ratios (100-300 pptv) of gaseous NH_3 and aerosol NO_3^- on JD 213-214, ≈ 8-10 times lower than HNO_3, we suggest that the heterogeneous formation of NH_4NO_3 aerosol is relatively insignificant on these particular days. For these hours, the conservation of HNO_3 between our two sampling levels is supported by the small difference (-2 to 6%) in the ratio of $[HNO_3]/[HNO_3 + NO_3^-$ aero.] between the sampling heights (Table 3.3).

3.4.2 Inferential (DDIM) HNO_3 deposition velocities

The DDIM method, as employed in this study, is essentially a measure of the turbulent (aerodynamic) and diffusive (boundary layer) resistances to deposition. In one respect, the DDIM results could be viewed as a physical upper limit to the HNO_3 deposition velocity. Thus, MBR deposition velocities dramatically greater than the DDIM V_d (e.g., 11.2 v. 5.9 cm s^{-1} at 10:30 on JD 214 (Table 3.3)) should be viewed with caution.

The general correlation between V_d calculated via the MBR and DDIM methods (r^2=0.60) (Figure 3.3), has been previously noted by Lee et al. [1994] over a lava surface. The similarity between these two methods of determining V_d also gives some support to the assumption that the surface (or canopy) resistance (R_c) for HNO_3 is generally small. By assuming that the total resistance (R_T) is equal to $[V_{d(MBR)}]^{-1}$, it is possible to solve for R_c as the residual resistance (i.e., R_T-[R_a+R_b]). The fact that $V_{d(DDIM)}$ is usually equal to or smaller than $V_{d(MBR)}$ means that R_a and R_b sufficiently describe the resistance to HNO_3 deposition. This can also result in the calculation of a negative R_c (Table 3.3). While negative resistance values are not physically possible, they imply that R_c is negligible for this system or that R_a and R_b are too large.

The calculated DDIM deposition velocities (Table 3.4, Figure 3.6) are in agreement with other previous measurements over mixed and deciduous forests [Hicks and Meyers, 1988; Meyers et al., 1989]. A summertime diel cycle for the V_d of HNO_3 at West Point, NY [Hicks and Meyers, 1988] starts with nighttime values around 0.5 cm s^{-1} and rapidly increases between 0500-0800 to reach a midday maximum of ≈ 6 cm s^{-1}, and then decreases after 1600 to nighttime levels. It is encouraging that these results are quite similar to what we observed at Harvard Forest (Figure 3.6a), however this similarity only verifies that the diel cycles of u an u. are comparable over these two mixed forest canopies.

Table 3.4. Summary of summertime deposition statistics at UNH sampling times and selected surface wind direction sectors[¶]. Statistics include: number of samples (n), 25th percentile (25%), standard deviation (s.d.), and 75th percentile (75%).

	Statistic	All Sectors	NW	E	SW
V_d^*	n	449	247	75	127
(cm s^{-1})	25%	2.90	3.14	2.24	3.55
	median	4.57	3.81	3.06	4.89
	mean	4.72	5.16	3.23[A]	4.72
	s.d.	2.52	2.78	1.52	2.11
	75%	6.36	6.96	4.22	6.37
Flux HNO_3^*	n	444	242	75	127
(μmol m^{-2} hr^{-1})	25%	-1.51	-1.14	-1.67	-3.29
	median	-3.03	-2.44	-2.74	-14.3
	mean	-8.30	-3.97	-3.95	-19.1[B]
	s.d.	12.8	4.96	3.56	19.0
	75%	-8.96	-4.27	-5.05	-26.9
Flux NO_y^{**}	n	326	179	59	85
(μmol m^{-2} hr^{-1})	25%	-0.36	-0.25	-0.46	-0.62
	median	-1.02	-0.87	-1.06	-1.55
	mean	-1.70	-1.41	-1.40	-2.36[B]
	s.d.	2.43	1.91	1.66	2.86
	75%	-2.28	-1.97	-2.43	-3.42
Flux Ratio***	n	273	157	53	65
F HNO_3 / F NO_y	25%	0.71	0.46	0.84	1.78
	median	2.30	1.76	2.09	3.63
	mean	3.11	2.59	2.50	4.85[B]
	s.d.	4.41	4.41	4.18	4.18
	75%	4.80	3.98	4.45	6.66

[¶]Northwest (NW) wind sector is 270°-45°, east (E) is 45°-180°, and southwest (SW) is 180°-270°.
*V_d and Flux HNO_3 via DDIM.
**Flux NO_Y via eddy covariance.
***Flux ratio statistics reflect dataset with top and bottom 5% of values excluded (refer to text (sec. 4.4)).
[A]Significantly less than NW and SW wind sectors ($p < 0.05$).
[B]Significantly greater than NW and E wind sectors ($p < 0.05$).

3.4.3 HNO_3 and NO_Y fluxes

Average summertime diel cycles of HNO_3 and V_d are higher at midday (Figure 3.6), consequently peak HNO_3 deposition is calculated to occur between the hours of 1000-1400 EST (Figure 3.8a). While HNO_3 levels are significantly greater in air masses from the relatively urban SW as compared to the more rural NW [Lefer et al., 1997], both have similar average DDIM deposition velocities (Table 3.4). Thus, HNO_3 deposition is significantly larger ($p < 0.01$) in air masses coming from more polluted regions, with inferentially calculated fluxes averaging -19.1 and -3.97 μmol m^{-2} hr^{-1} for the SW and NW windsectors, respectively. Along with higher HNO_3 deposition, NO_Y deposition [Table 3.4; Munger et al., 1996] and the fraction of NO_Y present as HNO_3 [Lefer et al., 1997] are also greater in air masses from the SW windsector, suggesting that HNO_3 is the primary depositing species in NO_Y.

3.4.3.1 Flux differential. On JD 213-214 of 1995, both the MBR and DDIM HNO_3 deposition fluxes indicate that the deposition of HNO_3 is 3-4 times the NO_Y flux (Figure 3.4). The NO_Y flux is essentially a net flux of a few processes including: NO soil emissions, HNO_3 and NO_2 deposition, and perhaps the deposition of various organic nitrates. While no measurements of NO soil emissions have been made at Harvard Forest, below canopy profile measurements of NO_X ($NO + NO_2$) from the same tower suggest that minor NO soil emissions occur in the summertime. Previous measurements of the flux of NO_X ($NO + NO_2$) above forested canopies in Europe, have shown both emission and deposition [Walton et al., 1997 and references therein]. For a deciduous forest near Oak Ridge, Tennessee, Williams and Fehsenfeld [1991] measured an average NO emission rate of about 0.08 μmol NO m^{-2} hr^{-1} (range = 0.02 - 0.3 μmol m^{-2} h^{-1}). While Walton et al.[1997] indicate that NO emissions may be as high as 2 μmol m^{-2} hr^{-1} in some European forest systems, much of the emitted NO is quickly oxidized by O_3 to NO_2 which subsequently redeposits to the ground. Even the higher European NO soil emission rates (without sub-canopy NO oxidation) are significantly less than the average ($\pm$ std. error), -4.3 ($\pm$ 0.5) μmol m^{-2} hr^{-1}, difference between the DDIM HNO_3 and eddy NO_Y fluxes and do not explain this discrepancy.

Minor NO soil emissions at Harvard Forest combined with the deposition of NO_2 and organic nitrates results in a situation where net NO_Y deposition should be greater than HNO_3 deposition and not the reverse. Assuming that the NO_Y flux is correct, there are a few explanations for the disagreement between these two measurements, including the possibility that: (1) the tower site is micrometeorologically inappropriate for the inferential method (i.e., DDIM model does not apply to this site); (2) if DDIM model is valid, perhaps R_c (the

canopy resistance) is not zero; and (3) both flux determinations are measuring two fundamentally different things (i.e., the comparison is not valid).

These three issues can be addressed with information within our data and ancillary dataset for this site. Given that the top of the tower at Harvard Forest is 6-7 meters above a mixed canopy of approximately 23 m. it is possible that the relatively short fetch and large surface roughness of this forested site are not ideal for the inferential method. Brook et al. [1997] observed that hourly inferential HNO_3 deposition estimates are very sensitive to different aerodynamic regimes (e.g., forest-clearing vs. open grassland) and in these extreme situations typically have an uncertainty of $\pm$ 90. If this site is poorly suited for inferential models it is difficult to explain the fairly well constrained heat budget measurements of Moore et al. [1996] which suggest that the micrometeorological conditions are adequately captured by the instrumentation at this site. Similarly, if R_c is not assumed to be 0, it would, on average , have to be more than 2 times greater than the aerodynamic and boundary layer resistances. While R_c might not be 0, for a sticky gas like HNO_3 the canopy resistance is not the primary resistance to deposition in this system. Finally, since HNO_3 is typically less than 20% of NO_Y at this site [Lefer et al., 1997], it is likely that these two quantities have different atmospheric behaviors. If HNO_3 is the primary depositing NO_Y species, determining the net NO_Y flux can be challenging at times when HNO_3 is a minor component (i.e., less than 1%) of NO_Y. However, for a system in which none of the components of NO_Y are emitted in significant quantities and few other component species are known to deposit efficiently, it is difficult to explain HNO_3 deposition rates higher than the measured NO_Y flux.

3.4.3.2 Positive NO_Y fluxes. On average, hourly summer time NO_Y fluxes are negative (Figure 3.8a), however significant positive NO_Y fluxes (NO_Y emissions) do occur 10% of time in the 1991-1995 Harvard Forest dataset. Similarly, significant positive HNO_3 fluxes, as suggested by negative HNO_3 gradients, were observed for 8% of the UNH measurement periods (Table 3.1). While some positive NO_Y fluxes may result from soil NO emissions, many of the positive NO_Y fluxes occur after a rapid change from high to low NO_Y concentrations and result from the "storage" of NO_Y in the subcanopy. Since the canopy is a physical barrier to mixing, the below canopy environment responds more slowly to air mass changes aloft and can temporarily store NO_Y in the canopy atmosphere. Positive NO_Y fluxes can occur when the relatively higher sub-canopy NO_Y concentrations are mixed or flushed into the above canopy boundary layer. Thus, not all of the NO_Y (or HNO_3) that penetrates the canopy is deposited.

While this storage effect is removed when hourly fluxes are integrated on daily or monthly time scales [Munger et al., 1997], a few of these storage induced emission events are the source of much of the variability when comparing HNO_3 and NO_Y fluxes. It is interesting to note that by convention, the DDIM method assumes

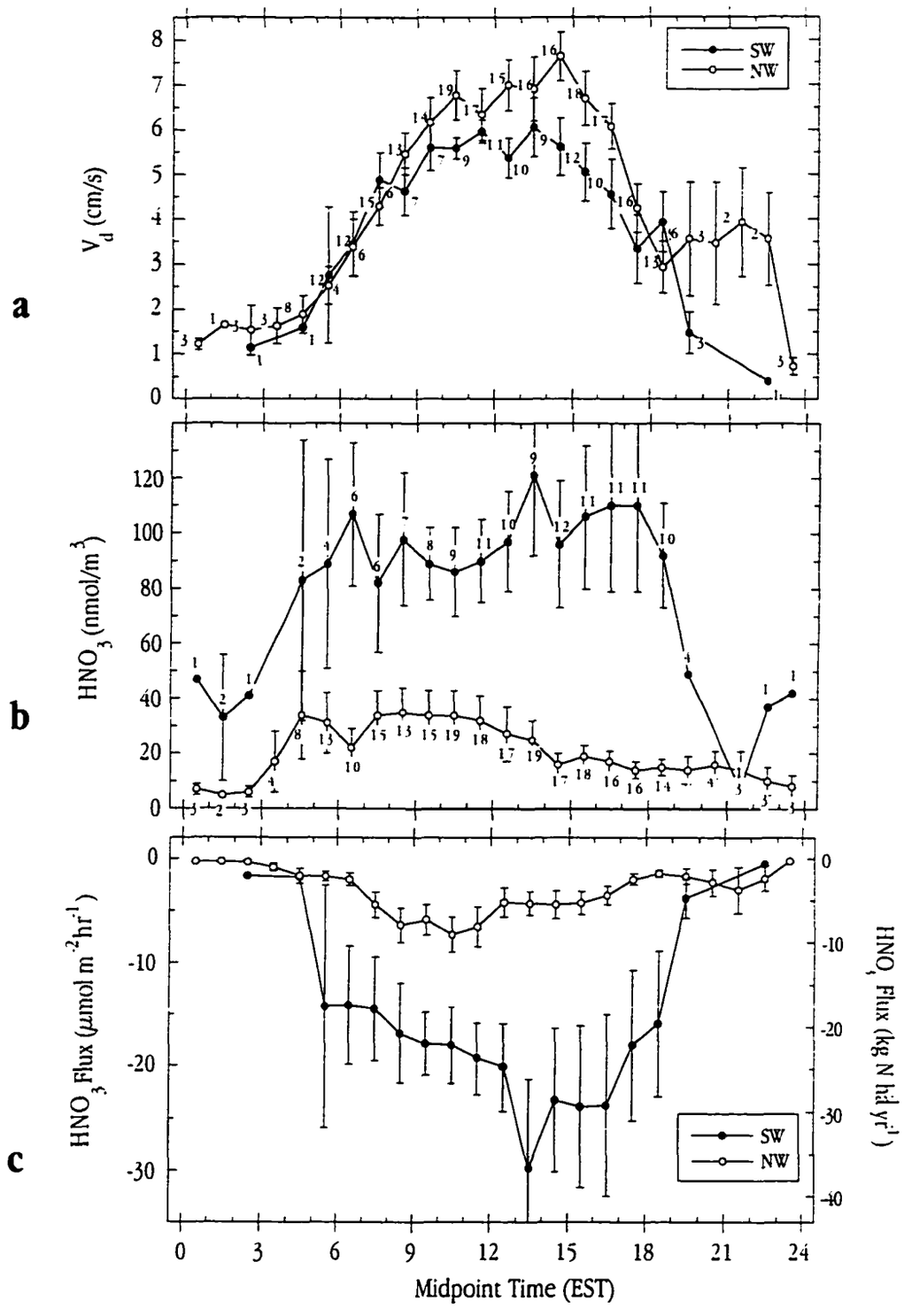

Figure 3.7. (a) Mean diel cycle of DDIM HNO_3 deposition velocity for the SW (filled symbol) and NW (open symbol) wind sectors during summertime sampling periods. Vertical bars correspond to standard error of mean. Values above or below symbols are number of samples.; (b) Same as Figure 3.7a, except for atmospheric HNO_3 concentration; (c) Same as Figure 3.7a, except for DDIM HNO_3 flux. Number of samples averaged are same as in Figure 3.7b.

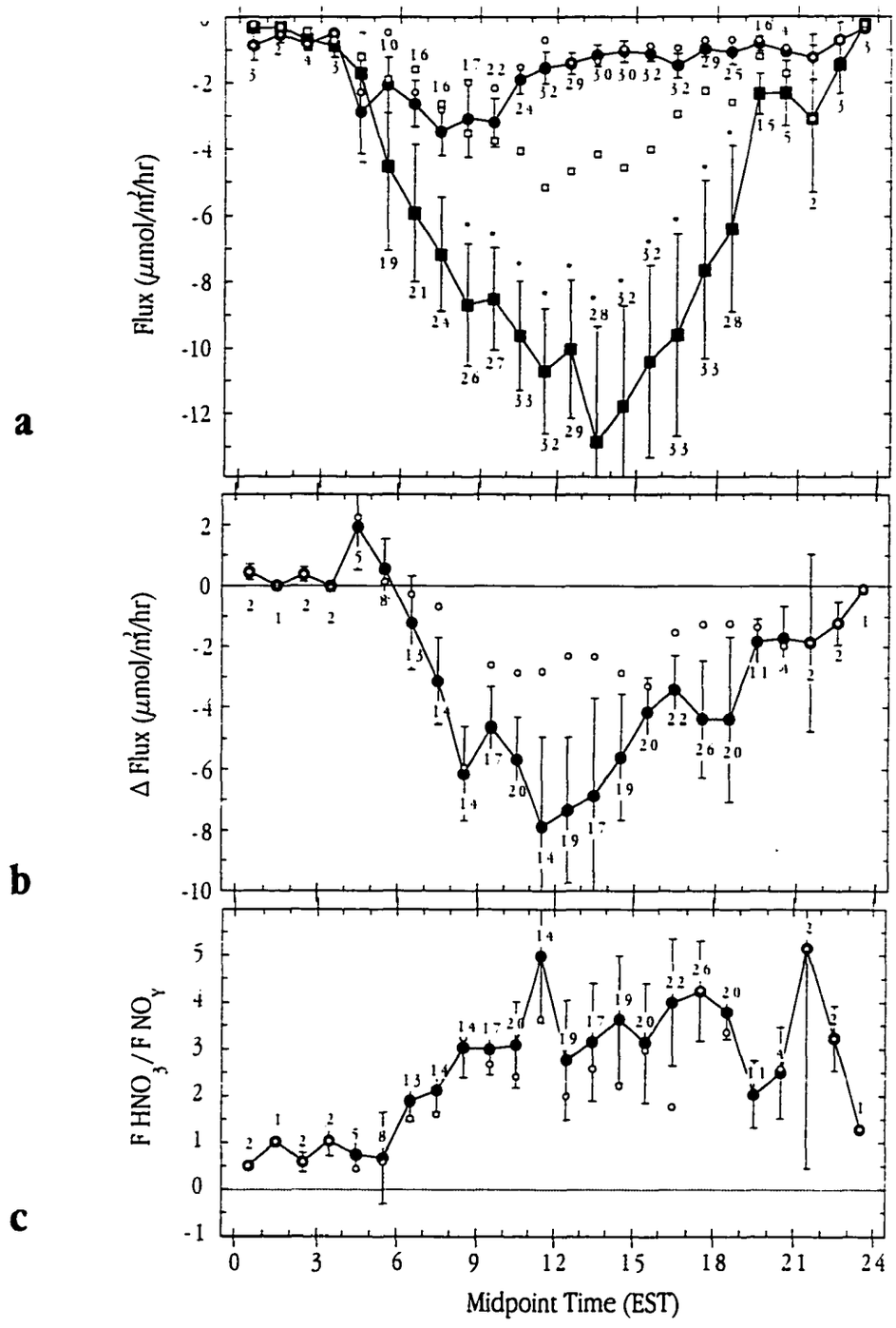

Figure 3.8 (a) Mean (filled symbol) and median (open symbol) diel cycle of DDIM HNO_3 (squares) and eddy NO_Y (circles) fluxes at 29-m for HNO_3 summertime sampling periods. Asterisks indicate mean fluxes of HNO_3 and NO_Y are significantly different ($p < 0.05$). Vertical bars correspond to standard error of mean. Values above or below symbols are number of samples.; (b) Same as Figure 3.8a. except for difference between HNO_3 and NO_Y fluxes. (c) Same as Figure 3.8a, except for ratio of DDIM HNO_3 flux to eddy NO_Y flux.

that HNO_3 is always depositing. Consequently, this may be considered another source of difference between the inferential HNO_3 and eddy covariance NO_Y fluxes. To minimize this storage effect and more accurately portray the central tendency of the flux comparison, the upper and minimum 5% of the data as well as any time periods with a negative Δ HNO_3 (Table 3.1) were removed from Figures 8b and 8c and the flux ratio in Table 3.4.

4.4.3 Bias in inferential HNO_3 flux measurements

While the inferential framework only allows for a one dimensional flux to occur , the assumption of only deposition is quite good for HNO_3, except for the instances of canopy storage described above. Additionally, the HNO_3 DDIM flux may be systematically biased if [HNO_3] and V_d are strongly correlated [Meyers et al., 1991]. Overall, [HNO_3] and V_d are generally uncorrelated, primarily due to the fact that HNO_3 concentrations are considerably higher in winds from the SW[Lefer et al., 1997] while the friction velocity and hence the V_d are not significantly different between the SW and NW wind sectors (Figure 3.7). Since winds from the SW contain the highest HNO_3 levels, hence result in the largest HNO_3 fluxes (Figure 3.7), it is worthwhile to investigate potential bias in these values.

Meyers et al. [1991] derived the following relationship to account for systematic bias resulting from this auto-correlation:

$$F = \sum V_d \cdot [HNO_3] = \overline{V_d} \cdot \overline{[HNO_3]} + \overline{V_d' \cdot [HNO_3]'} = \overline{V_d} \cdot \overline{[HNO_3]} + \sigma_{v_d} \sigma_{HNO_3} r_{v_d HNO_3} \quad [13]$$

where $\overline{V_d}$ and $\overline{[HNO_3]}$ are long-term averages, primes are deviations from the average, σ is the standard deviation, and r is the correlation coefficient. Due to the lack of sub-hourly HNO_3 sample resolution, it is not possible to evaluate the bias in our one hour fluxes. Consequently, 56 days with more than 10 hours of data coverage were used to calculate sums of the hourly HNO_3 fluxes on each day ($\sum$hourly). The $\sum$hourly fluxes were compared to daily average (DA) fluxes calculated by multiplying together the 10+ hour (daily) averages of V_d and [HNO_3] for each of the 56 days. Due to the poor general correlation overall, the "daily" averaging only underestimated the HNO_3 flux by less than 4%. As a worst case scenario, the more highly correlated ($r^2 = 0.53$) mean diel cycles of V_d and [HNO_3] for the SW sector (Figure 3.7) were used to perform the same comparison. For this model day, the sum of the hourly fluxes was -12.6 μmol m^{-2} hr^{-1} compared to the "daily" flux of -13.6 μmol m^{-2} hr^{-1}. The 8% deficit was accounted for by adding the $\sigma_{v_d} \sigma_{HNO_3} r_{v_d HNO_3}$ correction term which resulted in an adjusted "daily" flux of -13.7 μmol m^{-2} hr^{-1}. From this analysis it appears that the systematic error

due to the correlation of V_d and $[HNO_3]$ is generally small for this dataset and at most contributes a negative bias of less than 8%.

Although only a few samples were collected at night, it appears that between 1900-0700 EST that the mean HNO_3 and NO_Y fluxes not significantly different ($p > 0.05$) (Figure 3.8a). The greatest differences between the HNO_3 and NO_Y fluxes occur in the early afternoon (Figure 3.8) and when surface winds are from the SW wind sector (Table 3.4). Since these are the same general conditions in which HNO_3 levels are highest [Lefer et al., 1997], this may indicate a systematic bias to the DDIM flux estimates.

3.5 Conclusions

The HNO_3 deposition velocity over a fully leafed northeastern mixed forest was found to be ≈ 5 cm s^{-1} and shows diel variation resulting from changes in atmospheric turbulence. Estimates of HNO_3 deposition by both MBR and DDIM methods yielded similar values, indicating that the surface resistance of the forest canopy to the dry deposition of HNO_3 is very small or zero. Our inferential estimates of HNO_3 deposition suggest that the concentration of HNO_3 plays a larger role than atmospheric turbulence in determining the magnitude of the HNO_3 flux to the canopy.

Overall, the average and median summertime inferential HNO_3 fluxes were -8.30 and -3.03 μmol m^{-2} hr^{-1}, respectively. Our estimates of HNO_3 deposition were typically three times greater than the measured eddy covariance NO_Y flux. The average difference between these two fluxes is not significant during nighttime hours and varies diurnally, showing the largest difference in the afternoon. The magnitude of this flux difference is significantly larger than the range of soil emissions of NO measured from U.S. and European forests. It is likely that measurement errors or biases, tower siting issues, storage effects, and the fluxes of other NO_Y species are all contributing in some degree to the differences between the measured NO_Y and inferred HNO_3 fluxes.

A clearer understanding of net N deposition to mid-latitude forests will require a concerted effort to obtain more measurements of the atmosphere-biosphere exchange of both HNO_3 and NO_Y. The comparison of these data to model results, as well as an examination of the DDIM models themselves, is vital before HNO_3 deposition can be confidently applied to forest ecosystems. This effort becomes more essential when one considers that inferential models are commonly used to calculate HNO_3 deposition at dry deposition monitoring sites in this country and elsewhere.

3.6 Acknowledgments

This research was funded by the US Department of Energy's (DOE) National Institute for Global Environmental Change (NIGEC) through the NIGEC Northeast Regional Center at Harvard University (DOE Cooperative Agreement DE-FC03-90ER61010). Financial support does not constitute an endorsement by the DOE of the views expressed in this article/report. The work at the University of New Hampshire (UNH) is sported by subcontract 901214-HAR#4 from Harvard University, under the Northeast Regional Center of NIGEC, to the Research Foundation of UNH. The excellent technical assistance of Eric Scheuer and comments by Jack Dibb are gratefully acknowledged

3.7 References

Aber, J.D., Nitrogen cycling and nitrogen saturation in temperate forest ecosystems, *Trends in Ecology and Evolution*, 7 (7), 220-223, 1992.

Aber, J.D., K.J. Nadelhoffer, P. Steudler, and J.M. Melillo, Nitrogen saturation in northern forest ecosystems. *BioScience*, *39* (6), 378-386, 1989.

Åren, G., Model analysis of some consequences of acid precipitation on forest growth, in *Ecological effects of acid deposition*, pp. 233-244, National Swedish Environment Protection Board, Solna, 1983.

Brook, J.R., F. Di-Giovanni, S. Cakmak, and T.P. Meyers, Estimation of dry deposition velocity using inferential models and site-specific meteorology—uncertainty due to siting of meteorological towers, *Atmospheric Environment*, *31* (23), 3911-3919, 1997.

Bytnerowicz, A., P.R. Miller, D.M. Olszky, P.J. Dawson, and C.A. Fox, Gaseous and particulate air pollution in the San Gabriel Mountains of southern California, *Atmospheric Environment*, *21*, 1804-1814, 1987.

Dollard, G.J., D.H.F. Atkins, T.J. Davies, and C. Healy, Concentrations and dry deposition velocities of nitric acid, *Nature*, *326*, 481-483, 1987.

Droppo, J.G., Concurrent measurements of ozone dry deposition using eddy correlation and profile flux methods, *Journal of Geophysical Research*, *90*, 2111-2118, 1985.

Dyer, A.J., and B.B. Hicks, Flux-gradient relationships in the constant flux layer, *Quart. J. Royal Meteorol. Soc.*, *96*, 715-721, 1970.

Erisman, J.W., Acid deposition to nature areas in the Netherlands: Part I. methods and results, *Water, Air, and Soil Pollution*, *71*, 51-80, 1993.

Garratt, J.R., and B.B. Hicks, Momentum, heat, and water vapour transfer to and from natural and artificial surfaces, *Quart. J. Royal Meteorol. Soc.*, *99*, 680-687, 1973.

Geigert, M.A., N.P. Nikolaidis, D.R. Miller, and J. Heitert, Deposition rates for sulfur and nitrogen to a hardwood forest in northern Connecticut, USA, *Atmospheric Environment*, *28* (9), 1689-1697, 1994.

Goulden, M.L., J.W. Munger, S.-M. Fan, B.C. Daube, and S.C. Wofsy, Measurements of carbon sequestration by long-term eddy covariance: methods and a critical evaluation of accuracy, *Global Change Biology*, *2*, 169-182, 1996.

Gschwandtner, G., K. Gschwandtner, K. Eldridge, C. Mann, and D. Mobley, Historic emissions of sulfur and nitrogen oxides in the United States from 1900 to 1980, *Journal of the Air Pollution Control Association*, *36*, 139-149, 1986.

Gunderson, P., Nitrogen deposition and the forest nitrogen cycle, *Forest Ecology and Management*, *44*, 15-28, 1991.

Hanson, P.J., and S.E. Lindberg, Dry deposition of reactive nitrogen compounds: a review of leaf, canopy, and non-foliar measurements, *Atmospheric Environment*, *25A* (8), 1615-1634, 1991.

Hicks, B.B., D.D. Baldocchi, T.P. Meyers, R.P. Hosker Jr., and D.R. Matt, A preliminary multiple resistance routine for deriving dry deposition velocities from measured quantities, *Water, Air, and Soil Pollution*, *36*, 311-330, 1987.

Hicks, B.B., and T.P. Meyers, Measuring and modelling dry deposition in mountainous areas. In *Acid deposition at high elevation sites*, edited by M.H. Unsworth and D. Fowler, pp. 541-552, Kluwer Academic Publishers, Dordrecht, 1988.

Hosker, R.P., Jr., and S.E. Lindberg, Review: atmospheric deposition and plant assimilation of gases and particles, *Atmospheric Environment*, *16*, 889-910, 1982.

Huebert, B.J., and C.H. Robert, The dry deposition of nitric acid to grass, *Journal of Geophysical Research*, *90* (D1), 2085-2090, 1985.

Kauppi, P.E., K. Mielikäinen, and K. Kuusela, Biomass and carbon budget of European forests, 1971-1990, *Science*, *256*, 70-74, 1992.

Klemm, O., R.W. Talbot, D.R. Fitzjarrald, K.I. Klemm, and B.L. Lefer, Low to middle tropospheric profiles and biosphere/troposphere fluxes of acidic gases in the summertime Canadian Taiga, *Journal of Geophysical Research*, *99* (D1), 1687-1698, 1994.

Kramm, G., and R. Dlugi, Modelling of the vertical fluxes of nitric acid, ammonia, and ammonium nitrate, *Journal of Atmospheric Chemistry*, *18*, 319-357, 1994.

Lamersdorf, N.P., and M. Meyer, Nutrient cycling and acidification of a northwest German forest site with high atmospheric nitrogen deposition, *Forest Ecology and Management*, *62*, 323-354, 1993.

Lee, G., L. Zhuang, B.J. Hubert, and T.P. Meyers, Concentration gradients and dry deposition of nitric acid vapor at the Mauna Loa Observatory, Hawaii, *Journal of Geophysical Research*, *98* (D7), 12,661-12,671, 1993.

Lefer, B.L., and R.W. Talbot, Aerosol nitrate and ammonium at a northeastern U.S. site, *Atmospheric Environment*, *submitted December* 1997.

Lefer, B.L., R.W. Talbot, and J.W. Munger, Nitric acid and ammonia at a rural northeastern U.S. site, *Journal of Geophysical Research*, *submitted December* 1997.

Logan, J.A., Nitrogen oxides in the troposphere: global and regional budgets, *Journal of Geophysical Research*, *88* (C15), 10,785-10,807, 1983.

Meixner, F.X., H.H. Franken, J.H. Duijzer, and R.M. van Aalst, Dry deposition of gaseous HNO_3 to a pine forest, in *Proceedings of the 16th International Technical Meeting on Air Pollution Modeling and its Applications*, edited by H. van Dop, pp. 23-35, Plenum Publishing Corporation, Lindau, Germany, 1988.

Meyers, T.P., and B.B. Hicks, Dry deposition of O_3, SO_2, and HNO_3 to different vegetation in the same exposure environment, *Environmental Pollution*, *53*, 13-25, 1988.

Meyers, T.P., B.J. Huebert, and B.B. Hicks, HNO_3 deposition to a deciduous forest, *Boundary-Layer Meteorology*, *49*, 395-410, 1989.

Meyers, T.P., B.B. Hicks, R.P.J. Hosker, J.D. Womack, and L.C. Satterfield, Dry deposition inferential measurement techniques–II. Seasonal and annual deposition rates of sulfur and nitrate, *Atmospheric Environment*, *25A* (10), 2361-2370, 1991.

Meyers, T.P., M.E. Hall, S.E. Lindberg, and K. Kim, Use of the modified Bowen-ratio technique to measure fluxes of trace gases, *Atmospheric Environment*, *30* (19), 3321-3329, 1996.

Moore, K.W., D.R. Fitzjarrald, R.K. Sakai, M.L. Goulden, J.W. Munger, and S.C. Wofsy, Seasonal variation in radiative and turbulent exchange at a deciduous forest in central Massachusetts, *Journal of Applied Meteorology*, *35*, 122-134, 1996.

Müller, H., G. Kramm, F. Meixner, G.J. Dollard, D. Fowler, and M. Possanzini, Determination of HNO_3 dry deposition by modified Bowen ratio and aerodynamic profile techniques, *Tellus*, *45B*, 346-367, 1993.

Munger, J.W., S.C. Wofsy, P.S. Bakwin, S.-M. Fan, M.L. Goulden, B.C. Daube, and A.H. Goldstein, Atmospheric deposition of reactive nitrogen oxides and ozone in a temperate deciduous forest and a subarctic woodland: 1. Measurements and mechanisms, *Journal of Geophysical Research*, *101* (D7), 12,639-12,657, 1996.

Munger, J.W., S.-M. Fan, P.S. Bakwin, M.L. Goulden, A.H. Goldstein, A.S. Colman, and S.C. Wofsy, Regional budgets for nitrogen oxides from continental sources: variations of rates for oxidation and deposition with season and distance from source regions, *Journal of Geophysical Research*, *in press*, 1997.

NADP/NTN, National Atmospheric Deposition Program/National Trends Network (NRSP-3), NADP/NTN Coordination Office, Natural Resource Ecology Laboratory, Colorado State University, Fort Collins, Colorado, February 17, 1997.

Nilsson, J., Critical loads for sulphur and nitrogen, in *Air Pollution and Ecosystems, Proc. Symp.*, edited by P. Mathy, pp. 85-91, D. Reidel Publishing Company, Dordrecht, Grenoble, 1978.

Peterson, B.J., and J.M. Melillo, The potential storage of carbon caused by eutrophication of the biosphere, *Tellus*, *37B*, 117-127, 1985.

Raupach, M.R., Anomalies in flux-gradient relationships over forest, *Boundary Layer Meteorology*, *16*, 467-486, 1979.

Schell, R.W., A historical perspective of atmospheric chemicals deposited on a mountain top peat bog in Pennsylvania, *International Journal of Goal Geology*, *8*, 147-173, 1987.

Schulze, E.-D., Air pollution and forest decline in a spruce *Picea abies* forest, *Science*, *244*, 776-783, 1989.

Schindler, D.W., and S.E. Bayley, The biosphere as an increasing sink for atmospheric carbon: estimates from increased nitrogen deposition, *Global Biogeochemical Cycles*, *7* (4), 717-734, 1993.

Talbot, R.W., A.S. Vijgen, and R.C. Harriss, Measuring tropospheric HNO_3: problems and prospects for nylon filter and mist chamber, *Journal of Geophysical Research*, *95* (D6), 7553-7542, 1990.

Vann, D.R., G.R. Strimbeck, and A.H. Johnson, Effects of ambient levels of airborne chemicals on freezing resistance of red spruce foliage, *Forest Ecology and Management*, *51*, 69-79, 1992.

Walton, S., M.W. Gallagher, and J.H. Duyzer, Use of a detailed model to study the exchange of NO_x and O_3 above and below a deciduous canopy, *Atmospheric Environment*, *31* (18), 2915-2931, 1997.

Wesely, M.L., and B.B. Hicks, Some factors that affect the deposition rates of sulfur dioxide and similar gases on vegetation, *Journal of the Air Pollution Control Association*, *27* (11), 1110-1116, 1977.

Williams, E.J., and F.C. Fehsenfeld, Measurement of soil nitrogen oxide emissions at three North American ecosystems, *Journal of Geophysical Research*, *96* (D1), 1033-1042, 1991.

CHAPTER 4

AEROSOL NITRATE AND AMMONIUM AT A NORTHEASTERN U.S. SITE

Abstract

Summertime measurements of the atmospheric concentrations and aerodynamic size distributions of NH_4^+, NO_3^- and other major aerosol species were made at a rural site in central Massachusetts between 1991-1995 to examine the nature of N aerosol chemistry and to estimate the importance of N aerosol dry deposition to the Harvard Forest. This northeastern U.S. site is primarily influenced by air masses advected from the rural northwest and more urban southwest wind sectors. The bulk aerosol can be described as a mixture of submicron ammonium (bi)sulfate aerosols with smaller amounts of soil derived particles. Approximately one third of the samples had an anion surplus of greater than 20%, which was assumed to result from unmeasured H^+ ions. Aerosols in surface winds from the southwest were rarely neutralized, especially when SO_4^{2-} concentrations were greater than ≈ 100 nmol m^{-3}. This result suggests that this may be an upper limit for atmospheric NH_x ($NH_3 + NH_4^+$) in this source region. Aerosol NO_3^- was observed at concentrations 4-8 times lower than NH_4^+, and while occasionally found in the fine mode, the majority of the NO_3^- was associated with supermicron soil derived Ca^{2+}. Elevated early morning NO_3^- concentrations not related to coarse soil particles were attributed to nighttime heterogeneous NO_3^- aerosol production via N_2O_5 or NO_3. Estimates of aerosol dry deposition suggest that despite the considerably higher NH_4^+ concentrations, the higher deposition velocity of supermicron NO_3^- results in similar dry deposition rates for both aerosol species (≈ 1 kg ha^{-1} yr^{-1}). These estimated aerosol fluxes are significantly smaller than the measured wet N input (≈ 8 kg ha^{-1} yr^{-1}) and, when combined with estimates of gaseous HNO_3 and NH_3 dry deposition, account for 20-40% of the total summertime N inputs to this forest ecosystem.

4.1 Introduction

Industrial and agricultural anthropogenic activities, including fossil fuel combustion, animal husbandry, and fertilizer application, have increased the fluxes of nitrogen oxides (NO_x = NO and NO_2) and ammonia (NH_3) to the atmosphere. Since NH_3 acts as the principal neutralizing agent for atmospheric acids and NO_x is involved in both the production and destruction of tropospheric ozone (O_3), changes in the mixing ratios of these nitrogen gases directly impact the chemistry of the troposphere. The human induced enhancement of NO_x and NH_3 emissions have also accelerated the rate of atmospheric N deposition [Schell, 1987]. Enhanced N deposition may have a fertilizing effect on N-limited ecosystems [Peterson and Melillo, 1985; Schindler and Bayley, 1993]. Forested portions of the terrestrial biosphere receiving N in excess of its biological needs have also experienced symptoms of nitrogen saturation [Aber et al., 1989] such as; soil acidification [van Breemen et al., 1987], nitrate (NO_3^-) leaching [van Miegroet et al., 1992], and decreased stand growth rates [Schulze, 1989].

The primary removal mechanisms of NO_x are through the oxidation of NO_2 to produce nitric acid (HNO_3) which, like NH_3, is highly soluble in precipitation and readily dry deposits to most surfaces. Another possible fate, for both HNO_3 and NH_3, is reaction with a gas or particle to produce N containing aerosols which are subsequently wet or dry deposited. A common example is the irreversible combination of NH_3 with sulfuric acid (H_2SO_4) to form submicron ammonium bisulfate (NH_4HSO_4) and/or ammonium sulfate ($(NH_4)_2SO_4$) aerosols. Alternatively, NH_3 can also react with HNO_3 to produce fine ammonium nitrate (NH_4NO_3) particles which are commonly unstable at the higher temperatures and relative humidities characteristic of the troposphere [Stelson et al., 1979; Stelson and Seinfeld, 1982]. In contrast, coarse mode (diameter $\geq 2.5\,\mu m$) aerosol NO_3^- can be produced by adsorption of HNO_3 on basic soil [Wolff, 1984] or seasalt particles [Savoie and Prospero, 1982]. A third mechanism of aerosol NO_3^- formation involves nighttime reactive N chemistry which produces gaseous NO_3 and N_2O_5, both of which may readily dissolve into wet aerosol surfaces to create particulate NO_3^- [Ehhalt and Drummond, 1982; Parrish et al., 1986; Li et al., 1993].

Several studies have strived to determine the relative importance of wet and dry atmospheric N inputs to forest ecosystems [e.g., Lovett and Lindberg, 1993; Geigert et al., 1994]. While many questions still remain, it has become apparent that wet deposition is considerably easier to quantify. Compared to gaseous dry deposition, aerosol deposition has received far less modeling and measurement attention [Erisman et al., 1997]. Thus far, the modeling of particle deposition to vegetated surfaces has employed process oriented, bulk resistance, or empirical approaches. Process oriented models describe the efficiency of particle removal

processes such as impaction, interception, and Brownian diffusion as a function of particle size and surface/canopy characteristics [Slinn, 1982]. In contrast, particle resistance models are quite similar to gaseous resistance models as both use meteorological variables to describe the aerodynamic resistance to transport through a turbulent surface layer and then through a viscous boundary layer surrounding vegetation elements [Hicks et al., 1987].

Eddy-covariance measurements of particle deposition to forested systems have confirmed model predictions that particle deposition velocities (V_d) are greater for larger particles and at unstable atmospheric conditions [Gallagher et al., 1997]. Process models by Slinn [1982] and Ruijgrok et al., [1997] have also considered additional effects, such as how surface wetness reduces particle rebound and the growth of submicron hydroscopic particles (e.g., ammonium sulfate) to diameters of several microns at high relative humidities (i.e., > 80%). Recent efforts have also focused on comparing these different models to each other and to traditional bulk deposition measurement techniques such as net throughfall [Erisman et al. , 1997].

In conjunction with studies determining the mixing ratios of NO_x, NO_y, HNO_3, and NH_3 [Munger et al., 1996; Lefer et al., 1997a] as well as the deposition fluxes of NO_y, HNO_3, and aqueous NO_3^- [Munger et al., 1996,1997; Lefer et al., 1997b], hourly measurements of particulate NH_4^+ and NO_3^- were obtained above and below a mixed temperate forest for a wide range of environmental conditions. The purposes of this study were: (1) to examine the importance of NH_4^+ and NO_3^- aerosols relative to aerosol acidity and other major ionic species at this rural site, (2) to determine the aerodynamic size distributions of the NH_4^+ and NO_3^- in these continental aerosols, (3) to identify the major N aerosol production pathways, and (4) to estimate summertime N aerosol inputs to this forested ecosystem and compare them to measured gaseous and precipitation N fluxes.

4.2 Methods

4.2.1 Site description

Located in a wooded, rural area of central Massachusetts, The Harvard Forest in Petersham (42°32', 72°11') is approximately 100 km west and northwest of the nearest large cities of Boston and Hartford, respectively. This 50 - 70 year old aggrading mixed forest (predominantly oak with maple, hemlock, and pine) has an average canopy height of 23-m near the 30-m Harvard University sampling tower. Harvard Forest typically receives air masses from both urban and rural source regions to the southwest (SW) and northwest (NW), respectively [Munger et al., 1996]. Significantly higher nitric acid (HNO_3) and lower ammonia (NH_3) mixing

ratios are associated with SW surface winds, while the reverse holds true for winds from the rural NW [Lefer et al., 1997a]. Other studies at this site have shown NH_3 levels to be low [Tjepkema et al., 1981], apparently suppressed by high levels of atmospheric sulfate [Lefer et al., 1997a]. In addition to the aerosol results discussed here, other related measurements at Harvard Forest include NO_y and O_3 deposition [Munger et al., 1996], HNO_3 deposition estimates [Lefer et al., 1997b], and radiative and turbulent exchange [Moore et al., 1996]. The University of New Hampshire (UNH) Harvard Forest (1991-1995) gas and aerosol dataset is available by anonymous ftp at io.harvard.edu.

4.2.2 Aerosol sampling methods

Between 1991-1995 hourly aerosol samples were continuously collected for 12-30 hour periods on 70 mostly summertime days [Lefer et al., 1997a]. These samples were collected on a 47-mm teflon membrane (Zefluor™, Gelman Products Inc.) in a custom made open-face teflon filter holder without a backup filter support. This filter holder assembly served as the prefilter to a mist chamber water soluble gas sampler. Potential positive and negative aerosol nitrate and ammonium sampling artifacts are discussed in Lefer et al. [1997a]. Aerosol samples were stored in a freezer for less than a week until the water soluble fraction was extracted in teflon tubes by application of 200 μL of MeOH and then two 5.0 mL aliquots of deionized water. Aerosol extracts were preserved with 100 μl of $CHCl_3$ and stored in 30-mL high density polyethylene amber bottles.

The hourly sampling protocol involved using three parallel samplers suspended at heights of 11, 24, and 29-m above ground to collect 45 min. integrated samples, with the remaining 15 min. available to exchange filter holders, collect field blanks, and remove samples from the mist chamber. Operating at a flowrate of 30 standard liters per minute (slpm), this downward-facing filter collected a bulk sample of aerosol particles with a diameter between ≈ 10 nm [Dibb and Anderson, 1996 personal communication] and at least 50 μm for windspeeds typically observed at this site [Davies, 1968; Davies and Subari, 1982]. The flowrate and volume of the aerosol/mist chamber system was determined by three 0-50 slpm Teledyne Brown Engineering (Hampton, VA) integrating mass flowmeters. These three flowmeters were intercompared before and after each field mission (n=19) and typically agreed to within 8%. The sample volumes of the 11-m and 24-m levels were adjusted to agree with the flowmeter at the 29-m level. This flowmeter was recalibrated by the manufacturer each winter and was always found to be within 5% of the previous year.

A Graseby-Andersen (Smyrna, GA) Mark II cascade impactor was outfitted with Zefluor™ telfon membranes in the pre-separator, on the 8 collection plates behind each stage, and as a final back up filter to

obtain aerosol samples in 10 aerodynamic size fractions between approximately 25 and 0.035 μm. The Mark II impactor was mounted at the top of the forest canopy (≈ 22-m above ground) and operated at flowrate of 28.3 standard liters per minute (slpm) as monitored by a 0-50 slpm Teledyne Brown Engineering integrating mass flowmeter. Individual sampling runs were integrated for 48-72 hours to ensure sufficient aerosol mass on each impactor stage. Impactor filters were treated and analyzed in an identical manner to the aerosol sample processing procedures described above and in section 4.2.3. Integrated impactor samples were during the following mostly summertime periods in 1995 (12-15 June) and 1996 (11-13 March, 02-05 May, 31 May - 02 June, 21-23 September, and 26-29 September). Potential cascade impactor errors include the deposition of particles to internal surfaces (i.e., interstage losses) and the bounce-off of particles from an upper to a lower impactor stage [Rao and Whitby, 1987].

4.2.3 Chemical analysis

Aerosol samples were analyzed within 2 months of collection on two independent Dionex ion chromatographic (IC) systems (anion and cation) containing Rheodyne (Model 9010) injection valves and Dionex self regenerating chemical conductivity suppression. The anion IC was equipped with a Dionex AS4 column using a 0.4 mM Na_2CO_3 eluant. This anion system was used to quantify several aqueous ions including nitrate (NO_3^-), oxalate $(COO^-)_2$, and sulfate (SO_4^{2-}). Mono- and divalent cations including sodium (Na^+), ammonium (NH_4^+), calcium (Ca^{2+}), and magnesium (Mg^{2+}) were quantified on an Dionex CS-12 column with 20 mM methylsulfonic acid eluant. We used commercially available IC standards from E. Merck (Darmstat, Germany) and found that they compared to within 3% of NIST standards for NO_3^-, SO_4^{2-}, and NH_4^+. Sample peak areas were analyzed and correlated to 8 point calibration curves using Hewlett-Packard Chemstation (HP 3365 Series 2, version A.03.33). Both IC systems have an analytical precision of 3-5% for the species of interest here.

A series of teflon filter blanks were collected for each 5 hours of sampling. Aerosol blanks were attached to each mist chamber sampler, briefly hoisted up the tower, and subsequently handled and processed exactly like actual aerosol samples. The average (± s. d.) blank values for each species that were subtracted from the aerosol samples as follows (in nmol mL^{-1}): Na^+ (0.434 ± 0.923), NH_4^+ (0.072 ± 0.094), K^+ (0.257 ± 0.236), Mg^{2+} (0.023 ± 0.027), Ca^{2+} (0.107 ± 0.123), NO_3^- (0.154 ± 0.252), SO_4^{2-} (0.047 ± 0.097), $(COO^-)_2$ (below detection limit of 0.02), Cl^- (0.087 ± 0.092), and PO_4^{3-} (0.557 ± 0.912). Using an extraction water volume of 10.0 mL, and average air volume of 1.35 m^3, and twice the blank value (or detection limit) results in calculated detection limits (in nmol m^{-3}) for each species of: Na^+ (6.43), NH_4^+ (1.07), K^+ (3.81), Mg^{2+} (0.34).

Ca^{2+} (1.59), NO_3^- (2.28), SO_4^{2-} (0.70), $(COO^-)_2$ (0.30), Cl^-(1.29), and PO_4^{3-} (8.25). The uncertainties assigned to the reported aerosol concentrations were calculated using a propagation of errors analysis that placed equal weight on the following uncertainties associated with: IC system, air volume measurement, extract volume, and the variability of the blank. All the reported aerosol concentrations , except Na^{2+}, have an uncertainty of less than ± 20%. Due to the higher and more variable Na^{2+} blank values, Na^{2+} concentrations have an uncertainty of ± 30%.

Summertime (June, July, and August) aerosol data were edited according to the charge balance as described by the following ratio R:

$$R = \frac{[\Sigma Cations - \Sigma Anions]}{[\Sigma Cations + \Sigma Anions]} \quad [1]$$

where ∑Cations = sum of Na^+, NH_4^+, K^+, Mg^{2+}, and Ca^{2+} in neq. m^{-3} and ∑Anions = sum of SO_4^{2-}, NO_3^-, $(COO^-)_2$, Cl^-, and PO_4^{3-} also in neq. m^{-3}. Considering the analytical uncertainties of each ion concentration and the additive errors in the calculation of R, the 59% of the aerosol samples (n = 332) with R values within ± 0.2 were assumed to have a charge balance of essentially 1. R values greater than 0.2 most likely reflect problems typically signified by a missing a value for SO_4^{2-}, and consequently these 52 samples were removed from the dataset. The remaining 33% of the samples (n = 185) contained a significant surplus of anions (i.e. R < - 0.2) most likely resulting from an unmeasured hydrogen ions (H^+) [Pierson et al., 1989]. Thus, for all samples with R less than 0.2, the difference between the cationic and anionic equivalent concentrations was assumed to be equal to unmeasured H^+ ions.

4.2.4 N particle deposition estimates

The flux of an aerosol species can be defined as the product of the aerosol concentration and the dry deposition velocity (V_d) of the associated aerosol. Estimates of NH_4^+ aerosol V_d were calculated using empirical relationships established from aerodynamic gradient measurements of SO_4^{2-} deposition to a mature Douglas fir forest in Holland as observed by Wyers and Duyzer [1997], hereafter referred to as W&D97, to be:

$$V_{d(NH_4^+)} = 0.0444 u_*^{1.47} \quad [2]$$

where u_* is friction velocity. Given that this relationship was developed for a dense coniferous forest with a leaf area index (LAI) of more than 2 times greater than at Harvard Forest, a parameterization of submicron aerosol deposition to a grassland system [Wesely et al., 1985] is also included for comparison. For their grassland system, Wesely et al. [1985], hereafter referred to as W85, used the eddy covariance technique to empirically define the deposition for submicron sulfate particles as a function of turbulence and stability such that:

$$V_{d(NH_4^+)} = 0.002u_* \qquad \text{for stable conditions } (L > 0) \qquad [3]$$

and

$$V_{d(NH_4^+)} = 0.002u_*\left(1+(-300/L)^{2/3}\right) \qquad \text{for unstable conditions } (L < 0) \qquad [4]$$

where u_* is the friction velocity (cm s^{-1}) and L is the Monin-Obukhov stability length scale defined as:

$$L = -\rho C_p u_*^3 T / kgQ_H \qquad [5]$$

where ρ is air density, C_p is heat capacity of air, T is absolute air temperature, k is von Karmon's constant (0.4), g is the acceleration due to gravity, and Q_H is the sensible heat flux. Complementary to W&D97, Gallagher et al. [1997], hereafter referred to as G97, made eddy covariance measurements of submicron particles fluxes, also at the Speulder Forest in Holland, and modeled their empirical parameterization after W85 such that:

$$V_{d(NH_4^+)} = 0.0135u_*d_p\left(1+(-300/L)^{2/3}\right) \qquad [6]$$

where d_p is the diameter of an aerosol particle between 0.1-0.5 μm. The V_d of aerosol NO_3^- was assumed to be a function of turbulence such that:

$$V_{d(NO_3^-)} = 0.1u_* \qquad [7]$$

4.3 Results

4.3.1 Aerosol composition

Ammonium and SO_4^{2-} are the principle ionic constituents of the aerosol at Harvard Forest, together accounting for 50-80% of the measured charge in the water soluble fraction (Figure 4.1). Table 4.1 contains more detailed statistical information on these two dominant species as well as NO_3^- and H^+. On average, NH_4^+ is found at a level insufficient to neutralize all the SO_4^{2-}, suggesting that much of the aerosol was a mixture of NH_4HSO_4, $(NH_4)_2SO_4$, and on occasion H_2SO_4. Aerosols from rural NW windsector typically contained lower levels of NH_4^+ and SO_4^{2-} and a charge balance close to neutrality. In contrast, aerosols from the more urban SW sector had a median anionic surplus of approximately 13% or 32 neq. m^{-3} (Figure 4.1, Table 4.1). The SW aerosol was associated with significantly higher levels of NO_3^- and $(COO^-)_2$ and twice the total soluble aerosol mass (Table 4.1) as the aerosol in air masses from the less polluted NW. Aerosol NO_3^- was commonly found at concentrations some 4 to 8 times less than particulate NH_4^+ (Figure 4.1).

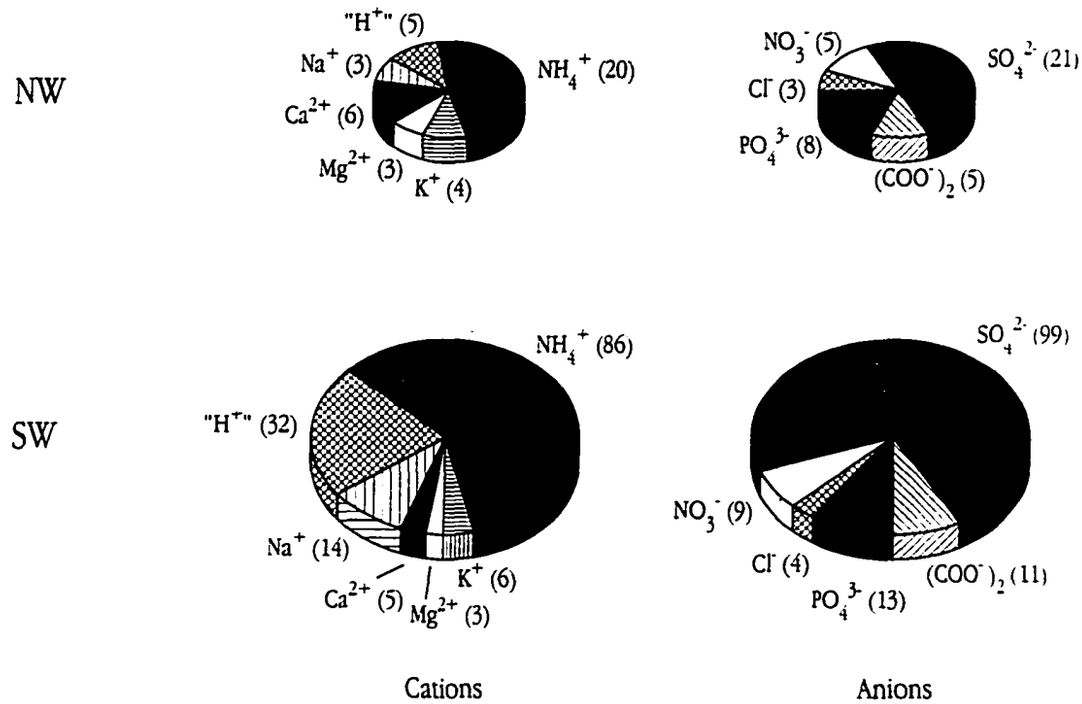

Figure 4.1 The 1991-1995 median summertime aerosol composition at 29-m. in nanoequivalents m^{-3} for northwest (NW = 270°-45°) and southwest (SW = 180°-270°) surface windsectors. "H^+" represents the total hydrogen ion concentration as estimated from the charge balance (see text). Sample number (n) for NH_4^+, SO_4^{2-}, and "H^+" was 224 for the NW and 138 for the SW sectors. Sample n for other species (NW, SW sectors respectively) was as follows: Na^+ (130, 77), Ca^{2+} (132, 109), Mg^{2+} (143, 112), K^+ (150, 117), NO_3^- (178, 120), $(COO^-)_2$ (99, 93), Cl^-(28, 7), and PO_4^{3-}(16, 21).

Table 4.1. Summary of major ionic species for Harvard Forest aerosol for summertime sampling between 1991-1995 at selected surface wind direction sectors[¶]. Statistics include: number of samples (n), 25th percentile (25%), standard deviation (s.d.), and 75th percentile (75%).

	Statistic	All Sectors	NW	E	SW
NH_4^+	n	517	224	113	138
(nmol m^{-3})	25%	12.8	8.51	21.5	27.9
	median	35.5	19.8	34.4	85.9
	mean	60.4	54.1	44.9	82.1[A]
	s.d.	71.1	71.8	38.3	58.6
	75%	94.3	69.4	57.5	119
SO_4^{2-}	n	517	224	113	138
(nmol m^{-3})	25%	7.93	5.91	11.1	19.9
	median	18.9	10.6	16.9	49.6
	mean	50.4	37.6	33.9	85.9[A]
	s.d.	71.7	56.7	42.5	76.9
	75%	62.1	34.7	44.5	145
NO_3^-	n	445	178	108	120
(nmol m^{-3})	25%	3.56	2.62	4.15	5.47
	median	6.31	4.92	5.44	9.41
	mean	9.77	7.75[B]	9.05	14.8[A]
	s.d.	10.2	7.54	8.05	14.4
	75%	11.9	10.1	11.6	18.7
"H^+"[‡]	n	517	224	113	138
(neq. m^{-3})	25%	-1.9	-2.1	-5.6	2.5
	median	6.1	4.7	0.9	31
	mean	39	20	20	93[A]
	s.d.	84	54	53	110
	75%	32	15	33	160
Molar Ratio	n	517	224	113	138
$[NH_4^+] / [SO_4^{2-}]$	25%	1.0	1.1	1.1	0.87
	median	1.5	1.6	1.7	1.2
	mean	1.6	1.7	1.7	1.3[A]
	s.d.	0.8	1.0	0.8	0.5
	75%	2.0	2.0	2.0	1.6
Total Soluble Mass	n	514	224	112	137
(g m^{-3})	25%	1470	1110	1850	3480
	median	3290	2180	2940	9800
	mean	6820	5440	4990	11400[A]
	s.d.	7430	7270	4420	8520
	75%	9800	5390	8050	18900

[¶]Northwest (NW) wind sector = 270-45°, east (E) = 45-180°, and southwest (SW) = 180-270°.
[A]Significantly greater than NW and E wind sectors ($p < 0.001$).
[B]Significantly less than E wind sector ($p < 0.05$).
[‡]"H^+" is assumed to be the difference between the $\sum$cations and $\sum$anions (see text).

Phosphate and Cl^- were present in less than 10% of the samples and were always in amounts less than 15% of the total sum of anions. While both species were included in the median composite Harvard Forest aerosol (Figure 4.1), their relevance to the overall ion balance at this site was minimal, thus they are not included in further discussion.

4.3.2 Size distributions of selected species

The average concentration normalized size distributions of NH_4^+ and SO_4^{2-} are quite similar with peak concentrations of both of these ions occurring in the same two impactor stages representing aerodynamic diameters between 0.43 and 1.1 μm (Figure 4.2). The average (± std. deviation) mass median diameter (MMD) of NH_4^+ and SO_4^{2-} for all the cascade impactor samples was determined to be 0.63 ± 0.07 and 0.64 ± 0.10 μm, respectively, which is similar to the acidic SO_4^{2-} average MMD of ≈0.7 μm reported by Pierson et al. [1989] for the eastern U.S.. The concentration normalized averages in Figures 2 and 3 represent impactors collected for a wind variety of atmospheric environments, in both polluted and clean air masses sampled between the months of March and October. For both NH_4^+ and SO_4^{2-}, the atmospheric concentrations were much higher in the air masses from the polluted SW, however , the concentration normalized aerodynamic size distributions for the NW and SW were indistinguishable from each other. This dominant submicron mode is characteristic of aerosols formed from gas-phase reactions and suggests that gaseous SO_2 is being oxidized to sulfuric acid (H_2SO_4) and/or reacting with NH_3 to form fine NH_4HSO_4 and $(NH_4)_2SO_4$.

Aerosol NO_3^- was typically associated with coarse particles having an average MMD of 4.8 ± 1.5 μm, which is slightly less than the MMD of 5.6 ± 0.84 μm observed for Ca^{2+} (Figure 4.3). All seven sampling events produced NO_3^- size distributions with a similar coarse mode, however two of these periods also contained a significant amount of accumulation mode submicron particles (0.43 - 1.1 μm). This phenomenon lowered the overall NO_3^- MMD and produced the relatively large standard deviation for the submicron range of the NO_3^- size distribution (Figure 4.3). The size distributions of NO_3^- and Ca^{2+} are similar, with the vast majority of the their respective mass in particles larger than 2.1 μm(Figure 4.3).

4.3.3 Aerosol species relationships

Aerosol NH_4^+ was always highly correlated with SO_4^{2-}. For lower concentrations of SO_4^{2-} (< 100 nmol m^{-3}), the NH_4^+/SO_4^{2-} molar ratio was commonly close to 2 and rarely less than 1, corresponding to $(NH_4)_2SO_4$ and a mixture of NH_4HSO_4 aerosols (Figure 4.4a). About 100 nmol m^{-3} of NH_4^+ appears to be a common upper limit of NH_x ($NH_3 + NH_4^+$) in air masses from the SW, since SO_4^{2-} concentrations above this same level were rarely neutralized. This relationship also suggests the presence of sulfuric acid (H_2SO_4) particles in these

polluted air masses. For comparison, Figure 4.4b shows fully neutralized aerosols observed during a week with less polluted air generally from the north and west wind sectors.

Despite the similarities between their size distributions, overall aerosol NO_3^- and Ca^{2+} were not highly correlated. However, NO_3^- and Ca^{2+} were correlated ($r^2 > 0.5$) in some individual air masses at NO_3^- to Ca^{2+} mole ratios ranging from 7 to 0.3 (Figure 4.5). In general, air masses with lower HNO_3 mixing ratios have lower aerosol NO_3^-, with the amount of Ca^{2+} as secondary factor. In some cases, elevated concentrations of aerosol NO_3^- were observed in the early morning and were not associated with enhanced levels of particulate Ca^{2+} (Figure 4.6).

Many of the aerosol species relationships described above occurred during an intensive sampling experiment in 09-20 June of 1995. This 11 day period was marked by a cold frontal passage followed by a period of warming air temperature as displayed by changes in air temperature, relative humidity, and wind direction (Figure 4.7). Corresponding changes in gas and aerosol levels are recorded in Figure 4.8. A cascade impactor run during this intensive collected a $(COO^-)_2$ size distribution that was quite similar to NH_4^+ and SO_4^{2-} (Figure 4.9).

4.3.4 Estimates of N particle deposition

The overall average summertime diel concentrations and corresponding estimates of V_d for NH_4^+ and NO_3^- are presented in Figure 4.10. Figure 4.11 displays the average diel N aerosol concentrations for the SW and NW windsectors. Overall NH_4^+ levels were generally around 60 nmol m^{-3} during the day and about a third lower at night. Air masses from the SW quadrant contained higher concentrations of NH_4^+ and NO_3^- during the day (Figure 4.11). Mean concentrations of aerosol NO_3^- are greatest in the first half of the day and gradually decrease through the night (Figures 10 and 11). For both species, the deposition models are highly dependent on u_* and thus display similar diel behavior for V_d. In the early afternoon, average hourly deposition velocities peaked at 2.3 and 6.2 cm s^{-1} for NH_4^+ and NO_3^-, respectively, while lower values were estimated for nighttime conditions (Figure 4.10). In Figure 4.10 the two Dutch parameterizations [Wyers and Duyzer, 1997; Gallagher et al., 1997] result in significantly greater NH_4^+ deposition velocities compared to the relationship derived for grassland system [Wesely et al., 1985]. Since u_* was not significantly different for the NW and SW windsectors, the calculated deposition velocities of NH_4^+ and NO_3^- did not change as a function of windsector. The overall maximum hourly average V_d for each species translates into deposition fluxes of 4.2 and 2.4 μmol N m^{-2} hr^{-1} for NH_4^+ and NO_3^-, respectively. In the late morning, higher N aerosol concentrations from the SW resulted in larger average NH_4^+ and NO_3^- deposition fluxes, both on the order of 5 μmol N m^{-2} hr^{-1} (Figure 4.11).

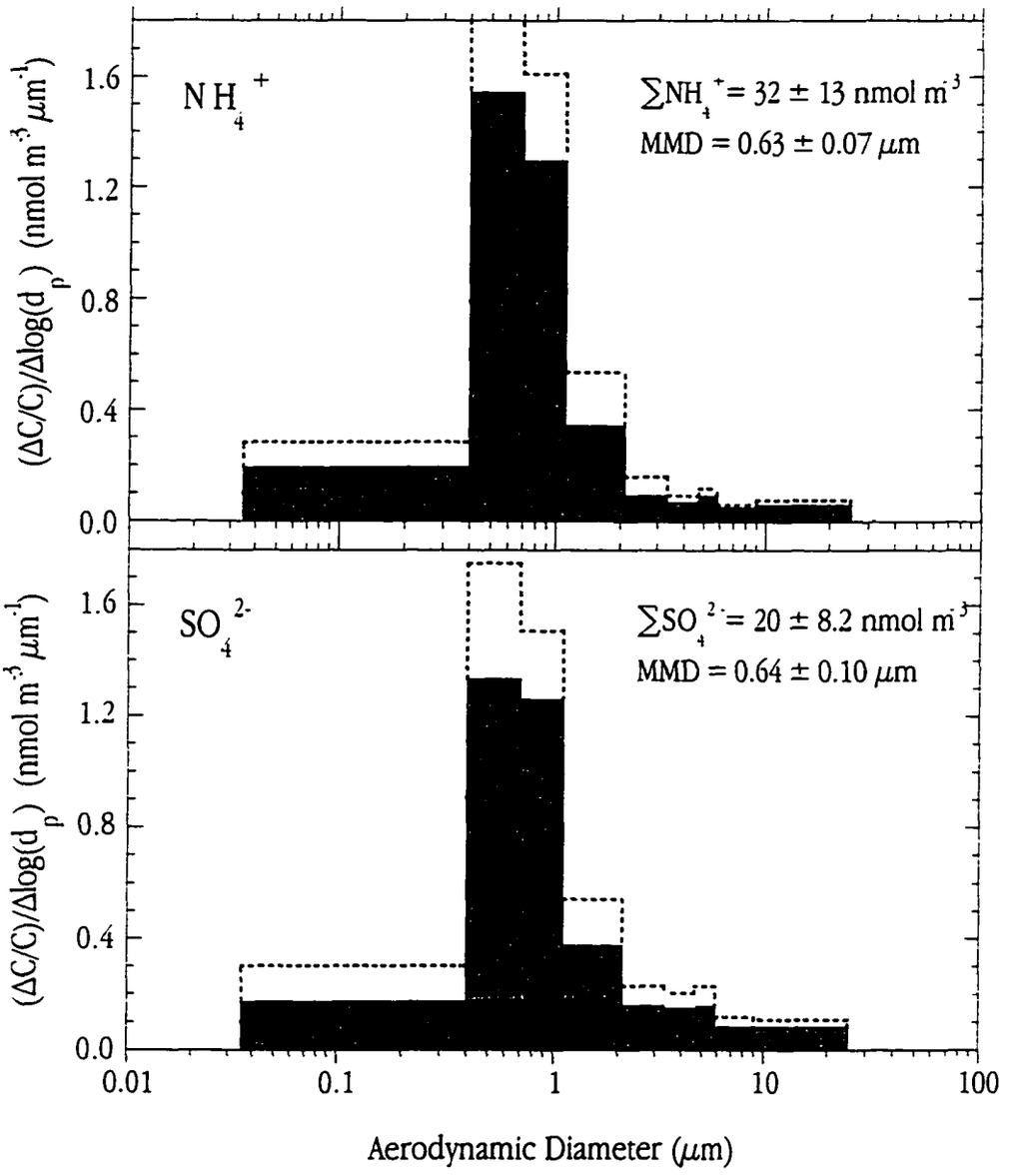

Figure 4.2 Normalized aerodynamic size distribution for aerosol sampled during summers of 1995 and 1996 (n = 7). Solid and dashed lines represent average and one standard deviation (above and below), respectively. The total of the 9 stages compared well with a bulk aerosol sample collected over the same time interval. The average (± std. dev.) concentration (a sum of the 9 stages) and mass median diameter (MMD) for the 7 impactor runs are also shown for both species.

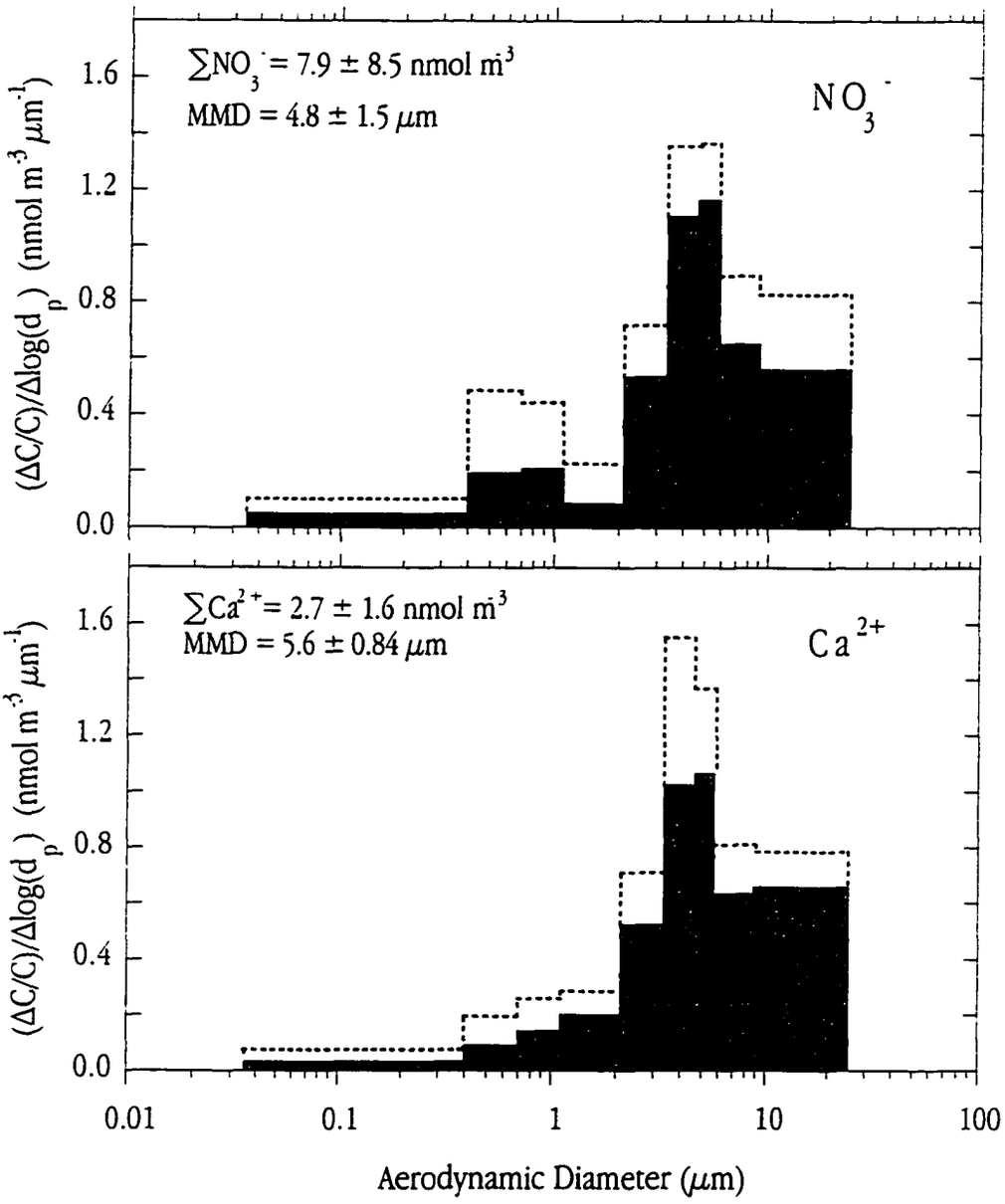

Figure 4.3 Normalized aerodynamic size distribution for aerosol sampled during summers of 1995 and 1996 (n = 7). Solid and dashed lines represent average and one standard deviation (above and below), respectively. The total of the 9 stages compared well with a bulk aerosol sample collected over the same time interval. The average (± std. dev.) concentration (a sum of the 9 stages) and mass median diameter (MMD) for the 7 impactor runs are also shown for both species.

4.4 Discussion

4.4.1 Rural and urban aerosol signals

The range and average concentrations for NH_4^+, SO_4^{2-}, NO_3^- at Harvard Forest (Table 4.1) are similar to results observed in previous summertime studies of aerosol composition at rural eastern and northeastern U.S. sites such as University Park, PA [Lewin et al., 1986], Newton, CT [Keeler et al., 1991], and Whiteface Mtn., NY [Kelly et al., 1984; Miller et al., 1993]. Nonetheless, Pierson et al. [1989] sampled aerosols from Allegheny Mtn., PA and measured average concentrations of NH_4^+, SO_4^{2-}, and H^+ more than twice as high as those found at Harvard Forest. However, the overall average from one site can be a misleading statistic as all of the above studies noticed higher concentrations and more acidic aerosol in the maritime and continental tropic air masses from the S and SW, respectively, and cleaner less acidic aerosol in faster moving continental polar air masses from the northwest [Parekh and Hussain, 1982]. During a particular study period, the frequency of winds from the midwestern U.S. as well as the synoptic-scale meteorology (rainy vs. dry periods) will heavily influence the reported average concentrations. Of the above mentioned sites, Allegheny Mtn., PA is also closest to the midwestern source region and Harvard Forest is the furthest, suggesting that remoteness from a source provides more opportunity for the wet removal of pollutants enroute or perhaps the greater influence of winds from a clean air source region.

At Harvard Forest, the contrast between the SW urban pollution signal and the more rural NW source region is also evident in "pollutant" trace gases such as HNO_3, NO, NO_y, O_3, and CO [Munger et al., 1996; Lefer et al., 1997a]. The NW and SW median composite aerosol composition in Figure 4.1 could probably be described as rural and urban aerosol signals, respectively. The median SO_4^{2-} concentration of 11 nmol m^{-3} measured in surface winds from the NW sector was similar to the 15 nmol m^{-3} observed by Kelly et al. [1983] in "clean air" episodes sampled at Whiteface Mtn., NY, while the SO_4^{2-} data from the SW sector contains pollution events with levels as high as those observed by Tanner et al. [1979] sampling in New York City (see case study in sec. 4.3).

4.4.2 Factors regulating aerosol NH_4^+ at Harvard Forest

Aside from a few notable exceptions of southern California [Appel et al., 1978] and Denver [Countess et al., 1980], it is well established that continental aerosols in the U.S. are primarily composed of a mixture of submicron ammonium sulfate salts and sulfuric acid [Stevens et al., 1978; Milford and Davidson, 1987]. This

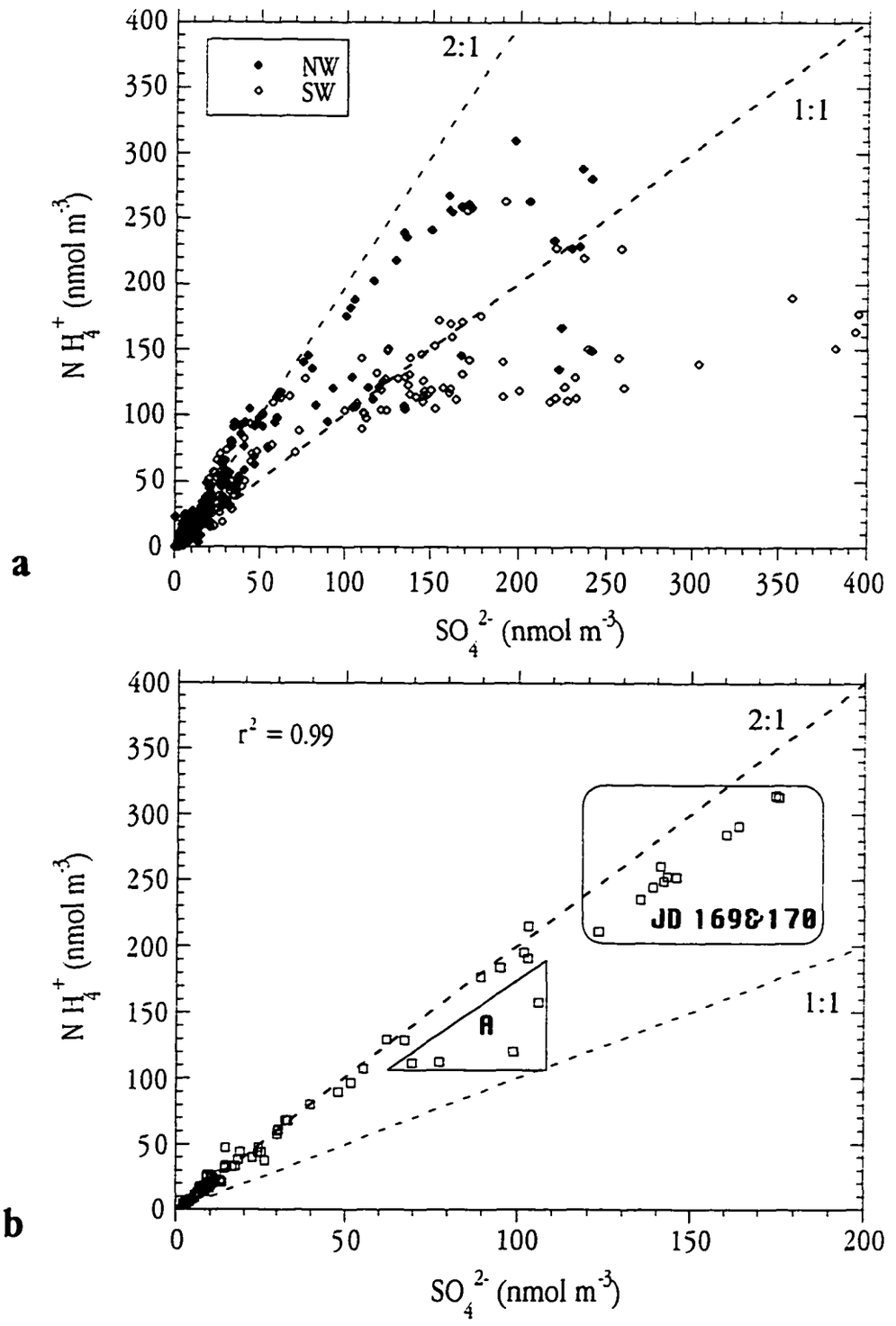

Figure 4.4 Relationship between NH_4^+ and SO_4^{2-} for: (a) aerosol samples collected between 1993-1995 for SW (n = 152) and NW (n = 290) surface wind direction sectors, and (b) samples collected between 09-21 June, 1995 (n = 87). Error bars were omitted for clarity. Letter A refers to a specific event during this case study period (see text and Figure 4.8).

also appears to be the case for Harvard Forest, especially considering the prominent submicron peaks in the size distributions of both NH_4^+ and SO_4^{2-} aerosols (Figure 4.2) and the dominance of these two ions in the overall aerosol composition (Figure 4.1). Mean (± std. dev.) NH_4^+/SO_4^{2-} molar ratios of 1.7 (± 1.0) for the NW and 1.3 (± 0.5) for the SW also indicate that both air masses lack sufficient levels of NH_x to completely neutralize atmospheric H_2SO_4. The greater acidity of the polluted SW air can also be inferred from the larger "H^+" concentrations (i.e., cation deficit) observed for these air masses (Table 4.1).

Given the agricultural source of NH_3 and its higher levels in the NW sector [Lefer et al., 1997a], one might expect the rural (NW) aerosol to contain higher NH_4^+ levels. Nonetheless, air masses from the NW contain, on average, almost a third less particulate NH_4^+ than winds from the polluted SW (Table 4.1). Having an atmospheric lifetime on the order of several hours to a few days, NH_3 is considered to be a local pollutant [Georgii and Gravenhorst, 1977]. However, once converted to a fine aerosol, NH_4^+ can travel relatively long distances in the atmosphere [Asman and Janssen, 1987]. In addition to being a principal source of S to the eastern U.S. [Pierson et al., 1989], the midwest also hosts significant agricultural activities which emit large amounts of NH_3 [Harriss and Michaels, 1982]. Since tropical air masses approaching New England from the SW are relatively slower moving than those of polar origin [Keeler et al., 1991], perhaps these highly acidic air masses have, on average, more time to fully oxidize SO_2 to H_2SO_4 and titrate out essentially all the NH_3 enroute.

At Harvard Forest it appears that the mixing ratios of NH_3 are suppressed, and thus the concentrations of aerosol NH_4^+ are enhanced, by the high acidic SO_4^{2-} levels in air reaching this site [Lefer et al., 1997a]. At aerosol SO_4^{2-} levels below 50 nmol m^{-3}, there is typically more than enough NH_3 between the source region and our site to completely neutralize H_2SO_4 to $(NH_4)_2SO_4$ as indicated by the proximity of these points to the 2:1 molar ratio line in Figure 4.4a. Aerosol NH_4^+ concentrations in SW pollution events rarely exceed 100 nmol m^{-3} (Figure 4.4a), suggesting that this is a general limit to the NH_x levels in these air masses. As a result, pollution events with SO_4^{2-} levels higher than 100 nmol m^{-3} appear to contain an increasing faction of H_2SO_4 (Figure 4.4a) with intermediate SO_4^{2-} levels resulting in a mixture of $(NH_4)_2SO_4$ and NH_4HSO_4. Interestingly, the highest particulate NH_4^+ events are indeed observed in the rural NW windsector (Figure 4.4a), suggesting that on rare occasions this continental polar air contains "pollution" levels of SO_4^{2-} which are almost completely neutralized by high rural NH_3 emissions.

4.4.3 Factors regulating aerosol NO_3^- at a continental site

Away from marine influences, aerosol nitrate has been observed to be associated with a submicron NH_4NO_3 and supermicron soil aerosols [Wolff, 1984]. Although substantial concentrations of volatile NH_4NO_3

aerosols lead to significant sampling artifacts [Appel et al., 1981, 1988], high levels of atmospheric sulfate create an environment where the irreversible reactions producing ammonium(bi)sulfate salts dominate. Thus they prevent substantial NH_4NO_3 formation until all the acidic SO_4^{2-} is neutralized [Tang et al. 1980]. The acidic nature of the Harvard Forest aerosol and the low ambient NH_3 mixing ratios indicate that NH_4NO_3 is a minor aerosol species at this site. This idea is further supported by the average Harvard Forest NO_3^- aerosol size distribution (Figure 4.3) which places 86% of the mass of NO_3^- in particles aerodynamically greater than 1 μm. A similar particulate NO_3^- distribution was observed by Kadowaki [1976] for summer continental aerosols. The correlation between the NO_3^- and Ca^{2+} size distributions (Figure 4.3) also implies that the primary mechanism of aerosol NO_3^- formation at this site is the adsorption of gaseous HNO_3 onto basic soil particles. While two of the seven NO_3^- distributions did contain significant levels of submicron NO_3^-, in both cases the submicron NO_3^- loading was still considerably less than that in the coarse fraction.

While the similarities between their size distributions suggest a direct correlation between the bulk aerosol concentrations of NO_3^- and Ca^{2+}, this is generally not the case. However, some individual air masses display a linear relationships between NO_3^- and Ca^{2+} (Figure 4.5). Since the mechanism of coarse NO_3^- aerosol formation involves the adsorption of HNO_3 onto a particle surface, and not the combination of two gaseous molecules, the molecular ratio of these two ionic species is not required to be constant. The factors controlling NO_3^- loading on a particular soil particle have not been identified but could include: particle surface area, particle surface pH, and the ratio between the concentration of HNO_3 and the number of soil particles. A lower number of soil particles in the atmosphere will result in fewer coarse NO_3^- aerosols, however, if exposed to a high level of HNO_3, each particle could be associated with a greater NO_3^- loading. Similarly, HNO_3 should have a greater affinity for a more basic soil particle, or a particle with more surface area or a greater number of positively charged adsorption sites.

The lowest NO_3^- to Ca^{2+} ratio (0.3) occurred on JD 165, a day influenced by NW winds that contained high Ca^{2+} concentrations and low HNO_3 mixing ratios (100-400 pptv). Two days later, an air mass also from the NW brought similar Ca^{2+} levels to Harvard Forest, except HNO_3 levels where considerably higher ranging from 1000-2000 pptv resulting in a higher NO_3^- to Ca^{2+} ratio of 2 (Figure 4.5). Although it is conceivable that the soluble NO_3^- was associated with soil particles before becoming airborne, it would be surprising that soil particles from the same general source region sampled two days apart would have such different NO_3^- levels. These linear relationships may reflect various dilution levels of a previously produced coarse nitrate rich air mass.

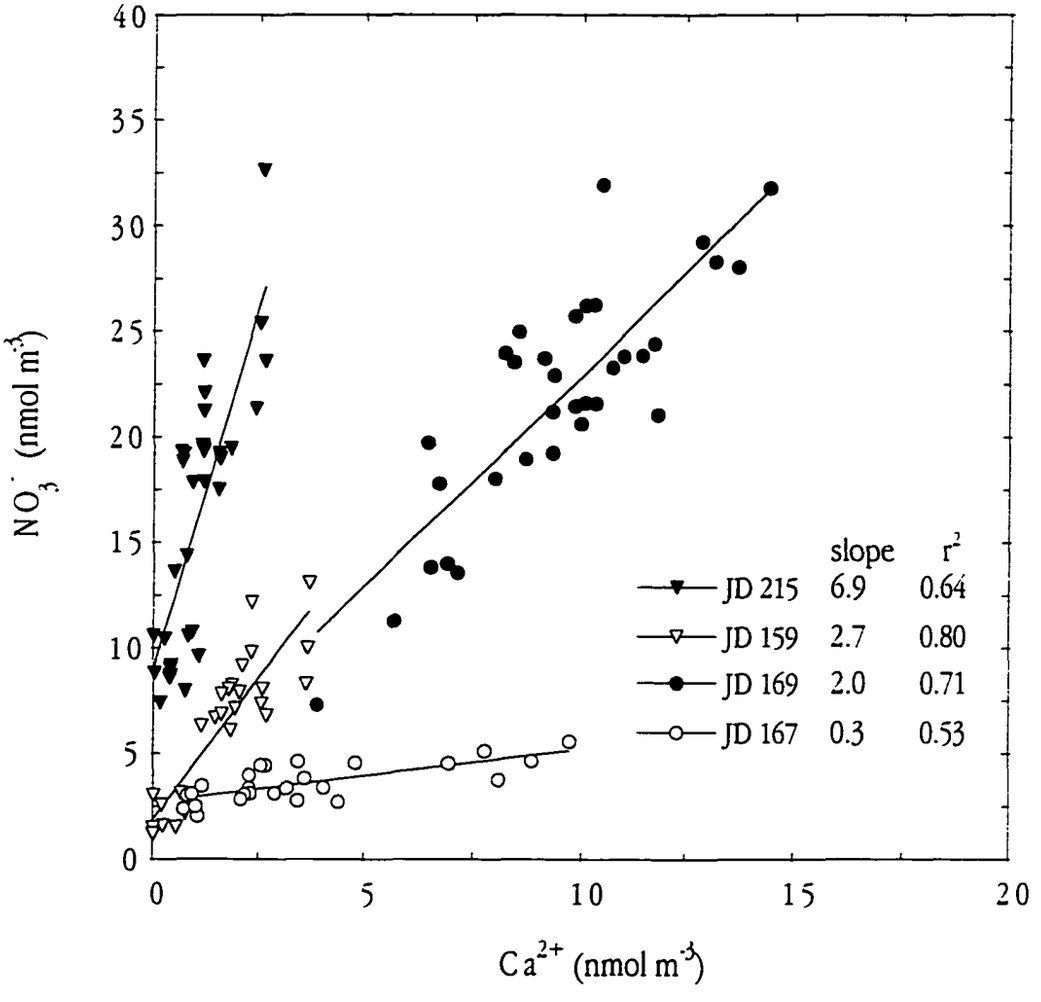

Figure 4.5 Linear relationship with slope and correlation coefficient (r^2) observed for NO_3^- and Ca^{2+} in bulk aerosol samples for select Julian days (JD) in 1995. Error bars omitted for clarity.

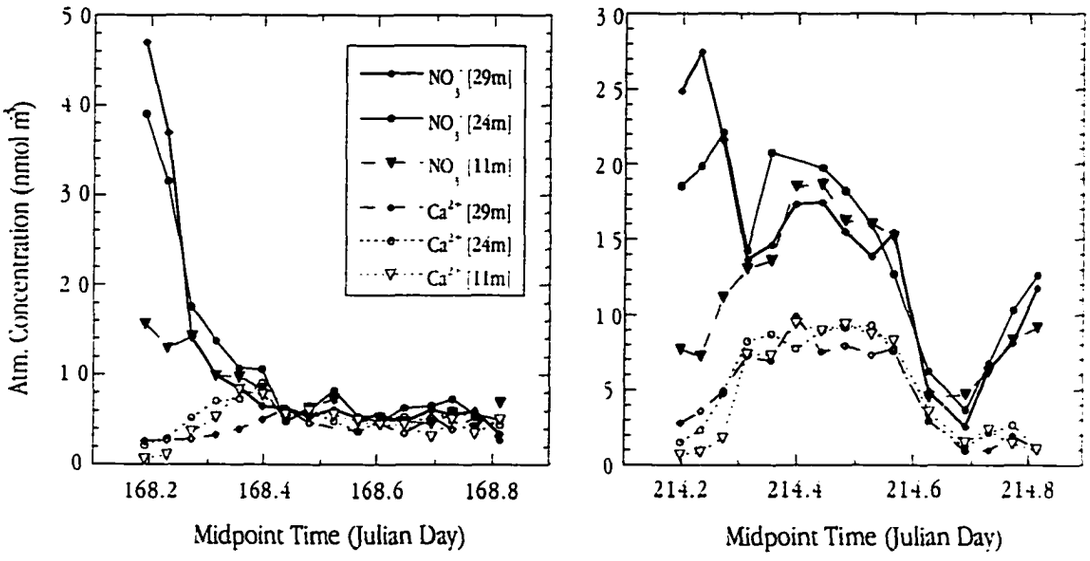

Figure 4.6 Elevated early morning levels of aerosol NO_3^- were not associated with coarse particle Ca^{2+}. Data shown above for 17 June (JD 168) and 02 August (JD 214) of 1995 represent 2 of 7 similar events observed that summer.

On several occasions elevated levels of aerosol NO_3^- were observed in the night and early morning hours (Figure 4.6). Since these aerosol NO_3^- "events" did not occur in conjunction with coarse particle Ca^{2+} or enhanced NH_3 mixing ratios, it is likely that a mechanism other than the adsorption of HNO_3 on soil particles or reaction with NH_3 is responsible. Alternative scenarios for these events include the nighttime production of NO_3 and N_2O_5 by reaction of NO_2 with O_3:

$$NO_2 + O_3 \rightarrow NO_3 + O_3 \qquad [11]$$

$$NO_2 + NO_3 \xleftrightarrow{M} N_2O_5 \qquad [12]$$

both of which may ultimately create aerosol NO_3^- via reaction on particle surfaces:

$$N_2O_5 + H_2O \xrightarrow{particle} 2HNO_3 \qquad [13]$$

[Richards, 1983]. Parrish et al. [1986] also suggested that NO_3 can directly react with wet aerosols to produce aerosol NO_3^-. Evidence of the nighttime production of NO_3, N_2O_5, and HNO_3 at Harvard Forest has been suggested by significant increases in NO_X, NO_Y, and HNO_3 in the early morning hours [Munger et al., 1996; Lefer et al., 1997a]. Other studies above forest areas have indicated that HNO_3 from the residual mixed layer of the previous day is mixed down in the early morning as the nocturnal boundary layer erodes [Trainer et al., 1991; Kleinman et al., 1994].

Currently, there is not enough evidence to confirm that the higher early morning HNO_3 and NO_3^- levels result from reactions involving N_2O_5. Given the low Ca^{2+} concentrations during these early morning NO_3^- events, if the NO_3^- production described in Equation 13 is occurring at Harvard Forest, it is most likely occurring on small particles and not on large basic soil particles as suggest by Richards [1983] and Wolff [1984]. The enhanced levels of fine mode aerosol NO_3^- observed in a few impactor runs (Figure 4.3) were observed during periods of acidic aerosols and low ambient NH_3. Thus, regardless of the source of the HNO_3, this submicron NO_3^- could easily result from the scavenging of HNO_3 by wet sulfate aerosol surfaces.

4.4.4 June 1995 case study

During intensive sampling, N aerosol and gas samples were collected between 09-20 of June 1995 (JD 160-171) at Harvard Forest from the top of a 20-m walkup tower. Hourly samples were collected between 1000-1400 and 2200-0200 EDT each day. The first half of the study was dominated by a cold front passage (JD 163, Event A) that brought cooler temperatures, overcast skies, and a 2-day period of 100% humidity and scattered rain (Figure 4.7). This was followed by clearer and drier conditions with temperatures gradually increasing to midday highs of around 30°C for last 3 days. The cool period (approximately between JD

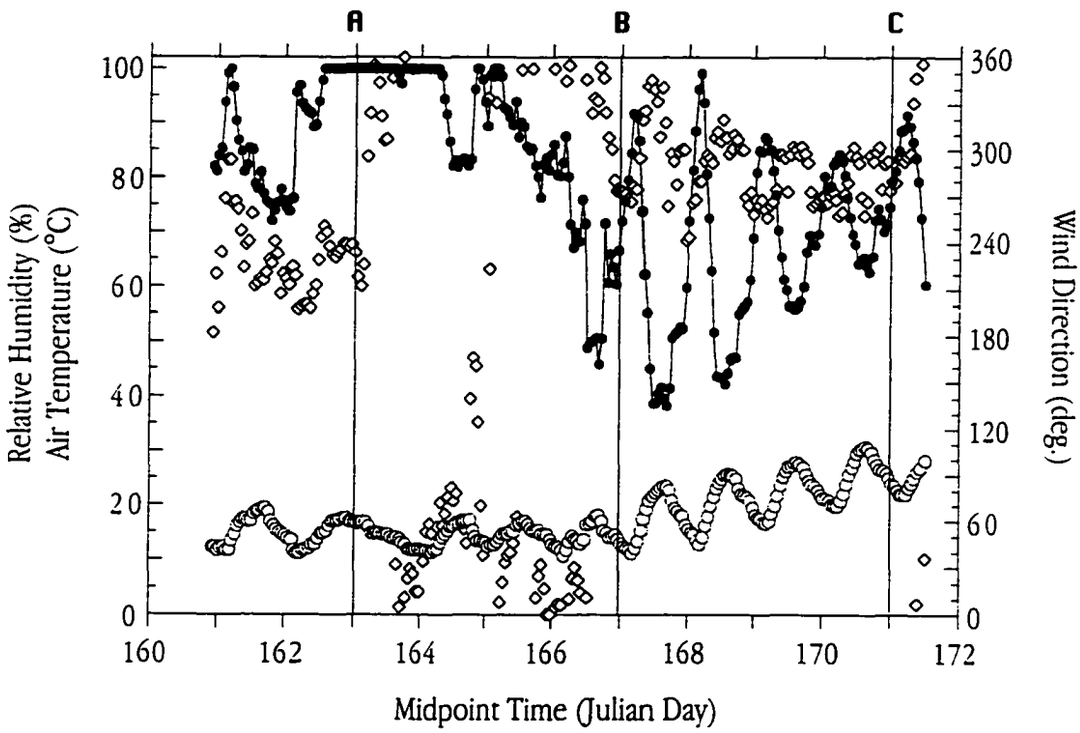

Figure 4.7 Continuous hourly averages of air temperature (open circle), relative humidity (filled circle with connection line) and wind direction (open diamond) for the case study period between 09-20 of June 1995 (JD 160.8-171.6). See text (section 4.4.4) for explanation of events A, B, and C.

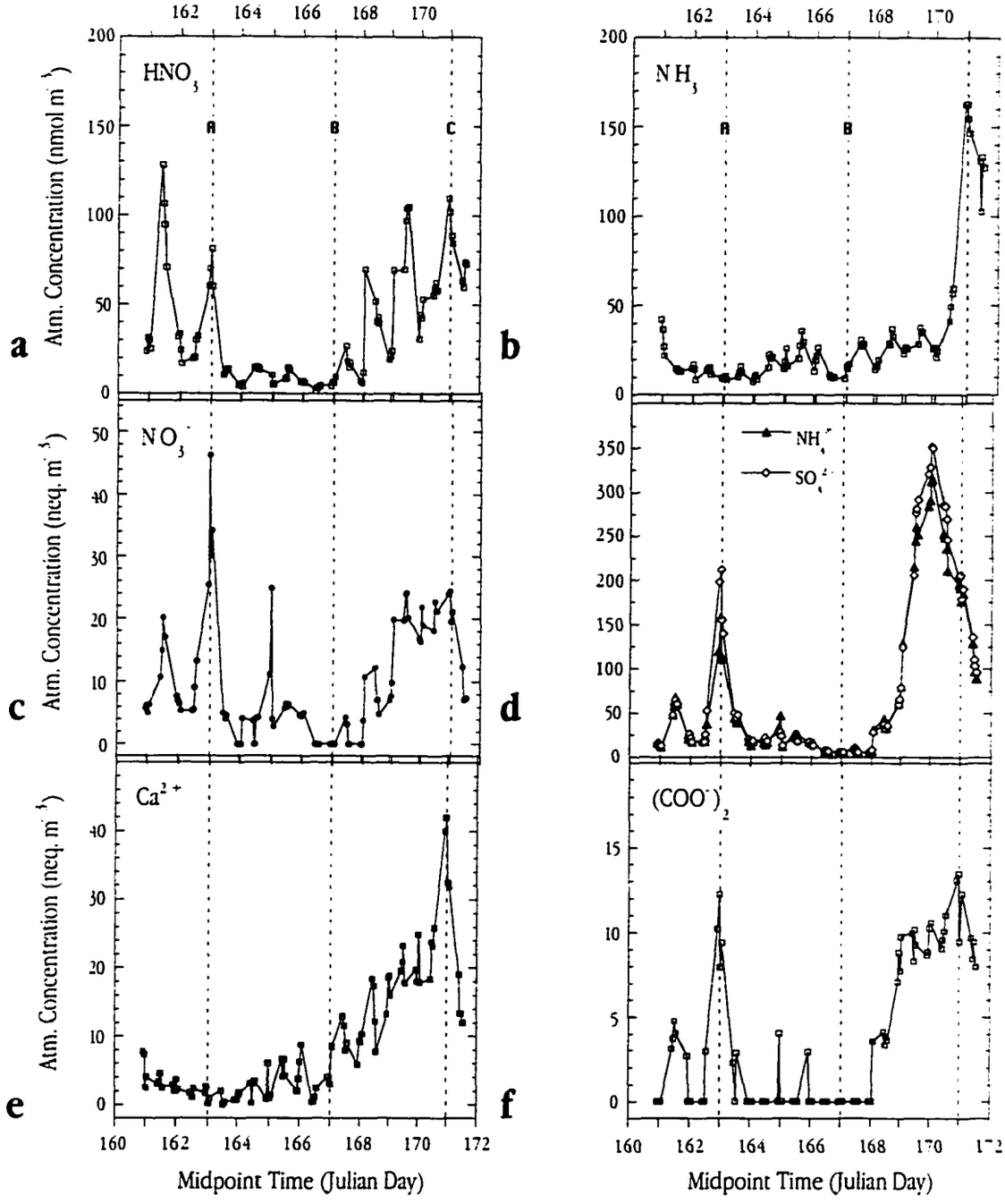

Figure 4.8 Atmospheric concentrations of select gas and aerosol species at Harvard Forest from the top of a 20 meter walk up tower for the case study period between 09-20 of June 1995 (JD 160.8-171.6). Lines connecting points to not indicate continuous sampling. Hourly sampling occurred from 1000-1400 and 2200-0200 EDT each day. Error bars were omitted for clarity. See text (section 4.4.4) for explanation of events A, B, and C.

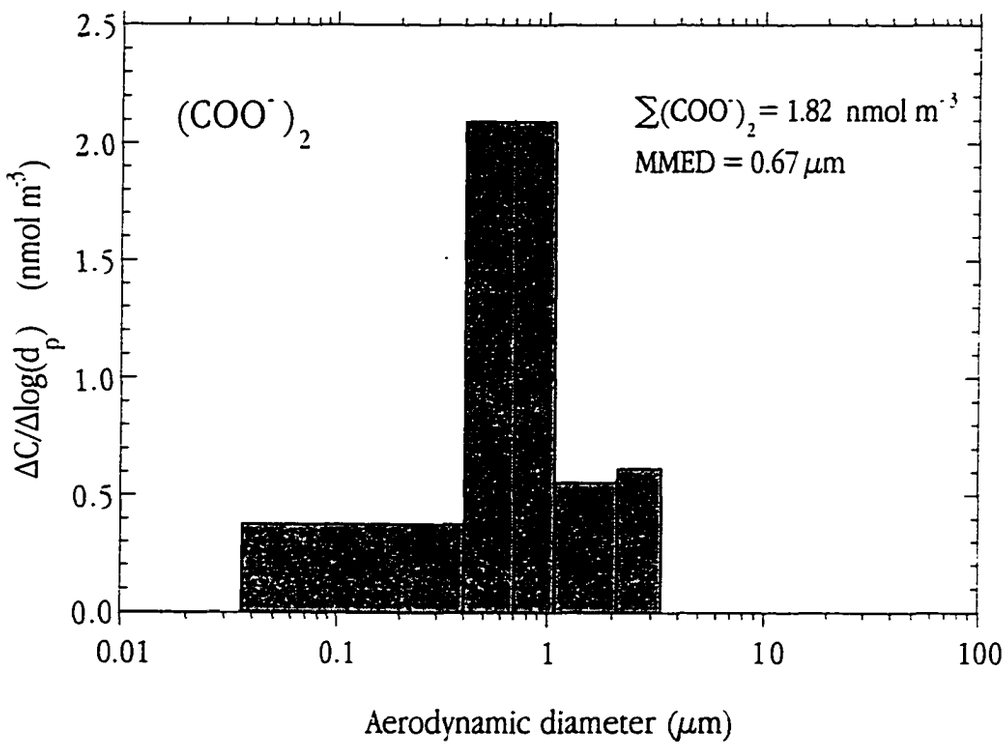

Figure 4.9 Aerodynamic size distribution for particulate oxalate ($(COO^-)_2$) from the top of a 20 m walk up tower at Harvard Forest. Sample was collected between 12-16 June (JD 163-166) of 1995.

162-167) was characterized by winds from the north and east, with winds changing to the west (240-300°) on JD 168 (Event B) and remaining that way until the last hours of the experiment (Figure 4.7).

The time series of selected N gas and aerosol species during this case study period (Figure 4.8) displays many of the factors regulating NH_4^+ and NO_3^- aerosols at Harvard Forest. Immediately noticeable are low levels of all these soluble species during the overcast and wet period between JD 163-167. In general, HNO_3, NO_3^-, and $(COO^-)_2$ track each other, although the particulate NO_3^- concentrations are typically 5-10 times lower than HNO_3 with $(COO^-)_2$ approximately half of aerosol NO_3^-. The correlation between NO_3^- and $(COO^-)_2$ strongly implies a pollution source for $(COO^-)_2$ [Norton, 1983]. An impactor collected between JD 163-166 of this case study shows all of the $(COO^-)_2$ in the submicron mode (Figure 4.9), indicating that aerosol $(COO^-)_2$ is formed from reactions involving a gas, perhaps oxalic acid ($(COOH)_2$). A water soluble gas that forms $(COO^-)_2$ in solution was previously observed over eastern Canada [Lefer et al., 1994] suggesting that this fine mode aerosol $(COO^-)_2$ may form when gaseous $(COOH)_2$ reacts with wet aerosol surfaces. While it is not known how a gas such as $(COOH)_2$ would compete with H_2SO_4 or HNO_3 for reaction with NH_3, given the similarity of the two size distributions, it is also plausible that $(COO^-)_2$ aerosols result from the heterogeneous production of ammonium oxalate.

The HNO_3 and aerosol NO_3^-, NH_4^+, SO_4^{2-}, and $(COO^-)_2$ concentrations peak at midnight of JD 163 (Event A) may result for the rapid and coherent transport of pollutants ahead of the front as a consequence of increased temperature and pressure gradients. In general, the NH_x levels during this case study were high enough to completely neutralized the atmospheric SO_4^{2-} to $(NH_4)_2SO_4$ aerosols, except prior to this frontal passage (Event A) and during a second large pollution episode on JD 169 and 170 (Figures 4b and 7).

Event A was an air mass with low Ca^{2+} concentrations yet it contained the highest aerosol NO_3^- levels of the study period, consequently most of the aerosol NO_3^- must have been in the submicron fraction at this time. The low NH_3 levels and unneutralized nature of the SO_4^{2-} aerosol during Event A are unlikely conditions to form NH_4NO_3 aerosols. While it is not possible to determine the origin of this NO_3^-, the high humidities during this nighttime event are favorable for heterogeneous reactions involving N_2O_5 (Eq. 11, 12, and 13). The gradual increase in aerosol NO_3^- for the second half of the experiment (after Event B) is mirrored by an increase in Ca^{2+} concentrations. The presence of coarse NO_3^- aerosol was confirmed in the impactor sample collected between events A and B.

Except during the overcast period, NH_3 and aerosol NH_4^+ display divergent behavior with NH_3 concentrations remaining low except when NH_4^+ and SO_4^{2-} levels decrease after midnight of JD 171 (Event C)

as winds shifted back to the north (Figure 4.8). The lower nitrate and high NH_3 and soil Ca^{2+} concentrations during Event C suggest this air mass may have originated in a rural agricultural region to the north.

4.4.5 N particle deposition estimates

In general, deposition models have predicted particle deposition velocities lower than those observed by direct measurement methods, particularly for forested systems [Wesely et al., 1983, 1985; Gallagher et al., 1997]. Given that the empirical deposition relationships used in this study (W&D97, G97) were determined for a system with a considerably larger leaf area index (LAI) than at Harvard Forest (> 2 x difference) these NH_4^+ deposition estimates should be considered an upper limit. Similarly, the grassland parameterization of Wesely et al. [1985] might represent a lower limit of the NH_4^+ flux at Harvard Forest (Figure 4.10). The three different empirical estimates of the NH_4^+ deposition velocity at Harvard Forest averaged (± std. dev.) 1.3±0.86, 0.71±0.54, and 0.17±0.13 cm s^{-1} for W&D97, G97, and W85, respectively. The middle of this range (G97) compares well with the eddy covariance measurements of Hicks et al. [1989] for a deciduous forest (Oak Ridge, TN) which averaged about 1 cm s^{-1} during the daytime and dropped close to zero at night. It is interesting to note the long term average during the study was 0.6 cm s^{-1}, a period in which the LAI was approximately 50% of the summertime maxima.

The disparities between W&D97 and G97 estimates may not be significant considering the uncertainties associated with each method and fundamental differences between flux-profile and eddy covariance techniques. Perhaps the two techniques are also measuring two different things, as the optical particle counter employed by G97 may not measure supermicron ammonium sulfate (formed at high relative humidities) and other coarse SO_4^{2-} particles present in the Dutch atmosphere [Gallagher et al., 1997].

Considering the bimodal or predominantly coarse nature of NO_3^- aerosol at many continental sites, it is not yet possible to measure the eddy covariance flux of supermicron aerosols with current particle counting instrumentation. As a result few direct measurements of NO_3^- aerosol nitrate deposition have been made. Nitrate particle fluxes are measurable using flux-profile methods but even this method can be challenging in regions with high ambient NH_3 concentrations like Holland [W&D97]. Ruijgrok et al. [1997] synthesized the dry deposition measurements at Speulder forest to develop a detailed process oriented model which estimates NO_3^- deposition velocities greater than 1 cm s^{-1}. This same model estimated an average (± std. dev.) base cation V_d of 5.1± 3.9 cm s^{-1}. Given that the bulk of the NO_3^- aerosol at Harvard Forest is typically associated with coarse particle Ca^{2+}, our average V_d estimate for NO_3^- was 4.8 ± 2.5, which corresponds to a Stokes settling velocity for a 27 μm particle with a density of 2.2 g cm^{-3}.

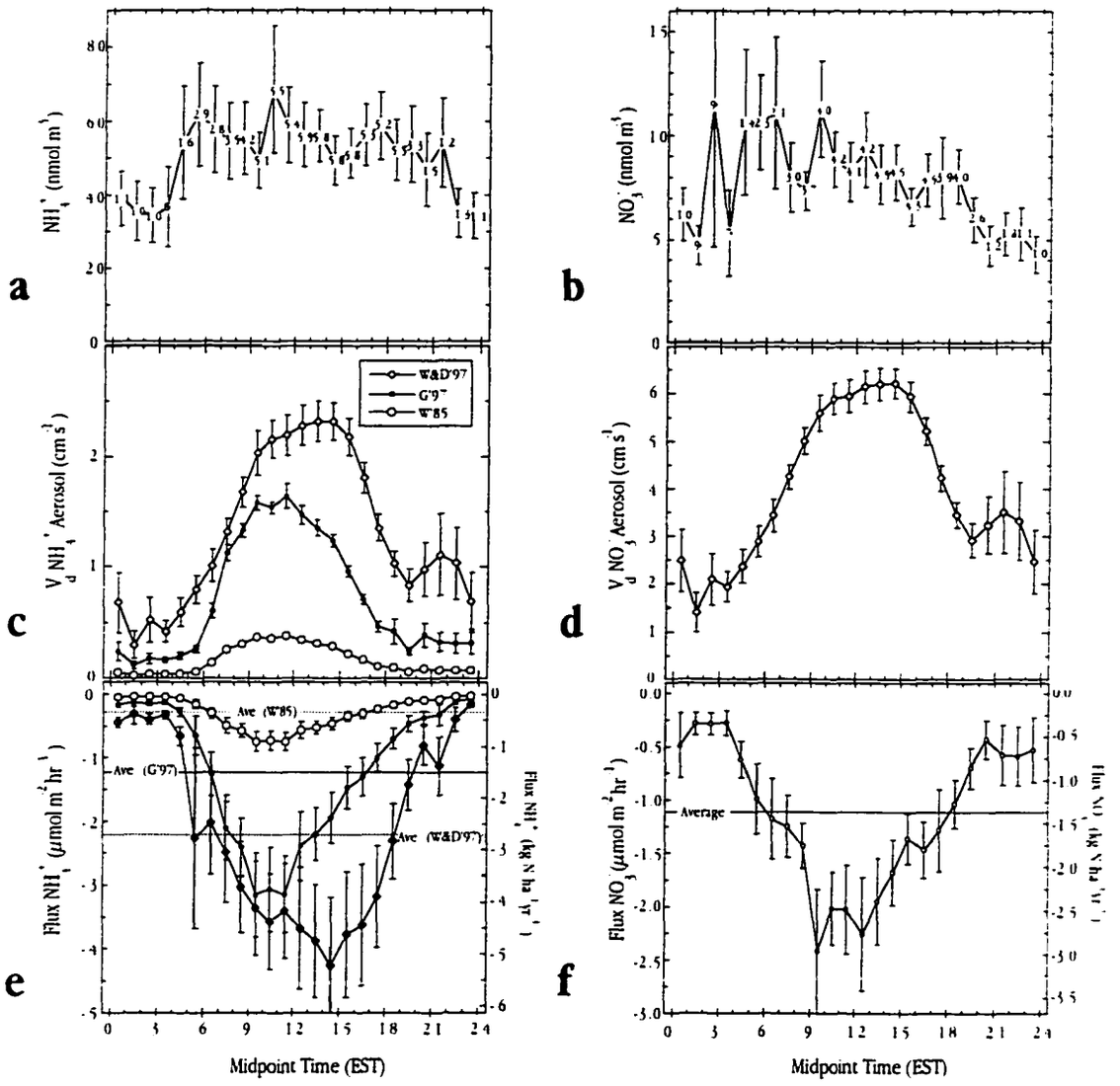

Figure 4.10 Average 1991-1995 summertime diel cycle of (a) NH_4^+ and (b) NO_3^-. Mean diel cycles of aerosol deposition velocity for NH_4^+ and NO_3^- are shown in panels (c) and (d), respectively. Deposition velocities were determined by different empirical models as a function of friction velocity (see section 4.2.4). Also shown is the diel average of the resulting estimates of the dry deposition flux of (e) NH_4^+ and (f) NO_3 for the different models. Vertical error bars represent ± standard error. Numbers in panels a and b are sample n for NH_4^+ and NO_3^- data, respectively, and apply to other diel cycles in panels c, d, e, and f.

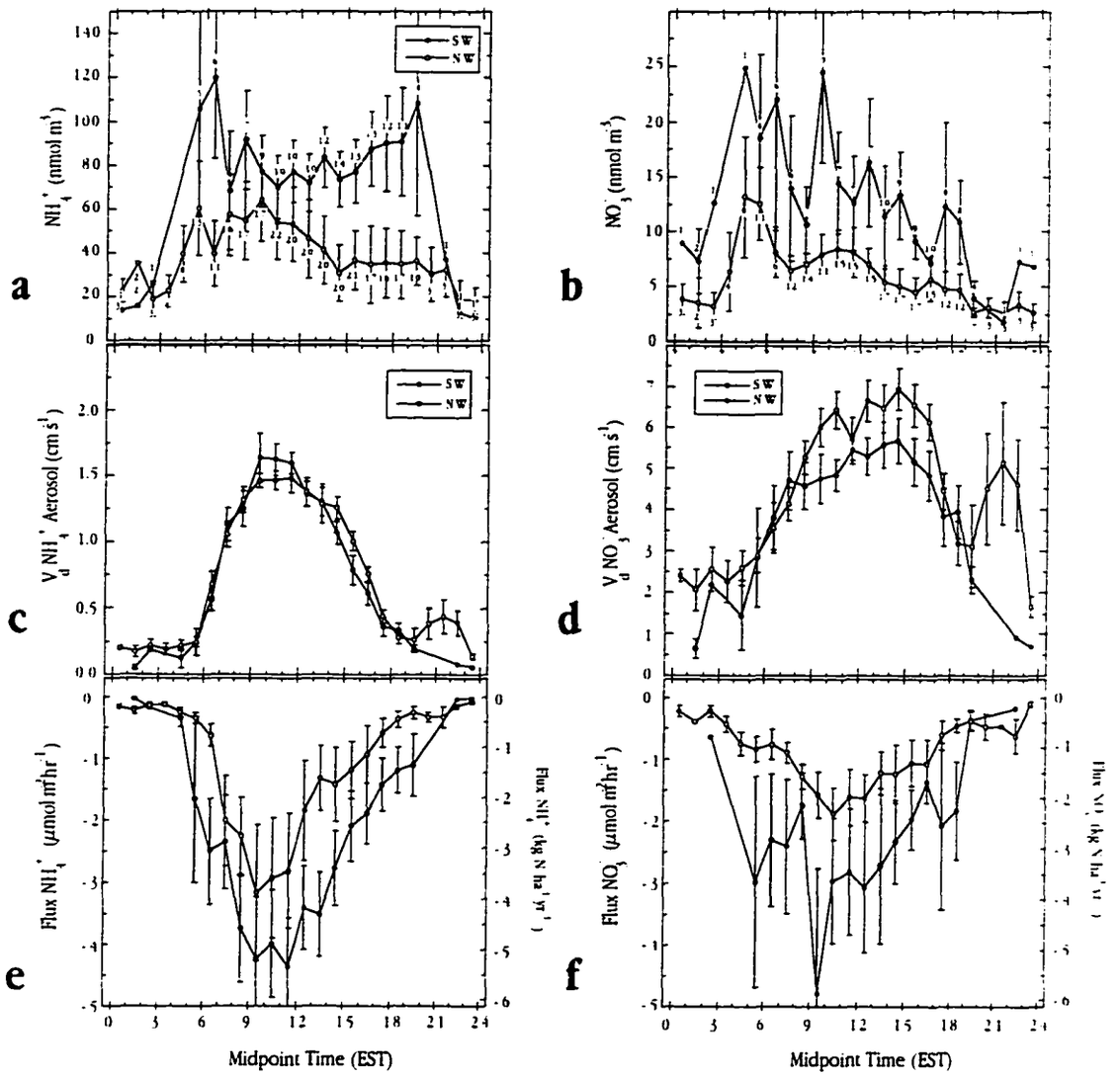

Figure 4.11 Average 1991-1995 summertime diel cycles of (a) NH_4^+ and (b) NO_3^- for SW and NW wind sectors. Filled and open circles represent SW and NW data respectively. Numbers near symbol are the sample n for SW and NW windsectors. Sample n in upper two panels apply to all the respective NH_4^+ and NO_3^- data. Vertical error bars represent ± standard error. The mean diel cycles of aerosol deposition velocity in SW/NW windsectors for NH_4^+ and NO_3^- are shown in panels (c) and (d), respectively. Symbols and error bars are the same as above.. Deposition velocities were determined by empirical models as a function of friction velocity. Gallagher et al. [1997] empirical model was used for panel c (see section 4.2.4). Also shown is the diel average of the resulting estimates of the dry deposition flux for the two dominant windsector of (e) NH_4^+ and (f) NO_3^-.

Alternatively, Lindberg and Lovett [1985] developed a method of determining coarse NO_3^- deposition to polycarbonate petri dishes suspended above and within forest canopy systems. Results from the application of this technique to a series of 9 forested sites near the eastern coast of the U.S. as part of the Integrated Forest Study revealed average annual coarse NO_3^- deposition fluxes ranging from 0.06 nmol N m^{-2} hr^{-1} atop White Face Mtn., NY to 1.5 nmol N m^{-2} hr^{-1} in the Great Smoky Mountains National Park [Lovett and Lindberg, 1993]. The upper end of this range compares well with the average (1.2 nmol N m^{-2} hr^{-1}) estimate of NO_3^- deposition at Harvard Forest.

4.4.5 Comparison of N deposition fluxes at Harvard Forest

Summertime deposition flux estimates for both particulate and gaseous N were calculated from average summertime atmospheric concentrations and a range of species-specific deposition velocities (Table 4.2). While NH_x is the principle form of atmospheric N at Harvard Forest, NO_3^- dominates the dry deposition flux accounting for the input of 2 - 8 kg N ha^{-1} yr^{-1} (Table 4.2). This paradox has been observed at several other eastern sites [Lovett and Lindberg, 1993] and at Harvard Forest results from the partitioning of 69% of NH_x in a fine mode aerosol that deposits slowly. In comparison, 78% of atmospheric NO_3^- is on average found as efficiently depositing gaseous HNO_3 [Hanson and Lindberg, 1991]. Although NO_3^- concentrations are typically 4-8 times lower than aerosol NH_4^+, the significantly higher deposition velocities of coarse particle NO_3^- results in similar deposition fluxes for these two species. Furthermore, in contrast to HNO_3, NH_3 can be deposited to and emitted from forest ecosystems [Langford and Fehsenfeld, 1992] further reducing total NH_x deposition. Given the low NH_3 mixing ratios at this site it is likely that NH_3 emission is also occurring at Harvard Forest [Lefer et al., 1997a], which is factored into these estimates by using $V_{d(NH3)}$ which ranges from -2 (emission) to 3 cm s^{-1} (deposition) (see Table 4.2).

The nearest National Acid Deposition Program (NADP) wet deposition monitoring site is located approximately 10 miles to the SW of Harvard Forest at the Quabbin Reservoir (Site MA08). Munger et al. [1997] has shown that the concentration of dissolved NO_3^- in precipitation samples collected at Harvard Forest are in good agreement with those measured at MA08. Average 1991-1996 summertime wet NO_3^- and NH_4^+ deposition values at MA08 are 5.26 and 3.02 kg N ha^{-1} yr^{-1}, respectively. The wet deposition fluxes also show the same trend of higher NO_3^- inputs compared to NH_4^+, suggesting that gaseous HNO_3 is more easily incorporated into falling precipitation than NH_4^+ aerosols.

At Harvard Forest, the upper range of the dry deposition estimates are equal to or greater than the measured wet deposition flux for both NH_x and NO_3^- (Table 4.2). Wet NO_3^- deposition and dry HNO_3

Table 4.2. Comparison of summertime gas and aerosol N dry deposition estimates to measured wet fluxes for Harvard Forest area.

Species	Ave. Conc. ± Std. dev. (nmol m^{-3}) (pptv)	V_d (cm s^{-1})	Estimated Flux (kg N ha^{-1} yr^{-1}) (μmol m^{-2} hr^{-1})	Measured Flux (kg N ha^{-1} yr^{-1})	Total N Flux (kg N ha^{-1} yr^{-1})
$HNO_{3(g)}$	36.9 ± 46.6[A] (828)	1 - 6[A]	(-1.1) - (-6.9) (-0.9) - (-5.6)	(-1.66)[G] [NO_Y]	
$NO_3^-{}_{(p)}$	9.77 ± 10.2[B] (219)	1 - 5[C]	(-0.3) - (-1.5) (-0.25) - (-1.25)	----	
$NO_3^-{}_{(aq)}$	----	----	----	(-5.26)[D]	
				Total Dry NO_3^-	(-1.4) - (-8.4)
				Total NO_3^-	(-6.7) - (-14) [(-7.2) - (-8.4)][H]
$NH_{3(g)}$	10.3 ± 11.3[A] (231)	(-2) - 3[E]	0.6 - (-1.0) 0.5 - (-0.8)	----	
$NH_4^+{}_{(p)}$	60.4 ±71.1[B] (1350)	0.2 - 1[F]	(-0.4) - (-1.9) (-0.3) - (-1.5)	----	
$NH_4^+{}_{(aq)}$	----	----	----	(-3.02)[D]	
				Total Dry NH_X	(-0.2) - (-2.9)
				Total NH_X	(-2.8) - (-5.8)
				Total Dry N	(-1.6) - (-11.3)
				Total Wet N	(-8.28)
				Total N	(-9.9) - (-20) [(-11) - (-14)][H]
NO_Y	6560±2530[G] (6560)	0.1 - 0.3[G]	(-1.2) - (-3.6)	(-1.66)[G]	

[A]Lefer et al. [1997b].
[B]This Study.
[C]Ruijgrok et al., [1997], V_g for diameter of 12-27 μm and density of 2.2 g cm^{-3} from equations in Baron and Willeke [1993].
[D]1991-1996 average for Quabbin Reservoir, MA (Site MA08) of U.S. National Acid Deposition Program [1997].
[E] Duyzer et al., [1987].
[F]Wyers and Duyzer [1997]; Ruijgrok et al., [1997]
[G]Munger et al. [1996]
[H]Assuming Flux HNO_3 = Flux NO_Y

deposition are probably the two largest atmospheric N fluxes to the Harvard Forest, suggesting that aerosol N, and NH_x in general, are less important sources of N to this system. It is important to note that the higher N dry deposition fluxes of gaseous [Lefer et al., 1997b] and particulate N (Figure 4.11) in air masses from the polluted SW adds a dimension of temporal variability to N dry deposition. This combined with the episodic nature of wet deposition highlights the fact that the relative importance of wet and dry N depositions changes from year to year. Nevertheless, assuming that the average conditions experienced between 1991-1995 are "typical" for this forest ecosystem and that the measured NO_Y deposition [Munger et al., 1996] is equal to the HNO_3 flux [Lefer et al., 1997b], it is possible to limit the range of total dry N deposition to 2 - 6 kg N ha^{-1} yr^{-1}, or 19 - 42% of the total estimated N inputs to the Harvard Forest.

4.5 Conclusions

Ammonium is the dominant N aerosol species at Harvard Forest, typically found at summertime concentrations of approximately 60 nmol m^{-3}, which is 4-8 times greater than that of particulate NO_3^-. As a whole, the aerosol at this continental site has a bimodal distribution with NH_4^+, SO_4^{2-} and H^+ accounting for the majority of submicron fraction. Aerosol NO_3^- is present in both the coarse and fine modes, with the majority of the NO_3^- associated with supermicron Ca^{2+} aerosols.

Overall, the aerosol acidity is not completely balanced by NH_4^+, with the more acidic particles arriving from the polluted SW. Ammonium levels in these polluted air masses are insufficient to neutralize SO_4^{2-} concentrations greater than ≈ 100 nmol m^{-3}, which may help define an upper limit to the NH_x emissions from this region. The primary method of particulate NO_3^- production appears to be the adsorption of gaseous HNO_3 onto basic soil particles. However, elevated NO_3^- particulate levels in the early morning not associated with coarse aerosol Ca^{2+} indicates that the heterogeneous production of NO_3^- aerosol via N_2O_5 may also be occurring.

Although aerosol NO_3^- concentrations were significantly lower than submicron NH_4^+, the higher V_{dl} of these coarse particles resulted in similar dry deposition estimates, on the order of 1 kg N ha^{-1} yr^{-1} for both aerosol N species. These aerosol dry deposition fluxes are considerably smaller than measured N wet deposition (≈ 8 kg N ha^{-1} yr^{-1}) and estimates of gaseous HNO_3 inputs (1-7 N ha^{-1} yr^{-1}) to this forest ecosystem.

4.6 Acknowledgments

This research was funded by the US Department of Energy's (DOE) National Institute for Global Environmental Change (NIGEC) through the NIGEC Northeast Regional Center at Harvard University (DOE Cooperative Agreement DE-FC03-90ER61010). Financial support does not constitute an endorsement by the DOE of the views expressed in this article/report. The work at the University of New Hampshire (UNH) is supported by subcontract 901214-HAR#4 from Harvard University, under the Northeast Regional Center of NIGEC, to the Research Foundation of UNH. We would like to thank Harvard University, especially Bill Munger and Steven Wofsy, for allowing us access to their data and the help with our sampling efforts at Harvard Forest. The excellent technical assistance of Eric Scheuer and comments by Jack Dibb are also gratefully acknowledged. The UNH gas and aerosol dataset for Harvard Forest is available via anonymous ftp at io.harvard.edu in the directory pub/nigec/UNH and the www-as.harvard.edu Web site.

4.7 References

Aber, J.D., K.J. Nadelhoffer, P. Steudler, and J.M. Melillo, Nitrogen saturation in northern forest ecosystems, *BioScience*, *39* (6), 378-386, 1989.

Appel, B.R., E.L. Kothny, E.M. Hoffer, G.M. Hidy, and J.J. Wesolowski, Sulfate and nitrate data from the California aerosol characterization experiment (ACHEX), *Environmental Science & Technology*, *12* (4), 418-425, 1978.

Appel, B.R., Y. Tokiwa, and M. Haik, Sampling of nitrates in ambient air, *Atmospheric Environment*, *15*, 283-289, 1981.

Appel, B.R., Y. Tokiwa, E.L. Kothny, R. Wu, and V. Povard, Evaluation of procedures for measuring atmospheric nitric acid and ammonia, *Atmospheric Environment*, *22* (8), 1565-1573, 1988.

Asman, W.A.A., and A.J. Janssen, A long-range transport model for ammonia and ammonium for Europe, *Atmospheric Environment*, *21* (10), 2099-2119, 1987.

Baron, P.A., and K. Willeke, Gas and particle motion, in *Aerosol measurement: principles, techniques, and applications*, edited by K. Willeke, and P.A. Baron, pp. 23-40, Van Nostrand Reinhold, New York, 1993.

Countess, R.J., G.T. Wolff, and S.H. Cadle, The Denver winter aerosol: a comprehensive chemical characterization, *Journal of the Air Pollution Control Association*, *30*, 1194-1200, 1980.

Davies, C.N., The entry of aerosols into sampling tubes and heads, *British Journal of Applied Physics*, ser.2,*1*, 921-392, 1968.

Davies, C.N., and M. Subari, Aspiration above wind velocity of aerosols with thin-walled nozzles facing at right angles to the wind direction, *Journal of Aerosol Science*, *13* (1), 59-71, 1982.

Duyzer, J.H., A.M.H. Bouman, R.M. van Aalst, and H.S.M.A. Diederen, Assessment of dry deposition fluxes of NH_3 and NH_4^+ over natural terrains, in *EURASAP, 13-15 April 1987*, edited by W.A. H. Asman and H.S.M. A. Diederen, National Institute of Public Health, Bilthoven, The Netherlands, 1987.

Ehhalt, D.H., and J.W. Drummond, The tropospheric cycle of NO_x, in *Chemistry of the unpolluted and polluted troposphere*, edited by H.W. Georgii, and W. Jaeschke, pp. 219-251, D. Reidel, Hingham, MA, 1982.

Erisman, J.W., G. Draaijers, J. Duyzer, P. Hofschreuder, N. van Leeuwen, F. Römer, W. Ruijgrok, P. Wyers, and M. Gallagher, Particle deposition to forests—Summary of results and application, *Atmospheric Environment*, *31* (3), 321-332, 1997.

Gallagher, M.W., K.M. Beswick, J. Duyzer, H. Westrate, T.W. Choularton, and P. Hummelshøj, Measurements of aerosol fluxes to Speulder Forest using a micrometeorological technique, *Atmospheric Environment*, *31* (3), 359-373, 1997.

Geigert, M.A., N.P. Nikolaidis, D.R. Miller, and J. Heitert, Deposition rates for sulfur and nitrogen to a hardwood forest in northern Connecticut, USA, *Atmospheric Environment*, *28* (9), 1689-1697, 1994.

Georgii, H.-W., and G. Gravenhorst, The ocean as a source or sick of reactive trace-gases, *Pure Appl. Geophys.*, *115*, 503-511, 1977.

Hanson, P.J., and S.E. Lindberg, Dry deposition of reactive nitrogen compounds: a review of leaf, canopy and non-foliar measurements, *Atmospheric Environment*, *25A* (8), 1615-1634, 1991.

Harriss, R.C., and J.T. Michaels, Sources of atmospheric ammonia, paper presented at the second symposium on the composition of the nonurban Troposphere, Am. Meteorol. Soc., Williamsburg, VA, , 1982.

Hicks. B.B., D.D. Baldocchi, T.P. Meyers, R.P. Hosker Jr., and D.R. Matt, A preliminary multiple resistance routine for deriving dry deposition velocities from measured quantities, *Water, Air, and Soil Pollution*, *36*, 311-330, 1987.

Hicks, B.B., D.R. Matt, R.T. McMillen, J.D. Womack, M.L. Wesley, R.L. Hart, D.R. Cook, S.E. Lindberg, R.G. de Pena, and D.W. Thomson, A field investigation of sulfate fluxes to a deciduous forest, *Journal of Geophysical Research*, *94* (D10), 13003-13011, 1989.

Kadowaki, S.; Size distribution of atmospheric total aerosols, sulfate, ammonium and nitrate particulates in the Nagoya area, *Atmospheric Environment*, *10*, 39-43, 1976.

Keeler, G.J., J.D. Spengler, and R.A. Castillo, Acid aerosol measurements at a suburban Connecticut site, *Atmospheric Environment*, *25A* (3/4), 681-690, 1991.

Kelly, T.J., R.L. Tanner, L. Newman, P.J. Galvin, and J.A. Kadlecek, Trace gas and aerosol measurements at a remote site in the northeast U.S., *Atmospheric Environment*, *18* (12), 2565-2576, 1984.

Kleinman, L., Y.-N. Lee, S.R. Springston, L. Nunnermacker, X. Zhou, R. Brown, K. Hallock, P. Klotz, D. Leahy, J.H. Lee, and L. Newman, Ozone formation at a rural site in the southeastern United States, *Journal of Geophysical Research*, *99* (D2), 3469-3482, 1994.

Langford, A.O., and F.C. Fehsenfeld, Natural Vegetation as a Source or Sink for Atmospheric Ammonia - A Case Study, *Science*, *255* (5044), 581-583, 1992.

Lefer, B.L., R.W. Talbot, R.C. Harriss, J.D. Bradshaw, S.T. Sandholm, Olson, G.W. Sachse, J. Collins, M.A. Shipham, D.R. Blake, K.I. Klemm, K. Gorzelska, and J. Barrick, Enhancement of acidic gases in biomass-burning impacted air masses over Canada, *Journal of Geophysical Research*, *99* (D1), 1721-1738, 1994.

Lefer, B.L., R.W. Talbot, and J.W. Munger, Nitric acid and ammonia at a rural northeastern U.S. site, *Journal of Geophysical Research*, *submitted November*, 1997a.

Lefer, B.L., R.W. Talbot, and J.W. Munger, Deposition of nitric acid vapor to a mid-latitude forest, *Atmospheric Environment*, *submitted November*, 1997b.

Lewin, E.E., R.G. DePena, and J.P. Shimshock, Atmospheric gas and particle measurements at a rural northeastern U. S. site, *Atmospheric Environment*, *20* (1), 59-70, 1986.

Li, S.-M., K.G. Anlauf, and H.A. Wiebe, Heterogeneous nighttime production and deposition of particle nitrate at a rural site in North America during summer 1988, *Journal of Geophysical Research*, *98* (D3), 5139-5157, 1993.

Lindberg, S.E., and G.M. Lovett, Field measurements of particle dry deposition rates to foliage and inert surfaces in a forest canopy, *Environmental Science & Technology*, *19* (3), 238-244, 1985.

Lovett, G.M., and S.E. Lindberg, Atmospheric deposition and canopy interactions of nitrogen in forests, *Canadian Journal of Forest Research*, *23*, 1603-1616, 1993.

Milford, J.B., and C.I. Davidson, The sizes of particulate sulfate and nitrate in the atmosphere - a review, *Journal of the Air Pollution Control Association*, *37* (2), 125-134, 1987.

Miller, E.K., J.A. Panek, A.J. Friedland, J. Kadlecek, and V.A. Mohnen, Atmospheric deposition to a high-elevation forest at Whiteface Mountain, New York, USA, *Tellus*, *45B*, 209-227, 1993.

Moore, K.W., D.R. Fitzjarrald, R.K. Sakai, M.L. Goulden, J.W. Munger, and S.C. Wofsy, Seasonal variation in radiative and turbulent exchange at a deciduous forest in central Massachusetts, *Journal of Applied Meteorology*, *35*, 122-134, 1996.

Munger, J.W., S.C. Wofsy, P.S. Bakwin, S.-M. Fan, M.L. Goulden, B.C. Daube, and A.H. Goldstein, Atmospheric deposition of reactive nitrogen oxides and ozone in a temperate deciduous forest and a subarctic woodland: 1. Measurements and mechanisms, *Journal of Geophysical Research*, *101* (D7), 12,639-12,657, 1996.

Munger, J.W., S.-M. Fan, P.S. Bakwin, M.L. Goulden, A.H. Goldstein, A.S. Colman, and S.C. Wofsy, Regional budgets for nitrogen oxides from continental sources: variations of rates for oxidation and deposition with season and distance from source regions, *Journal of Geophysical Research*, *in press*, 1997.

NADP/NTN, National Atmospheric Deposition Program (NRSP-3)/National Trends Network, Coordination Office, Natural Resource Ecology Laboratory, Colorado State University, Fort Collins, Colorado, 80523, February 17, 1997.

Norton, R.B., J.M. Roberts, and B.J. Huebert, Tropospheric oxalate, *Geophysical Research Letters*, *10* (7), 517-520, 1983.

Parekh, P.P., and L. Hussain, Ambient sulfate concentrations and windflow patterns at Whiteface Mountain, New York, *Geophysical Research Letters*, *9* (1), 79-82, 1982.

Parrish, D.D., R.B. Norton, M.J. Bollinger, S.C. Liu, P.C. Murphy, D.L. Albritton, F.C. Fehsenfeld, and B.J. Huebert, Measurements of HNO_3 and NO_3^- particulates at a rural site in the Colorado mountains, *Journal of Geophysical Research*, *91* (D5), 5379-5393, 1986.

Peterson, B.J., and J.M. Melillo, The potential storage of carbon caused by eutrophication of the biosphere, *Tellus*, *37B*, 117-127, 1985.

Pierson, W.R., W.W. Brachaczek, R.A. Gorse Jr., S.M. Japar, J.M. Norbeck, and G.J. Keeler, Atmospheric acidity measurements on Allegheny Mountain and the origins of ambient acidity in the northeastern United States, *Atmospheric Environment*, *23* (2), 431-459, 1989.

Rao, A.K., and K.T. Whitby, Non-ideal collection characteristics of inertial impactors—Cascade impactors, *Journal of Aerosol Science*, *9*, 87-100, 1987.

Richards, L.W., Comments on the oxidation of NO_2 to nitrate—day and night, *Atmospheric Environment*, *17* (2), 397-402, 1983.

Ruijgrok, W., H. Tieben, and P. Eisinga, The dry deposition of particles to a forest canopy: a comparison of model and experimental results, *Atmospheric Environment*, *31* (3), 399-415, 1997.

Savoie, D.L., and J.M. Prospero, Particle size distribution of nitrate and sulfate in the marine atmosphere, *Geophysical Research Letters*, *9* (10), 1207-1210, 1982.

Schell, R.W., A historical perspective of atmospheric chemicals deposited on a mountain top peat bog in Pennsylvania, *International Journal of Goal Geology*, *8*, 147-173, 1987.

Schindler, D.W., and S.E. Bayley, The biosphere as an increasing sink for atmospheric carbon: estimates from increased nitrogen deposition, *Global Biogeochemical Cycles*, 7 (4), 717-734, 1993.

Schulze, E.-D., Air pollution and forest decline in a spruce (Picea abies) forest, *Science*, *244*, 776-783, 1989.

Slinn, W.G.N., Predictions for particle deposition to vegetative canopies, *Atmospheric Environment*, *16*, 1785-1794, 1982.

Stelson, A.W., and J.H. Seinfeld, Relative humidity and pH dependence of the vapor pressure of ammonium nitrate-nitric acid solutions, *Atmospheric Environment*, *16*, 993-1000, 1982.

Stelson, A.W., S.K. Friedlander, and J.H. Seinfeld, A note on the equilibrium relationship between ammonia and nitric acid and particulate ammonium nitrate, *Atmospheric Environment*, *13*, 369-371, 1979.

Stevens, R.K., T.G. Dzubay, G. Russworm, and D. Rickel, Sampling and analysis of atmospheric sulfates and related species, *Atmospheric Environment*, *12*, 55-, 1978.

Tang, I.N., On the equilibrium partial pressures of nitric acid and ammonia in the atmosphere, *Atmospheric Environment*, *14*, 819-828, 1980.

Tanner, R.L., W.H. Marlow, and L. Newman, Chemical composition correlations of size-fractionated sulfate in New York City aerosol, *Environmental Science & Technology*, *13* (1), 75-78, 1979.

Tjepkema, J.D., R.C. Cartica, and H.F. Hemond, Atmospheric concentration of ammonia in Massachusetts and deposition on vegetation, *Nature*, *249*, 445-446, 1981.

Trainer, M., M.P. Buhr, C.M. Curran, F.C. Fehsenfeld, E.Y. Hsie, S.C. Liu, R.B. Norton, D.D. Parrish, E.J. Williams, B.W. Gandrud, B.A. Ridley, J.D. Shetter, E.J. Allwine, and H.H. Westberg, Observations and modeling of the reactive nitrogen photochemistry at a rural site, *Journal of Geophysical Research*, *96* (D2), 3045-3063, 1991.

van Breemen, N., J. Mulder, and J.J.M. van Grinsven, Impacts of acid atmospheric deposition on woodland soils in The Netherlands: II N-transformations, *Soil Science Society of America Journal*, *51*, 1634-1640, 1987.

van Miegroet, H., D.W. Cole, and N.W. Foster, Nitrogen distribution and cycling, in *Atmospheric deposition and forest nutrient cycling*, edited by D.W. Johnson, and S.E. Lindberg, pp. 178-196, Springer-Verlag, New York, 1992.

Wesely, M.L., D.R. Cook, and R.L. Hart, Fluxes of gases and particles above a deciduous forest in wintertime, *Boundary-Layer Meteorology*, *27*, 237-255, 1983.

Wesely, M.L., D.R. Cook, R.L. Hart, and R.E. Speer, Measurements and parameterization of particulate sulfur dry deposition over grass, *Journal of Geophysical Research*, *90* (D1), 2131-2143, 1985.

Wolff, G.T., On the nature of nitrate in coarse continental aerosols, *Atmospheric Environment*, *18* (5), 997-981, 1984.

Wyers, G.P., and J.H. Duyzer, Micrometeorological measurement of the dry deposition flux of sulphate and nitrate aerosols to coniferous forest, *Atmospheric Environment*, *31* (3), 333-343, 1997.

CHAPTER 5

CONCLUDING REMARKS

5.1 General Conclusions

(1) This rural northeastern U.S. site receives air masses from a variety of source regions resulting in mean and median HNO_3 and aerosol N (NH_4^+ and NO_3^-) levels approximately 4 times higher when surface winds were from the urban SW as opposed to the more aged air from the rural NW wind sector. Gaseous NH_3, which has a primarily agricultural source, was the only N species to have significantly higher mixing ratios in air from the rural NW. Thus, mesoscale meteorology plays a dominant role in determining the air mass source regions and hence the levels of atmospheric N at the Harvard Forest.

(2) Higher HNO_3 and aerosol NO_3^- mixing ratios in the early morning provide evidence of entrainment of these species from aloft in the newly developing mixed layer. This behavior is consistent with theories of nocturnal heterogeneous HNO_3 and aerosol NO_3^- production in the "fossil" mixed layer.

(3) On average HNO_3 makes up about 20% of NO_Y at midday. PAN and other organic nitrates are believed to make up a significant fraction of NO_Y at Harvard Forest. The sum of the measured NO_Y species (NO, NO_2, HNO_3, and NO_3^-) typically account for 60-80% of the summertime NO_Y over the course of a day. However, the fact that unmeasured NO_Y species comprise ≈ 75% of the $\{NO_Y\text{-}NO_X\}$ in surface winds from the NW and E sectors suggests the significant production of organic nitrates in these air masses.

(4) NH_3 mixing ratios and the NH_3/NH_X partitioning ratio appear to be controlled by atmospheric SO_4^{2-} levels. High levels of acidic SO_4^{2-} in the air above Harvard Forest typically suppress gaseous NH_3 concentrations below the predicted NH_3 compensation point. Thus implying that this particular N limited ecosystem and other forest ecosystems in the northeastern U.S. are routinely losing reduced N to the atmosphere via low level canopy NH_3 emissions. This dual (chemical and biological) mechanism of NH_3 regulation was observed to be an exponential function of air temperature, however the canopy mediated portion of this control appears to shut down when the ecosystem experiences physiological strains such as water stress.

(5) The HNO_3 deposition velocity over a fully leafed northeastern mixed forest was found to be ≈ 5 cm s^{-1} and shows diel variation resulting from changes in atmospheric turbulence. Estimates of HNO_3

deposition by both MBR and DDIM methods yielded similar values, indicating that the surface resistance of the forest canopy to the dry deposition of HNO_3 is very small or zero. These estimates of HNO_3 deposition suggest that the concentration of HNO_3 plays a larger role than atmospheric turbulence in determining the magnitude of the HNO_3 flux to the canopy.

(6) Our estimates of HNO_3 deposition were typically three times greater than the measured eddy covariance NO_Y flux. The average difference between these two fluxes is not significant during nighttime hours and varies diurnally, showing the largest difference in the afternoon. While multiple factors contribute to a larger uncertainty associated with the DDIM method, much of the discrepancy is not attributable to a specific factor. It is likely that measurement biases, storage effects, and the fluxes of other NO_Y species are all contributing to the differences between the measured NO_Y and inferred HNO_3 fluxes.

(7) Ammonium is the dominant N aerosol species at Harvard Forest, typically found at summertime concentrations of approximately 60 nmol m^{-3}, which is 4-8 times greater than that of particulate NO_3^-. In general, the aerosol at this continental site has a bimodal distribution with NH_4^+, SO_4^{2-} and H^+ accounting for the majority of submicron fraction. Aerosol NO_3^- is present in both the coarse and fine modes, with the majority of the NO_3^- associated with supermicron Ca^{2+} aerosols.

(8) Overall, the aerosol acidity is not completely balanced by NH_4^+, with the more acidic particles arriving from the polluted SW. Ammonium levels in these polluted air masses are insufficient to neutralize SO_4^{2-} concentrations greater than ≈ 100 nmol m^{-3}, which may help define an upper limit to the NH_X emissions from this region.

(9) Although aerosol NO_3^- concentrations were significantly lower than submicron NH_4^+, the higher V_d of these coarse particles resulted in similar dry deposition estimates, on the order of 1 kg N ha^{-1} yr^{-1} for both aerosol N species. These aerosol dry deposition fluxes are considerably smaller than measured N wet deposition (≈ 8 kg N ha^{-1} yr^{-1}) and estimates of gaseous HNO_3 inputs (1-7 N ha^{-1} yr^{-1}) to this forest ecosystem.

5.2 Future Directions

While this project has been fairly successful in identifying the primary mechanisms that produce and regulate the atmospheric levels of HNO_3, NH_3, and aerosol N at this rural northeastern U.S. site, the magnitude of and factors controlling the dry deposition of N to this forest ecosystem are still not well understood. In this regard, future experiments in this area should focus on more and improved measurements of HNO_3 dry deposition. Determining the reasons for the gap between HNO_3 and NO_Y fluxes is critical to establishing confidence in our ability to model HNO_3 dry deposition to other forest ecosystems. Furthermore, changes in

the designs of future experiments (e.g., taller tower, shorter sampling times), may allow for the quantification of NH_3 fluxes at this site, which will make it possible to verify if these N-limited ecosystems are indeed losing NH_3 and if so, what is the magnitude of this flux on an annual basis.

In addition, this thesis points to several potentially fruitful research topics that were beyond the scope of this work. This N gas and aerosol dataset should be a valuable resource for the atmospheric modeling community with specific uses including: NO_Y photochemistry, HNO_3 production rates/mechanisms, and the partitioning of ammonium and nitrate between gas and aerosol species. Consequently, the entire UNH Harvard Forest trace gas and aerosol dataset is available via anonymous ftp at io.harvard.edu.

More work along the same lines as this project is needed to positively determine if N_2O_5 and/or NO_3 are involved in the heterogeneous production of HNO_3 and/or aerosol NO_3^- at this site. Similarly, more N gas and aerosol measurements may further define the temperature dependence between SO_4^{2-}, NH_3, and NH_4^+. These types of relationships could prove to be helpful for estimating total N deposition at monitoring sites in which NH_3 measurements are not being made.

Furthermore, 20-40% of the NO_Y at this site is still not accounted for by the measured species (NO_X, HNO_3, NO_3^- aerosol) at this site. The significant quantities of non-methane hydrocarbons emitted from this forest ecosystem highlight the potential importance of organic nitrates at this site. The fact that some of these N containing compounds may also have significant deposition velocities emphasizes the need for the identification and quantification of these organic species.

Using average atmospheric concentrations for N gas and aerosol at the Harvard Forest and a range of species-specific N dry deposition velocities it is estimated 2-12 kg N ha^{-1} yr^{-1} are deposited to this forest ecosystem. Considering that wet deposition typically contributes 8 kg N ha^{-1} yr^{-1}, this system is potentially receiving a significant amount of N each year, perhaps in excess of its biological requirements. The considerable range on these values needs to be reduced to adequately measure the consequences of the human induced increase of atmospheric N on the biosphere.

CHAPTER 6

COMPLETE LIST OF REFERENCES

Aber, J.D., Nitrogen cycling and nitrogen saturation in temperate forest ecosystems, *Trends in Ecology and Evolution*, 7 (7), 220-223, 1992.

Aber, J.D., K.J. Nadelhoffer, P. Steudler, and J.M. Melillo, Nitrogen saturation in northern forest ecosystems, *BioScience*, *39* (6), 378-386, 1989.

Aneja, V.P., C.S. Clairborn, Z. Li, and A. Murthy, Trends, seasonal variations, and analysis of high-elevation surface nitric acid, ozone, and hydrogen peroxide, *Atmospheric Environment*, *28* (10), 1781-1790, 1994a.

Aneja, V.P., M. Das, D.-S. Kim, and B.E. Hartsell, Measurements and analysis of photochemical oxidants and trace gases in the rural troposphere of the southeast United States, *Israel Journal of Chemistry*, *34*, 387-401, 1994b.

Appel, B.R., and Y. Tokiwa, Atmospheric particulate nitrate sampling errors due to reactions with particulate and gaseous strong acids, *Atmospheric Environment*, *15*, 1087-1089, 1981.

Appel, B.R., E.L. Kothny, E.M. Hoffer, G.M. Hidy, and J.J. Wesolowski, Sulfate and nitrate data from the California aerosol characterization experiment (ACHEX), *Environmental Science & Technology*, *12* (4), 418-425, 1978.

Appel, B.R., Y. Tokiwa, and M. Haik, Sampling of nitrates in ambient air, *Atmospheric Environment*, *15*, 283-289, 1981.

Appel, B.R., S.M. Wall, Y. Tokiwa, and M. Haik, Simultaneous nitric acid, particulate nitrate and acidity measurements in ambient air, *Atmospheric Environment*, *14*, 549-554, 1980.

Appel, B.R., Y. Tokiwa, E.L. Kothny, R. Wu, and V. Povard, Evaluation of procedures for measuring atmospheric nitric acid and ammonia, *Atmospheric Environment*, *22* (8), 1565-1573, 1988.

Åren, G., Model analysis of some consequences of acid precipitation on forest growth, in *Ecological effects of acid deposition*, pp. 233-244, National Swedish Environment Protection Board, Solna, 1983.

Asman, W.A.A., and A.J. Janssen, A long-range transport model for ammonia and ammonium for Europe, *Atmospheric Environment*, *21* (10), 2099-2119, 1987.

Baron, P.A., and K. Willeke, Gas and particle motion, in *Aerosol measurement: principles, techniques, and applications*, edited by K. Willeke, and P.A. Baron, pp. 23-40, Van Nostrand Reinhold, New York, 1993.

Brook, J.R., F. Di-Giovanni, S. Cakmak, and T.P. Meyers, Estimation of dry deposition velocity using inferential models and site-specific meteorology—uncertainty due to siting of meteorological towers, *Atmospheric Environment*, *31* (23), 3911-3919, 1997.

Buhr, S.M., M.P. Buhr, F.C. Fehsenfeld, J.S. Holloway, U. Karst, R.B. Norton, D.D. Parrish, and R.E. Sievers, Development of a semi-continuous method for the measurement of nitric acid vapor and particulate nitrate and sulfate, *Atmospheric Environment*, *29* (19), 2609-2624, 1995.

Bytnerowicz, A., P.R. Miller, D.M. Olszky, P.J. Dawson, and C.A. Fox, Gaseous and particulate air pollution in the San Gabriel Mountains of southern California, *Atmospheric Environment*, *21*, 1804-1814, 1987.

Cadle, S.H., R.J. Countess, and N.A. Kelly, Nitric acid and ammonia in urban and rural locations, *Atmospheric Environment*, *16* (10), 2501-2506, 1982.

Cofer III, W.R., V.G. Collins, and R.W. Talbot, Improved aqueous scrubber for collection of soluble atmospheric trace gases, *Environmental Science & Technology*, *19* (6), 557-560, 1985.

Countess, R.J., G.T. Wolff, and S.H. Cadle, The Denver winter aerosol: a comprehensive chemical characterization, *Journal of the Air Pollution Control Association*, *30*, 1194-1200, 1980.

Crosley, D.R., Issues in the measurement of reactive nitrogen compounds in the atmosphere, Report # MP-94-035, SRI International, Menlo Park, March 1994.

Davies, C.N., The entry of aerosols into sampling tubes and heads, *British Journal of Applied Physics*, ser.2,*1*, 921-392, 1968.

Davies, C.N., and M. Subari, Aspiration above wind velocity of aerosols with thin-walled nozzles facing at right angles to the wind direction, *Journal of Aerosol Science*, *13* (1), 59-71, 1982.

Denmead, O.T., J.R. Freney, and J.R. Simpson, A closed ammonia cycle within a plant canopy, *Soil Biol. Biochem.*, *8*, 161-164, 1976.

Dentener, F.J., and P.J. Crutzen, Reaction of N_2O_5 on tropospheric aerosols: Impact on the global distributions of NO_x, O_3 and OH, *Journal of Geophysical Research*, *98*, 7149-7163, 1993.

Dollard, G.J., D.H.F. Atkins, T.J. Davies, and C. Healy, Concentrations and dry deposition velocities of nitric acid, *Nature*, *326*, 481-483, 1987.

Droppo, J.G., Concurrent measurements of ozone dry deposition using eddy correlation and profile flux methods, *Journal of Geophysical Research*, *90*, 2111-2118, 1985.

Duyzer, J.H., A.M.H. Bouman, R.M. van Aalst, and H.S.M.A. Diederen, Assessment of dry deposition fluxes of NH_3 and NH_4^+ over natural terrains, in *EURASAP, 13-15 April 1987*, edited by W.A. H. Asman and H.S.M. A. Diederen, National Institute of Public Health, Bilthoven, The Netherlands, 1987.

Dyer, A.J., and B.B. Hicks, Flux-gradient relationships in the constant flux layer, *Quart. J. Royal Meteorol. Soc.*, *96*, 715-721, 1970.

Edgerton, E.S., T.F. Lavery, and R.P. Boksleitner, Preliminary data from the USEPA dry deposition network: 1989, *Environmental Pollution*, *75*, 145-156, 1992.

Ehhalt, D.H., and J.W. Drummond, The tropospheric cycle of NO_x, in *Chemistry of the unpolluted and polluted troposphere*, edited by H.W. Georgii, and W. Jaeschke, pp. 219-251, D. Reidel, Hingham, MA, 1982.

Erisman, J.W., Acid deposition to nature areas in the Netherlands: Part I. methods and results, *Water, Air, and Soil Pollution*, *71*, 51-80, 1993.

Erisman, J.W., G. Draaijers, J. Duyzer, P. Hofschreuder, N. van Leeuwen, F. Römer, W. Ruijgrok, P. Wyers, and M. Gallagher, Particle deposition to forests—Summary of results and application, *Atmospheric Environment*, *31* (3), 321-332, 1997.

Farquhar, G.D., P.M. Firth, R. Weselaar, and B. Weir, On the gaseous exchange of ammonia between leaves and the environment: determination of the ammonia compensation point, *Plant Physiology*, *66*, 710-714, 1980.

Forrest, J., D.J. Spandau, R.L. Tanner, and L. Newman, Determination of atmospheric nitrate and nitric acid employing a diffusion denuder with a filter pack, *Atmospheric Environment*, *16* (6), 1473-1485, 1982.

Gallagher, M.W., K.M. Beswick, J. Duyzer, H. Westrate, T.W. Choularton, and P. Hummelshøj, Measurements of aerosol fluxes to Speulder Forest using a micrometeorological technique, *Atmospheric Environment*, *31* (3), 359-373, 1997.

Garratt, J.R., and B.B. Hicks, Momentum, heat, and water vapour transfer to and from natural and artificial surfaces, *Quart. J. Royal Meteorol. Soc.*, *99*, 680-687, 1973.

Geigert, M.A., N.P. Nikolaidis, D.R. Miller, and J. Heitert, Deposition rates for sulfur and nitrogen to a hardwood forest in northern Connecticut, USA, *Atmospheric Environment*, *28* (9), 1689-1697, 1994.

Georgii, H.-W., and G. Gravenhorst, The ocean as a source or sick of reactive trace-gases, *Pure Appl. Geophys.*, *115*, 503-511, 1977.

Georgopoulos, G.P., and J.H. Seinfeld, Statistical distribution of air pollutant concentrations, *Environmental Science & Technology*, *15* (7), 401A-416A, 1982.

Goldstein, A.H., C.M. Spivakovsky, and S.C. Wofsy, Seasonal variations of nonmethane hydrocarbons in rural New England: Constraints on OH concentrations in northern latitudes, *Journal of Geophysical Research*, *100*, 21,023-21,033, 1995.

Goldstein, A.H., M.L. Goulden, J.W. Munger, S.C. Wofsy, and C.D. Geron, Season course of isoprene emissions from a midlatitude deciduous forest, *Journal of Geophysical Research*, *in press*, 1997.

Goulden, M.L., J.W. Munger, S.-M. Fan, B.C. Daube, and S.C. Wofsy, Exchange of carbon dioxide by a deciduous forest: response to interannual climate variability, *Science*, *271*, 1576-1578, 1996a.

Goulden, M.L., J.W. Munger, S.-M. Fan, B.C. Daube, and S.C. Wofsy, Measurements of carbon sequestration by long-term eddy covariance: methods and a critical evaluation of accuracy, *Global Change Biology*, *2*, 169-182, 1996b.

Gschwandtner, G., K. Gschwandtner, K. Eldridge, C. Mann, and D. Mobley, Historic emissions of sulfur and nitrogen oxides in the United States from 1900 to 1980, *Journal of the Air Pollution Control Association*, *36*, 139-149, 1986.

Gunderson, P., Nitrogen deposition and the forest nitrogen cycle, *Forest Ecology and Management*, *44*, 15-28, 1991.

Harriss, R.C., and J.T. Michaels, Sources of atmospheric ammonia, paper presented at the second symposium on the composition of the nonurban Troposphere, Am. Meteorol. Soc., Williamsburg, VA, , 1982.

Hanson, P.J., and S.E. Lindberg, Dry deposition of reactive nitrogen compounds: a review of leaf, canopy, and non-foliar measurements, *Atmospheric Environment*, *25A* (8), 1615-1634, 1991.

Hidy, G.M., Spatial and temporal distribution of airborne sulfate in parts of the U.S., *Atmospheric Environment*, *12*, 735-752, 1978.

Hicks, B.B., and T.P. Meyers, Measuring and modelling dry deposition in mountainous areas, In *Acid deposition at high elevation sites*, edited by M.H. Unsworth and D. Fowler, pp. 541-552, Kluwer Academic Publishers, Dordrecht, 1988.

Hicks, B.B., D.D. Baldocchi, T.P. Meyers, R.P. Hosker Jr., and D.R. Matt, A preliminary multiple resistance routine for deriving dry deposition velocities from measured quantities, *Water, Air, and Soil Pollution*, *36*, 311-330, 1987.

Hicks, B.B., D.R. Matt, R.T. McMillen, J.D. Womack, M.L. Wesley, R.L. Hart, D.R. Cook, S.E. Lindberg, R.G. de Pena, and D.W. Thomson, A field investigation of sulfate fluxes to a deciduous forest, *Journal of Geophysical Research*, *94* (D10), 13003-13011, 1989.

Hosker, R.P., Jr., and S.E. Lindberg, Review: atmospheric deposition and plant assimilation of gases and particles, *Atmospheric Environment*, *16*, 889-910, 1982.

Huebert, B.J., and C.H. Robert, The dry deposition of nitric acid to grass, *Journal of Geophysical Research*, *90* (D1), 2085-2090, 1985.

Kadowaki, S.; Size distribution of atmospheric total aerosols, sulfate, ammonium and nitrate particulates in the Nagoya area, *Atmospheric Environment*, *10*, 39-43, 1976.

Kauppi, P.E., K. Mielikäinen, and K. Kuusela, Biomass and carbon budget of European forests, 1971-1990, *Science*, *256*, 70-74, 1992.

Keeler, G.J., J.D. Spengler, and R.A. Castillo, Acid aerosol measurements at a suburban Connecticut site, *Atmospheric Environment*, *25A* (3/4), 681-690, 1991.

Keene, W.C., R.W. Talbot, M.O. Andreae, K. Beecher, H. Berresheim, M. Castro, J.C. Farmer, J.N. Galloway, M.R. Hoffmann, S.-M. Li, J.R. Maben, J.W. Munger, R.B. Norton, A.A.P. Pszenny, H. Puxbaum, H. Westberg, and W. Winiwarter, An intercomparison of measurement systems for vapor and particulate phase concentrations of formic and acetic acids, *Journal of Geophysical Research*, *94* (D5), 6457-6472, 1989.

Kelly, T.J., R.L. Tanner, L. Newman, P.J. Galvin, and J.A. Kadlecek, Trace gas and aerosol measurements at a remote site in the northeast U.S., *Atmospheric Environment*, *18* (12), 2565-2576, 1984.

Kleinman, L., Y.-N. Lee, S.R. Springston, L. Nunnermacker, X. Zhou, R. Brown, K. Hallock, P. Klotz, D. Leahy, J.H. Lee, and L. Newman, Ozone formation at a rural site in the southeastern United States, *Journal of Geophysical Research*, *99* (D2), 3469-3482, 1994.

Klemm, O., R.W. Talbot, D.R. Fitzjarrald, K.I. Klemm, and B.L. Lefer, Low to middle tropospheric profiles and biosphere/troposphere fluxes of acidic gases in the summertime Canadian Taiga, *Journal of Geophysical Research*, *99* (D1), 1687-1698, 1994.

Knoll, G.F., *Radiation detection and measurement*, 816 pp., John Wiley & Sons, New York, 1979.

Kramm, G., and R. Dlugi, Modelling of the vertical fluxes of nitric acid, ammonia, and ammonium nitrate, *Journal of Atmospheric Chemistry*, *18*, 319-357, 1994.

Lamersdorf, N.P., and M. Meyer, Nutrient cycling and acidification of a northwest German forest site with high atmospheric nitrogen deposition, *Forest Ecology and Management*, *62*, 323-354, 1993.

Langford, A.O., and F.C. Fehsenfeld, Natural Vegetation as a Source or Sink for Atmospheric Ammonia - A Case Study, *Science*, *255* (5044), 581-583, 1992.

Langford, A.O., F.C. Fehsenfeld, J. Zachariassen, and D.S. Schimel, Gaseous ammonia fluxes and background concentrations in terrestrial ecosystems of the United States, *Global Biogeochemical Cycles*, *6* (4), 459-483, 1992.

Lee, G., L. Zhuang, B.J. Hubert, and T.P. Meyers, Concentration gradients and dry deposition of nitric acid vapor at the Mauna Loa Observatory, Hawaii, *Journal of Geophysical Research*, *98* (D7), 12,661-12,671, 1993.

Lefer, B.L., and R.W. Talbot, Aerosol nitrate and ammonium at a northeastern U.S. site, *Atmospheric Environment*, *submitted December*, 1997.

Lefer, B.L., R.W. Talbot, R.C. Harriss, J.D. Bradshaw, S.T. Sandholm, J.O. Olson, G.W. Sachse, J. Collins, M.A. Shipham, D.R. Blake, K.I. Klemm, K. Gorzelska, and J. Barrick, Enhancement of acidic gases in biomass-burning impacted air masses over Canada, *Journal of Geophysical Research*, *99* (D1), 1721-1738, 1994.

Lefer, B.L., R.W. Talbot, and J.W. Munger, Nitric acid and ammonia at a rural northeastern U.S. site, *Journal of Geophysical Research*, *submitted December* 1997a.

Lefer, B.L., R. W. Talbot, and J. W. Munger, Deposition of nitric acid vapor to a mid-latitude forest, *Atmospheric Environment*, *submitted December*, 1997b.

Lewin, E.E., R.G. DePena, and J.P. Shimshock, Atmospheric gas and particle measurements at a rural northeastern U. S. site, *Atmospheric Environment*, *20* (1), 59-70, 1986.

Li, S.-M., K.G. Anlauf, and H.A. Wiebe, Heterogeneous nighttime production and deposition of particle nitrate at a rural site in North America during summer 1988, *Journal of Geophysical Research*, *98* (D3), 5139-5157, 1993.

Lindberg, S.E., and G.M. Lovett, Field measurements of particle dry deposition rates to foliage and inert surfaces in a forest canopy, *Environmental Science & Technology*, *19* (3), 238-244, 1985.

Lovett, G.M., and S.E. Lindberg, Atmospheric deposition and canopy interactions of nitrogen in forests, *Canadian Journal of Forest Research*, *23*, 1603-1616, 1993.

Logan, J.A., Nitrogen oxides in the troposphere: global and regional budgets, *Journal of Geophysical Research*, *88* (C15), 10,785-10,807, 1983.

Meixner, F.X., H.H. Franken, J.H. Duijzer, and R.M. van Aalst, Dry deposition of gaseous HNO_3 to a pine forest, in *Proceedings of the 16th International Technical Meeting on Air Pollution Modeling and its Applications*, edited by H. van Dop, pp. 23-35, Plenum Publishing Corporation, Lindau, Germany, 1988.

Meyers, T.P., and B.B. Hicks, Dry deposition of O_3, SO_2, and HNO_3 to different vegetation in the same exposure environment, *Environmental Pollution*, *53*, 13-25, 1988.

Meyers, T.P., B.J. Huebert, and B.B. Hicks, HNO_3 deposition to a deciduous forest, *Boundary-Layer Meteorology*, *49*, 395-410, 1989.

Meyers, T.P., B.B. Hicks, R.P.J. Hosker, J.D. Womack, and L.C. Satterfield, Dry deposition inferential measurement techniques–II. Seasonal and annual deposition rates of sulfur and nitrate, *Atmospheric Environment*, *25A* (10), 2361-2370, 1991.

Meyers, T.P., M.E. Hall, S.E. Lindberg, and K. Kim, Use of the modified Bowen-ratio technique to measure fluxes of trace gases, *Atmospheric Environment*, *30* (19), 3321-3329, 1996.

Milford, J.B., and C.I. Davidson, The sizes of particulate sulfate and nitrate in the atmosphere - a review, *Journal of the Air Pollution Control Association*, *37* (2), 125-134, 1987.

Miller, E.K., J.A. Panek, A.J. Friedland, J. Kadlecek, and V.A. Mohnen, Atmospheric deposition to a high-elevation forest at Whiteface Mountain, New York, USA, *Tellus*, *45B*, 209-227, 1993.

Moody, J.L., J.W. Munger, A.H. Goldstein, D.J. Jacob, and S.C. Wofsy, Harvard Forest regional-scale air mass composition by PATH (Patterns in atmospheric transport history), *Journal of Geophysical Research*, *submitted*, 1997.

Moore, K.W., D.R. Fitzjarrald, R.K. Sakai, M.L. Goulden, J.W. Munger, and S.C. Wofsy, Seasonal variation in radiative and turbulent exchange at a deciduous forest in central Massachusetts, *Journal of Applied Meteorology*, *35*, 122-134, 1996.

Müller, H., G. Kramm, F. Meixner, G.J. Dollard, D. Fowler, and M. Possanzini, Determination of HNO_3 dry deposition by modified Bowen ratio and aerodynamic profile techniques, *Tellus*, *45B*, 346-367, 1993.

Munger, J.W., S.C. Wofsy, P.S. Bakwin, S.-M. Fan, M.L. Goulden, B.C. Daube, and A.H. Goldstein, Atmospheric deposition of reactive nitrogen oxides and ozone in a temperate deciduous forest and a subarctic woodland: 1. Measurements and mechanisms, *Journal of Geophysical Research*, *101* (D7), 12,639-12,657, 1996.

Munger, J.W., S.-M. Fan, P.S. Bakwin, M.L. Goulden, A.H. Goldstein, A.S. Colman, and S.C. Wofsy, Regional budgets for nitrogen oxides from continental sources: variations of rates for oxidation and deposition with season and distance from source regions, *Journal of Geophysical Research*, *in press*, 1997.

NADP/NTN, National Atmospheric Deposition Program (NRSP-3)/National Trends Network, Coordination Office, Natural Resource Ecology Laboratory, Colorado State University, Fort Collins, Colorado, 80523, February 17, 1997.

Nilsson, J., Critical loads for sulphur and nitrogen, in *Air Pollution and Ecosystems, Proc. Symp.*, edited by P. Mathy, pp. 85-91, D. Reidel Publishing Company, Dordrecht, Grenoble, 1978.

Norton, R.B., J.M. Roberts, and B.J. Huebert, Tropospheric oxalate, *Geophysical Research Letters*, *10* (7), 517-520, 1983.

Ollinger, S.V., J.D. Aber, G.M. Lovett, S.E. Millham, R.G. Lathrop, and J.M. Ellis, A spatial model of atmospheric deposition for the northeastern U.S., *Ecological Applications*, *3* (3), 459-472, 1993.

Parekh, P.P., and L. Hussain, Ambient sulfate concentrations and windflow patterns at Whiteface Mountain, New York, *Geophysical Research Letters*, *9* (1), 79-82, 1982.

Parrish, D.D., M.P. Buhr, M. Trainer, R.B. Norton, J.P. Shimshock, C. Fehsenfeld, K.G. Anlauf, J.W. Bottenheim, Y.Z. Tang, H.A. Wiebe, J.M. Roberts, R.L. Tanner, L. Newman, V.C. Bowersox, K.J. Olszyna, E.M. Bailey, M.O. Rodgers, T. Wang, H. Berresheim, U.K. Roychowdhury, and K.L. Demerjian, The total reactive oxidized nitrogen levels and the partitioning between the individual species at six rural sites in eastern North America, *Journal of Geophysical Research*, *98* (D2), 2927-2939, 1993.

Parrish, D.D., R.B. Norton, M.J. Bollinger, S.C. Liu, P.C. Murphy, D.L. Albritton, F.C. Fehsenfeld, and B.J. Huebert. Measurements of HNO_3 and NO_3^- particulates at a rural site in the Colorado mountains, *Journal of Geophysical Research*, *91* (D5), 5379-5393, 1986.

Parrish, D.D., M. Trainer, M.P. Buhr, B.A. Watkins, and F.C. Fehsenfeld, Carbon monoxide concentrations and their relation to concentrations of total reactive oxidized nitrogen at two rural U.S. sites, *Journal of Geophysical Research*, *96* (D5), 9309-9320, 1991.

Peake, E., M.A. MacLean, and H.S. Sandhu, Total inorganic nitrate (particulate nitrate and nitric acid) observations in Calgary, Alberta, *Journal of the Air Pollution Control Association*, *35* (3), 250-253, 1985.

Peterson, B.J., and J.M. Melillo, The potential storage of carbon caused by eutrophication of the biosphere, *Tellus*, *37B*, 117-127, 1985.

Pierson, W.R., W.W. Brachaczek, R.A. Gorse Jr., S.M. Japar, J.M. Norbeck, and G.J. Keeler, Atmospheric acidity measurements on Allegheny Mountain and the origins of ambient acidity in the northeastern United States, *Atmospheric Environment*, *23* (2), 431-459, 1989.

Rao, A.K., and K.T. Whitby, Non-ideal collection characteristics of inertial impactors—Cascade impactors, *Journal of Aerosol Science*, *9*, 87-100, 1987.

Raupach, M.R., Anomalies in flux-gradient relationships over forest, *Boundary Layer Meteorology*, *16*, 467-486, 1979.

Richards, L.W., Comments on the oxidation of NO_2 to nitrate—day and night, *Atmospheric Environment*, *17* (2), 397-402, 1983.

Ruijgrok, W., H. Tieben, and P. Eisinga, The dry deposition of particles to a forest canopy: a comparison of model and experimental results, *Atmospheric Environment*, *31* (3), 399-415, 1997.

Savoie, D.L., and J.M. Prospero, Particle size distribution of nitrate and sulfate in the marine atmosphere, *Geophysical Research Letters*, *9* (10), 1207-1210, 1982.

Schell, R.W., A historical perspective of atmospheric chemicals deposited on a mountain top peat bog in Pennsylvania, *International Journal of Goal Geology*, *8*, 147-173, 1987.

Schindler, D.W., and S.E. Bayley, The biosphere as an increasing sink for atmospheric carbon: estimates from increased nitrogen deposition, *Global Biogeochemical Cycles*, *7* (4), 717-734, 1993.

Schlesinger, W.H., and A.E. Hartley, A global budget for atmospheric NH_3, *Biogeochemistry*, *15*, 191-211, 1992.

Schulze, E.-D., Air pollution and forest decline in a spruce *Picea abies* forest, *Science*, *244*, 776-783, 1989.

Spicer, C.W., J.E. Howes, T.A. Bishop, L.H. Arnold, and R.K. Stevens, Nitric acid measurement methods: an intercomparison, *Atmospheric Environment*, *16*, 1487-1500, 1982.

Slinn, W.G.N., Predictions for particle deposition to vegetative canopies, *Atmospheric Environment*, *16*, 1785-1794, 1982.

Stecher III, H.A., G.W. Luther III, D.L. MacTaggart, S.O. Farwell, D.R. Crosley, W.D. Dorko, P.D. Goldan, N. Beltz, U. Krischke, W.T. Luke, D.C. Thornton, R.W. Talbot, B.L. Lefer, E.M. Scheuer, R.L. Benner, J. Wu, E.S. Saltzman, M.S. Gallagher, and R.J. Ferek, Results of the Gas-Phase Sulfur Intercomparison Experiment (GASIE): Overview of experimental setup, results and general conclusions, *Journal of Geophysical Research*, *102* (D13), 16,219-16,236, 1997.

Stelson, A.W., and J.H. Seinfeld, Relative humidity and pH dependence of the vapor pressure of ammonium nitrate-nitric acid solutions, *Atmospheric Environment*, *16*, 993-1000, 1982.

Stelson, A.W., S.K. Friedlander, and J.H. Seinfeld, A note on the equilibrium relationship between ammonia and nitric acid and particulate ammonium nitrate, *Atmospheric Environment*, *13*, 369-371, 1979.

Stevens, R.K., T.G. Dzubay, G. Russworm, and D. Rickel, Sampling and analysis of atmospheric sulfates and related species, *Atmospheric Environment*, *12*, 55-, 1978.

Talbot, R.W., A.S. Vijgen, and R.C. Harriss, Measuring tropospheric HNO_3: problems and prospects for nylon filter and mist chamber, *Journal of Geophysical Research*, *95* (D6), 7553-7542, 1990.

Talbot, R.W., A.S. Vijgen, and R.C. Harriss, Soluble species in the Arctic summer troposphere: acidic gases, aerosols, and precipitation, *Journal of Geophysical Research* (D15), 16,531-16,545, 1992.

Talbot, R.W., J.E. Dibb, B.L. Lefer, E.M. Scheuer, J.D. Bradshaw, S.T. Sandholm, S. Smyth, D.R. Blake, N.J. Blake, G.W. Sachse, J.E. Collins, and G.L. Gregory, Large-scale distributions of tropospheric nitric, formic, and acetic acids over the western Pacific basin during wintertime, *Journal of Geophysical Research*, *In press*, 1997.

Tang, I.N., On the equilibrium partial pressures of nitric acid and ammonia in the atmosphere, *Atmospheric Environment*, *14*, 819-828, 1980.

Tanner, R.L., W.H. Marlow, and L. Newman, Chemical composition correlations of size-fractionated sulfate in New York City aerosol, *Environmental Science & Technology*, *13* (1), 75-78, 1979.

Tjepkema, J.D., R.C. Cartica, and H.F. Hemond, Atmospheric concentration of ammonia in Massachusetts and deposition on vegetation, *Nature*, *249*, 445-446, 1981.

Trainer, M., M.P. Buhr, C.M. Curran, F.C. Fehsenfeld, E.Y. Hsie, S.C. Liu, R.B. Norton, D.D. Parrish, E.J. Williams, B.W. Gandrud, B.A. Ridley, J.D. Shetter, E.J. Allwine, and H.H. Westberg, Observations and modeling of the reactive nitrogen photochemistry at a rural site, *Journal of Geophysical Research*, *96* (D2), 3045-3063, 1991.

Vann, D.R., G.R. Strimbeck, and A.H. Johnson, Effects of ambient levels of airborne chemicals on freezing resistance of red spruce foliage, *Forest Ecology and Management*, *51*, 69-79, 1992.

van Breemen, N., J. Mulder, and J.J.M. van Grinsven, Impacts of acid atmospheric deposition on woodland soils in The Netherlands: II N-transformations, *Soil Science Society of America Journal*, *51*, 1634-1640, 1987.

van Miegroet, H., D.W. Cole, and N.W. Foster, Nitrogen distribution and cycling, in *Atmospheric deposition and forest nutrient cycling*, edited by D.W. Johnson, and S.E. Lindberg, pp. 178-196, Springer-Verlag, New York, 1992.

Walton, S., M.W. Gallagher, and J.H. Duyzer, Use of a detailed model to study the exchange of NO_x and O_3 above and below a deciduous canopy, *Atmospheric Environment*, *31* (18), 2915-2931, 1997.

Wesely, M.L., and B.B. Hicks, Some factors that affect the deposition rates of sulfur dioxide and similar gases on vegetation, *Journal of the Air Pollution Control Association*, *27* (11), 1110-1116, 1977.

Wesely, M.L., D.R. Cook, and R.L. Hart, Fluxes of gases and particles above a deciduous forest in wintertime, *Boundary-Layer Meteorology*, *27*, 237-255, 1983.

Wesely, M.L., D.R. Cook, R.L. Hart, and R.E. Speer, Measurements and parameterization of particulate sulfur dry deposition over grass, *Journal of Geophysical Research*, *90* (D1), 2131-2143, 1985.

Williams, E.J., and F.C. Fehsenfeld, Measurement of soil nitrogen oxide emissions at three North American ecosystems, *Journal of Geophysical Research*, *96* (D1), 1033-1042, 1991.

Williams, E.J., S.T. Sandholm, J.D. Bradshaw, J.S. Schendel, A.O. Langford, P.K. Quinn, P.J. LeBel, S.A. Vay, P.D. Roberts, R.B. Norton, B.A. Watkins, M.P. Buhr, D.D. Parrish, J.G. Calvert, and F.C. Fehsenfeld, An intercomparison of five ammonia measurement techniques, *Journal of Geophysical Research*. *97* (D11), 11591-11611, 1992.

Wofsy, S.C., M.L. Goulden, J.W. Munger, S.-M. Fan, P.S. Bakwin, B.C. Daube, S.L. Bassow, and F.A. Bazzaz, Net exchange of CO_2 in a mid-latitude forest, *Science*, *260*, 1314-1317, 1993.

Wolff, G.T., On the nature of nitrate in coarse continental aerosols, *Atmospheric Environment*, *18* (5), 997-981. 1984.

Wyers, G.P., R.P. Otjes, and J. Slanina, A continuous-flow denuder for the measurement of ambient concentrations and surface-exchange fluxes of ammonia, *Atmospheric Environment*, *27A* (13), 2085-2090, 1993.

Wyers, G.P., and J.H. Duyzer, Micrometeorological measurement of the dry deposition flux of sulphate and nitrate aerosols to coniferous forest, *Atmospheric Environment*, *31* (3), 333-343, 1997.